In presenting the dissertation as a partial fulfillment of the requirements for an advanced degree from the Georgia Institute of Technology, I agree that the Library of the Institute shall make it available for inspection and circulation in accordance with its regulations governing materials of this type. I agree that permission to copy from, or to publish from, this dissertation may be granted by the professor under whose direction it was written, or, in his absence, by the Dean of the Graduate Division when such copying or publication is solely for scholarly purposes and does not involve potential financial gain. It is understood that any copying from, or publication of, this dissertation which involves potential financial gain will not be allowed without written permission.

3/17/65
b

THE EFFECT OF THE INTERMEDIATE PRINCIPAL STRESS ON THE STRENGTH OF ROCK

A THESIS

Presented to

The Faculty of the Graduate Division

by

Billy Bruce Mazanti

In Partial Fulfillment

of the Requirements for the Degree

Doctor of Philosophy

in the School of Civil Engineering

Georgia Institute of Technology

June, 1967

THE EFFECT OF THE INTERMEDIATE PRINCIPAL

STRESS ON THE STRENGTH OF ROCK

Approved:

Chairman

Date approved by Chairman: 5/27/67

DEDICATION

This thesis is dedicated to my wife, Jewel, for her patience and encouragement during the past years of my graduate study.

ACKNOWLEDGMENTS

Grateful acknowledgment of assistance is expressed to all who participated in the development of this work.

In particular, the writer wishes to thank Professor G. F. Sowers for his advice, guidance and instruction over the years past, during which he acted both as a teacher and a friend.

Special thanks also are extended to Dr. N. H. Wade for the efforts which he expended in the evaluation of the investigation, as well as to Dr. C. H. Weaver for serving as a reading committee member.

TABLE OF CONTENTS

LIST OF TABLES

LIST OF ILLUSTRATIONS

LIST OF SYMBOLS

σ	Normal Stress
σ_1	Major Principal Stress
σ_2	Intermediate Principal Stress
σ_3	Minor Principal Stress
σ_o	Octahedral Normal Stress
σ_r	Radial Stress in Hollow Cylinders
σ_z	Axial Stress in Hollow Cylinders
σ_θ	Tangential, or Circumferential, Stress in Hollow Cylinders
τ	Shear Stress
τ_o	Octahedral Shear Stress
ϕ	Mohr Friction Angle
δ	Slope of $1/2(\sigma_1 - \sigma_3)$ vs. $1/2(\sigma_1 + \sigma_3)$ Curve

SUMMARY

The necessity for more correct and precise representations of the strength of rock is becoming more acute. Extensive engineering projects such as the North American Air Defense Command Combat Operations Center at Colorado Springs, Colorado are being constructed deep underneath the earth's surface, deeper and deeper holes are being bored in search for oil as well as for geological information and the use of rock and rock-like materials in "ordinary" construction is based upon more radical stress conditions each day.

Considerable effort has been expended in the past ten years in order to define the strength parameters of rock and rock-like materials under various conditions of confinement and heat; however, one most important aspect has been greatly neglected. That is the effect of the intermediate principal stress on the strength of rock.

The testing techniques presently in use are generally capable of producing only two stress states with respect to the relative value of the intermediate principal stress. These are: (1) Major Principal Stress greater than the Intermediate Principal Stress which is equal to the Minor Principal Stress, and (2) Major Principal Stress equal to the Intermediate Principal Stress and greater than the Minor Principal Stress. In practice, these two states are probably not representative of many stress situations. Some few investigations have utilized equipment and techniques with the capabilities of producing other states of stress; however, the results from the use of such equipment is of

questionable value due to the system used and/or to the size of specimens tested.

Because of the limited amount of data available, the general effects on strength due to variation of the intermediate principal stress are not clear. Also, graphical representations of strength criteria must be dependent upon assumed behavior of the rock in this respect.

The purpose of the present investigation was to design a system of testing which will produce reliable results under three-dimensional loading and to perform tests on different types of rock in order to determine the effect on strength of the intermediate principal stress.

A system was selected which consisted of hollow cylinders of rock subjected to the combined effect of internal fluid pressure, external fluid pressure, and axial loads. The apparatus was designed to withstand any combination of internal and external pressures up to 10,000 psi. Its unique construction allows the use of any length of specimen and the system utilizes readily-available electrical insulation for membranes. It can be easily modified to allow for pore pressure measurements.

The strength specimens were cored from intact rock blocks in a single operation by the use of commercially-available, double-tube, diamond-tipped core bits.

Two different rocks were used in this study: (1) Indiana Limestone, a relatively porous rock, which exhibits "plasticity" at high confining pressures and (2) Stone Mountain Granite, a very low porosity, crystalline material which behaves in a brittle manner under the con-

fining pressures used in this study.

Tests were performed during which the ratio of the intermediate principal stress to the major principal stress was held constant for a given test. This ratio was varied, during the test series, from a value of zero up to a value of one. The minor principal stress was held constant during a given test. These conditions were produced by maintaining the internal fluid pressure constant while increasing both the external fluid pressure and the axial load. Internal confining pressures up to 2000 psi were utilized.

Failure of the specimens was by complete shear fracture although internal spalling occurred in some specimens prior to fracture.

The principal stresses at fracture were calculated on an elastic basis and two sets of failure stresses were analyzed. One set was those stresses at the internal surface of the cylinder and the second set consisted of "average" stresses.

Analysis of the results utilized conventional triaxial presentations as well as octahedral stresses. Failure surfaces were developed for the octahedral plane and compared with presently-used criteria.

It was concluded that the newly-developed apparatus is satisfactory for the study of the behavior of rocks under controlled, polyaxial stress states within the confining pressure capabilities of the cell. The strength was found to be a function of the intermediate principal stress and can be represented in terms of the ratio of the intermediate to the major principal stresses. A generalized relationship was developed which depends on a material constant. This constant can be evaluated by the use of the newly-developed equipment. The strength of

the rocks can be represented by straight-line failure surfaces on the octahedral plane. These failure surfaces were closely approximated by the Mohr criterion in the case of the granite and were intermediate between the Mohr and the Tresca criteria in the case of the Indiana limestone. The spalling phenomenon appears to be an important mechanism in the behavior of rocks under certain stress states and the conventional triaxial testing equipment probably prevents the occurrence of spalling.

CHAPTER I

STATEMENT OF THE PROBLEM

The strength of rock and rock-like materials has recently become a subject of considerable interest and investigation. The impetus for the studies is the realization of the fact that physical environmental conditions and character of stresses influence rock strength and deformational characteristics to unknown degrees. New situations are constantly developing in which man is altering the environment of rock masses and, in so doing, must be concerned with the stability of the rock system. Stability, in an engineering sense, does not signify the complete lack of deformation, but that the deformation be of an allowable amount, consistent with the purpose of the situation.

Typical of such situations is the drilling or boring of very deep holes into the earth. Oil companies are constantly opening deeper and deeper holes in their search for productive formations and geological investigations are being conducted to tremendous depths below the earth's surface. There, conditions of heat and pressure combinations are much in excess of that which has been previously experienced. Tunnels and mines are being developed to depths where past experience is lacking with respect to stable opening configurations and shoring practice. Many new engineering structures and complexes such as underground powerhouses are being located underground, in extremely large openings in rock formations. The practice of storing, for later retrieval, liq-

uids and gases in both man-made and natural cavities is increasing as is, also, the use of such openings for the *disposal* of contaminated gases, liquids, slurries and solids.

The lack of information with respect to the strength and deformational characteristics of rock under these conditions leads to the expenditure of unknown excesses in terms of human effort as well as money. This practice is inconsistent with the refinements being effected in other engineering areas and, as a consequence, some attention has been directed to the study of the factors involved.

Possibly the major efforts have been made by oil companies with smaller, piecemeal contributions by governmental agencies, other private enterprises and by educational institutions. With the use of "conventional" triaxial testing apparatus, modified, in some cases, to permit the application of high temperature, considerable work has been done on the effects of lateral confinement on the strength of rock. Usually these investigations have been carried out on specimens of intact rock, with and without obvious planes of weakness such as laminations, intrusion contacts, etc.

The knowledge gained from these investigations, as worthwhile as it is, still does not present the engineer with strength and deformational parameters which have been determined under conditions truly representative of those encountered in practice. Probably very seldom, if ever, do we find rock masses which are stressed such that two of the principal stresses are equal, although such is the manner in which the usual triaxial test is conducted. Also, in real situations, the changes in magnitude and direction of the principal stresses (or stress path)

from the natural conditions to the construction conditions probably never coincide with those of the triaxial test.

Consider, for example, the stress state in a rock mass far underground which is penetrated by a bore hole or shaft. Due to geologic disturbances, the lateral stresses (perpendicular to the vertical) are most likely different from the vertical stress and, in addition, there may be a continuous variation of lateral stress for different directions within the lateral plane. Due to the anisotropic nature of the rock, the deformational behavior will be different for the different directions. As the opening progresses towards a given point within the mass, the body stresses will change and the changes will be dependent upon the magnitude of the initial stresses as well as on the deformational interrelationships. The strength (or stability) of the system would be most appropriately represented by strength parameters determined by tests in which the stress states and changes in stress states approximate those expected in-situ.

The determination of the parameters is far from being easily accomplished. The knowledge of the particular initial stress states cannot be determined with any degree of certainty except by first disturbing the existing stress state and, by appropriate techniques, calculating the probable initial stress state. The analysis and the test techniques involved are beyond the scope of this paper; however, it should be recognized that considerable chance for error is possible.

Having arrived at a judicial estimate of the initial stresses, one could then set up a test program to evaluate the deformational and strength parameters on the basis of assumed stress changes. This would

involve tests in which the individual control of stresses in three orthogonal directions was possible. With this information and by the use of an appropriate mathematical analysis, the stability of the proposed structure could be determined and, if necessary, modifications to the design could be proposed.

It is readily apparent that the process just described is basically interrelated, with all calculations dependent upon certain assumptions regarding the behavior of the material under certain stress conditions. As a starting point, the generalized behavior of rock and rock-like materials must be determined under conditions which approach those in service. In order to accomplish this, it is necessary to develop equipment and testing techniques which can subject appropriate specimens to controlled, three-dimensional loading and to then determine appropriate representations of the strength parameters.

CHAPTER II

STRENGTH AND RUPTURE OF MATERIALS

Strength

There is no unique "strength" of materials unless what is indicated is the basic attraction of the individual atoms one to another. In the usual connotation, "strength" has to do with the resistance of a mass of the material to a force. The resistance to the force may be that which is available to prevent rupture or it may be that available to prevent "yield" or a certain amount of deformation. Regardless of which "resistance" is under consideration, the value in stress units is a function of the specimen size and shape as well as of the test procedure, the environment and the inherent characteristics of the material.

To further complicate the situation, many materials fail or rupture in a brittle manner while others behave plastically and still others exhibit a partially ductile behavior. Brittle behavior is evidenced by sudden fracture at small strains whereas plastic behavior consists of the absence of well-defined fracture planes together with large strains. The "failure" of either brittle or plastic materials is relatively easy to define and to determine experimentally. The "combination behavior" materials comprise a relatively large proportion of rocks and, consequently, bring into prominence the question of a suitable failure criterion. In addition, many of the naturally "brittle" materials exhibit a change in deformational characteristics with

increasing confining stress, passing through a "partially ductile" stage and finally becoming a "plastic" or ductile material.

The determination of *the* "failure" stress for a given specimen, then, depends upon its load-deformational characteristics, i.e., its stress-strain curve. In brittle failure, the maximum stress either coincides with the fracture, or occurs very quickly thereafter. With brittle fracture, the originally coherent mass is separated into a minimum of two and often into many distinct portions. On the other hand, a truly plastic or ductile failure is indicated by the attainment of a yield stress which then remains practically constant as the specimen continues to yield or flow without fracturing. Upon removal of the stresses, the plastic material will retain its coherence but maintain the dimensional changes which occurred. The partially ductile material will normally have a unique stress-strain curve which, after being initially straight (or practically straight) will exhibit a continuously varying slope, finally becoming essentially horizontal.

Generally, there are three methods in widespread acceptance for the determination of a "failure" stress of the partially ductile materials. One method utilizes the intersection of the extension of the straight line portions as the failure stress. The "offset" method consists of constructing a parallel to the initial straight line portion of the stress-strain curve, "offset" from the origin along the strain axis by some definite strain increment. The third method designates the failure stress as that stress corresponding to the point on the stress-strain curve where the rate of change of the slope becomes a minimum and the slope remains constant thereafter, i.e., the beginning of the final

straight-line segment. Figure 1 illustrates the three methods.

The Phenomenon of Rupture or Fracture

Rupture, or fracture, with reference to rock failure, may be defined as the separation of the mass into two or more distinct portions. It will be shown that on this basis, rupture or fracture may occur without collapse of the specimen, that is, at applied loads which are less than the maximum which a specimen can sustain.

Terzaghi (1) classified the failure of rock under compressive loads according to the inclination of the failure planes as splitting, shear or pseudo-shear. In a splitting failure, cracks form parallel to the direction of the major load and usually the cracks are intergranular. This obviously is primarily a tensile failure phenomenon wherein the tensile stresses are caused by end effects and a wedging action by the grains. Generally, such failures occur in the higher-strength, more rigid rocks. Shear failures are manifested in the translation of grains along some well-defined shear plane which may pass through or around individual grains. The pseudo-shear failure is a combination shear and tension fracture.

Of these three failure modes, the shear phenomenon is of primary interest since most rocks fail in such a manner. In brittle failures where shear planes are usually well developed, the surfaces of the shear planes are ordinarily covered with very fine granular particles of the fractured rock. This indicates either actual fracture of the individual crystals or the grinding of whole grains which have been torn from the matrix. In conjunction with the powdered substance there are usually

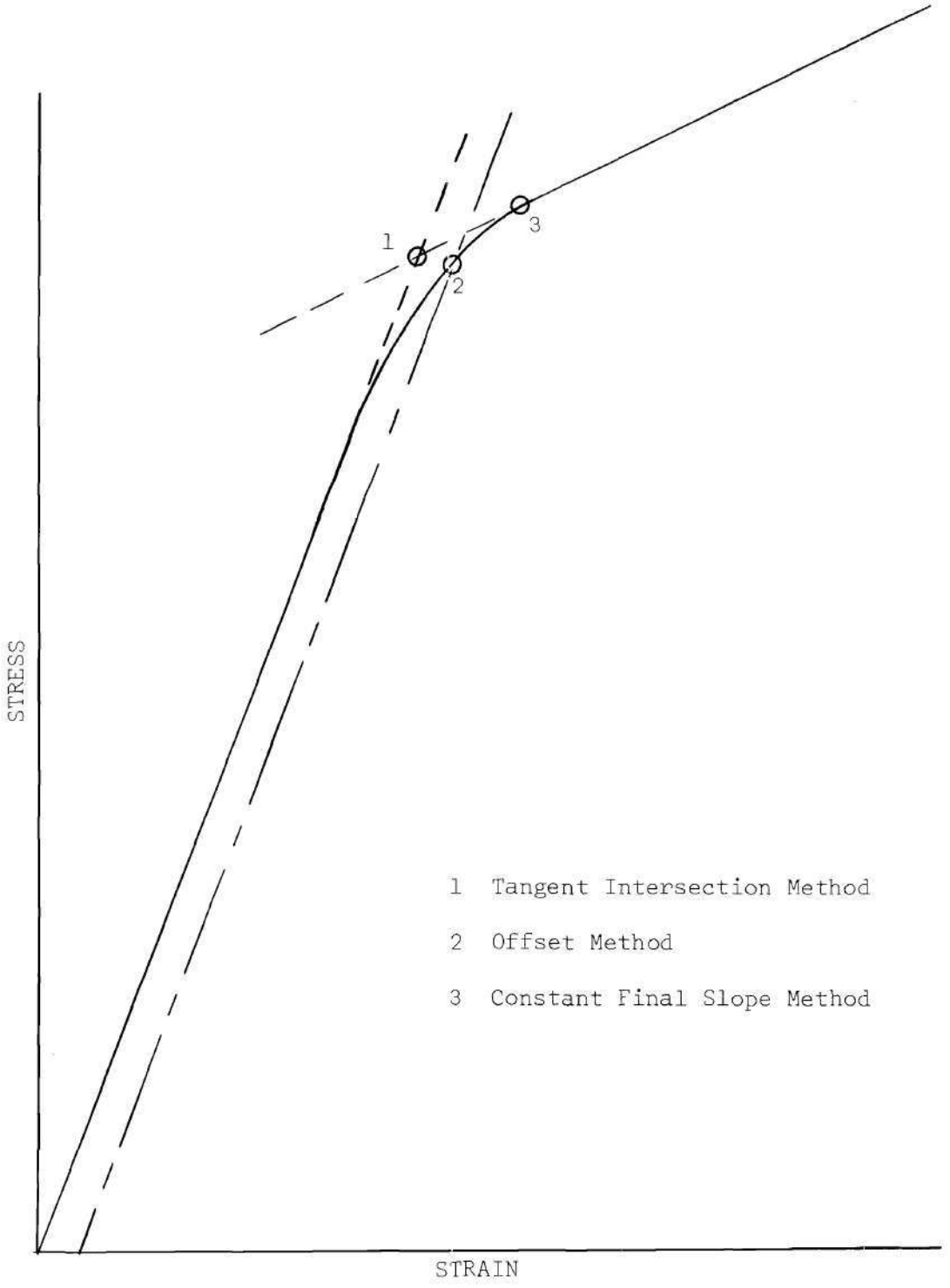

Figure 1. Methods for Determination of Failure Stress

freshly fractured grain faces. The granulation, or powdering, may be the result of movement along the shear plane occurring *after* the rupture and, therefore, may properly be assigned to testing techniques or equipment. Rather high energy is necessary to break the specimens and a corresponding amount of energy is stored in the testing machine in the form of recoverable elastic strain. Immediately after rupture of the specimen, the recoverable strain causes a definite amount of relative movement between the sheared portions with the probable consequence of granulation. Thus, when discussing a fracture mechanism, it may be misleading to consider the powdering as a part of the basic phenomena.

Ductile failure occurs in many rocks at low confinement and for many "normally brittle" materials at high confinement. There is considerable evidence indicating that all polycrystalline rocks will become ductile at sufficiently high confining pressures. For individual crystals, such may not be the case. For example, Bridgeman (2) reports the inability to cause platic flow in quartz crystals even when exposed to confining pressures of 18,000 Kg./sq.cm.

Another type of "rupture" has been observed under certain stress conditions. This is in the nature of a "scaling-off" of the inner surface of hollow cylinders, apparently in the form of small flakes or grains. The flaking can continue until it produces large eroded cavities. This action has been noted and recorded by Bridgeman (2) and Adams (3) in their experiments concerned with the failure of cavities in crystals and rocks under pressure. (The same phenomenon has been noted in this investigation.) In both cases, the specimens being tested were hollow cylinders subjected to stress systems so that there was little

or no restriction to such flaking action. The flaking occurs from a minor principal plane when the ratio of the intermediate principal stress to the major principal stress is "high" and the stress levels are of sufficient magnitude.

Failure by rupture is usually a sudden phenomena occurring at the maximum stress level for the specimen and, in addition, the strains at which rupture takes place will generally be rather small, on the order of 1 or 2 per cent.

Failure Theories and Graphical Representations of Strength

Many theories of failure have been advanced over the years in attempts to predict the strength of materials in general. Some have proved to be of considerable value in certain cases only, while others have been shown to be practically worthless. With respect to the characterization of strength of a wide range of materials, only a few have merit. Also, considering the possibility that all materials will yield plastically under sufficiently high confinement, it appears that there is *no* theory which can adequately predict the failure characteristics of materials in general. In fact, it is misleading to describe these as "theories of failure" since, in all cases, it is necessary to make physical tests to determine significant parameters for a given material. Instead, the terminology "failure criterion" is more appropriate.

The more widely utilized failure theories or criteria have been discussed by many authors in papers and books. These include Nadai (4)

and (5), Silverman (6) among others and consequently a detailed discussion of all will not be repeated here. Instead, those of prime interest and apparent usefulness will be discussed.

Mohr's Failure Criterion

Mohr's failure criterion is an extension of the "Maximum-Shear Theory." The maximum-shear theory indicates failure to be incipient when the shearing stress acting on any plane reaches a value equal to one-half of the unconfined compressive strength. Thus, there is neglected any influence of the normal stress acting on the shear plane, which is contrary to experimental results. Mohr extended this criterion to include the influence of the normal stress and included the maximum-shear theory value as a special case.

The stress system for any loading, including that of failure, is represented by a circle in a shearing stress--normal stress plot where an orthogonal coordinate system is utilized. For the τ (shearing stress) and σ (principal normal stress) axes, a series of limiting stress circles, experimentally determined, can be constructed and a failure envelope drawn tangent to the circles. Admissible combinations of shear and normal stress values must lie below the envelope which is represented mathematically by the relation $\tau = f(\sigma)$. The intermediate principal stress is considered to have no influence on the strength since the normal stress on the failure plane as well as the failure plane itself are assumed to be perpendicular to the direction of the intermediate principal stress.

The Mohr-Coulomb criterion has been extended to include presentation in a three-dimensional plot. The representation is included in

a later section of this work.

Representations of Failure Surfaces in Principal Stress Coordinates

There is increasing dependence upon the graphical representation of octahedral stresses in order to depict failure criterion. By utilizing a "three stress" coordinate system, the various failure criteria can be compared with experimental data and with each other. A complete discussion of the development of the failure surfaces is contained in the appendix and only the main points will be given here. As shown in the appendix, the failure envelopes appear as curves which indicate the intersection of the envelopes with an Octahedral plane.[1] Figure 2 shows the general relationships between the failure criteria which are normally utilized in soil and rock mechanics work. These include the Mohr-Coulomb, the von Mises (constant Octahedral Shear) and the Tresca (maximum shear).

These curves are symmetrical with respect to the three principal stresses and it is therefore sufficient to investigate only a 60° segment of the space. Point "A" in Figure 2 indicates the value of the octahedral shearing stress at failure (τ_o) as obtained in a "standard" triaxial test where $\sigma_1 > \sigma_2 = \sigma_3$. Point "B" is the corresponding value for a test performed such that $\sigma_1 = \sigma_2 > \sigma_3$. Values of τ_o for other cases ($\sigma_1 > \sigma_2 > \sigma_3$) fall between points A and B. The Mohr criterion assumes no influence of the intermediate principal stress and consequently produces a straight-line relation between A and B.

The abrupt discontinuities in the Mohr and the Tresca curves are

---

[1] An Octahedral plane is one of eight planes so inclined that their normals have direction cosines of $1/\sqrt{3}$ with the principal stress.

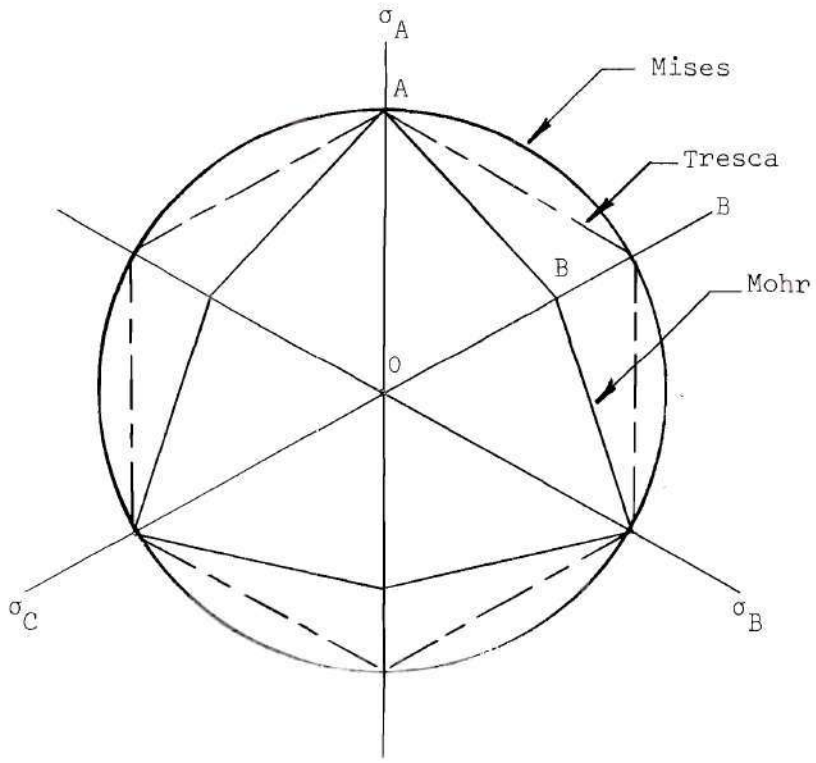

Figure 2. Octahedral Representation of Strength Criteria

points of some contention. It is generally believed that a more reasonable curve would not have such discontinuities; however, this belief has no scientific basis but is primarily due to observation of phenomenological action where calculations normally produce regular, smooth curves.

CHAPTER III

PURPOSE OF THE RESEARCH

The purpose of this study is to initiate investigation of the effect of the intermediate principal stress on the strength of rock.

At the present time, the equipment normally used for strength testing of rock is capable of producing only two basic stress states with respect to the relative value of the intermediate principal stress. In addition, there is doubt as to the validity of the results obtained from "extension" tests since the equipment may retard the formation of spalling failure. This means that basic equipment must be designed in order to perform the investigation.

The specimen shape will depend upon the system chosen for the application of stresses. If other than cubical or solid cylindrical specimens are necessary, the production of the specimen itself will be a major factor in the realiability of the results, consequently, considerable time and effort may be necessary in this respect.

The determination of the effect of the intermediate principal stress will involve an analysis of the data in terms of the usual two-dimensional representations as well as in terms of other representations such as the octahedral stress relationships.

It is recognized that an exhaustive study of the main topic, "the effect of the intermediate principal stress on the strength of rock," is beyond the scope of any single research effort such as this;

however, it is believed that after the development of suitable equipment and testing techniques, basic trends can be determined with respect to the importance of the intermediate principal stress. Such results could then serve as a guide to future studies which may furnish truly general relationships.

In view of the preceding discussion, the author proposed to accomplish the following:

1. To select a system for the study of the effect of the intermediate principal stress on rock strength.

2. To develop equipment and techniques for the production and testing of suitable specimens, and

3. To determine the effect on strength of the intermediate principal stress and to compare the results with certain failure criteria.

CHAPTER IV

EVALUATING STRENGTH IN THREE-DIMENSIONAL LOADING

Several basic methods are available for the application of controlled, triaxial stresses to rock specimens. Included, as being most appropriate for the present purposes, are the following:

1. Cubical or orthorhombic specimen with forces applied independently to the plane faces.

2. Solid cylinders under combined axial load, lateral fluid pressure and torsion.

3. Hollow cylinders under various combinations of external fluid pressure, internal fluid pressure, axial load and torsion.

The choice of a method for the investigation of the effect of the intermediate principal stress on strength depends to a large extent upon the material under investigation. As an example, the failure of metals can be studied quite satisfactorily by the use of hollow tubes subjected to almost unlimited combinations of axial load, internal and external fluid pressure and torsion. This is so because metal has reasonably high tensile strength and is impervious to the penetration of the fluid through the cylinder wall. With rock materials which, in general, must be tested under compressive stresses in order to be comparable to stress systems in real masses, and which also must be effectively jacketed from the confining fluids, the problem is much more complex. Each of the three cases listed as being possible choices of test systems will now be

discussed with respect to rock testing.

Cubical or Orthorhombic Specimens

Cubical specimens have been utilized for many years as standard shapes for compressive strength specimens; however, in this application, the stresses have been primarily uniaxial. Even so, serious problems arise with respect to lateral restraint effects between the loaded surface and the loading platens. In addition, care must be exercised in order to assure uniform stress distribution. This ordinarily is accomplished by producing relatively smooth specimen faces and providing a ball-and-socket type of loading head.

In uniaxial tests the consequences of the preceding considerations are of import, but when extended to the case of biaxial loading, the problems become much more complicated, and, for triaxial loading, the testing apparatus becomes more complex. In addition to the increasing complexity of the apparatus, the knowledge of the state of stress produced in the specimen becomes greatly diminished. An apparatus has been used at least in one case, in studies of rock strength, which would load on four faces of a cube; however, no records are available with respect to the testing on six faces of rock cubes.

Kjellman (7) developed equipment which permitted independent control of the three principal stresses on a cubical specimen of soil and had a maximum load capacity in each direction of 500 kg. and would not be suitable for rock. The equipment was exceedingly complex and bulky. In order to increase the load capacity of such a device to such a level as to be of value in rock testing, the size would probably be

prohibitive. In addition, it is hardly conceivable that the necessary high normal forces could be applied without the development of correspondingly high shearing stresses. Due to the difficulty of evaluating the magnitude of the shearing stresses, an accurate analysis of the failure stresses would be almost impossible.

In several investigations of the plane-strain behavior of soils (8, 9, 10), equipment has been devised which utilizes an orthorhombic specimen with two of the dimensions considerably greater than the third. This type of apparatus generally subjects the specimen to fluid pressure in addition to axial loads on the "small area" faces. In addition, then, to the problems associated with the cubical specimen apparatus, the jacketing of specimens of this shape becomes a major problem when concerned with high confining pressures. The production of specimens of this shape would entail rather large, precision diamond saws and considerable time would probably be involved in the cutting of each specimen. Each surface would then have to be precision ground in order to insure the proper distribution of the loads. If one assumes that the applied normal stresses are principal stresses, i.e., there is zero friction on these faces, then the internal stress state is quite simple.

Solid Cylinders

With the usual "triaxial" test chambers, it is not possible to perform truly "controlled triaxial stress" tests since two of the applied principal stresses are equal regardless of the manner in which the test is performed. In fact, the two possible failure stress states, one where $\sigma_1 > \sigma_2 = \sigma_3$ and the other where $\sigma_1 = \sigma_2 > \sigma_3$, are possibly

not comparable due to the stress histories of the specimens being different prior to the occurrence of failure, in that, in one case, the two equal valued stresses are maintained at the hydrostatic stress value while the major principal stress is increased and, in the second case, the minor principal stress is decreased from the hydrostatic value.

In order to accomplish a degree of control over the intermediate principal stress, torsional loads can be applied to the specimen in conjunction with confining pressure and axial loads. A decided disadvantage of this stress system is the non-homogeneous nature of the stresses as well as the variation of the torsional stresses from a value of zero at the axial center of the specimen to a maximum at the outer surface. Complications also arise in the knowledge of the stress system due to the necessary stress concentrations caused by the torsion applying mechanism. The application of torsional loads was used by Böker (11) in tests on marble and was accomplished by machining hexagonal ends on the specimens which fit into sockets and one end rotated relative to the other. Obviously, there is much time and expense involved in the preparation of such specimens and the jacketing of the specimens is also a major job. The accurate measurement of the torsional moment is a difficult operation when coupled with high confining fluid pressures. In past investigations on concrete, hollow cylinder specimens (12), a heavy "brake band" arrangement was used. Solid plugs, cemented to the specimen have also been used. This arrangement is probably more suitable since the twist could then be applied by rotation of the axial force piston.

Hollow Cylinders

Closed-end hollow cylinders, when subjected to different internal and external fluid pressure, are stressed so that the tangential (circumferential) stresses and the radial stresses are, in general, different. The value of each stress varies throughout the wall thickness of the specimen and these stresses are the principal stresses. If the cylinder is additionally loaded in the axial direction and the assumption is made that there are no shearing stresses on the ends, then the three principal stresses will act in the axial, the circumferential and the radial directions.

With respect to a given set of loading conditions, the stresses will be functions of the internal and the external diameters and of the radial distance from the inner wall. In general, the thinner the wall, the more uniform will be the stress across the wall for the circumferential stress; however, when the external and the internal fluid pressures are at different values, the radial stress varies from a value of one fluid pressure to a value equal to the other. This occurs from the inner face, where the radial pressure equals the internal fluid pressure to the outer face, where the radial pressure equals the external fluid pressure. Necessarily, then, for a given fluid pressure differential, the thinner the specimen wall, the greater the stress gradient will be.

In the case where the internal and the external fluid pressures are equal, the radial and the circumferential stresses are uniform, equal to the other as well as being equal in value to the fluid pressure. This produces a state of stress in a hollow cylinder which is comparable to that in a solid cylinder subjected to a confining fluid pressure.

Torsional loads may also be placed on the specimens. The stress effects from such loading are, in general, the same as with the solid specimens except that some of the non-uniformity of torsional stresses will be eliminated. The "brake band" arrangement for application of torsion would not be practical in cases where external confining pressures are used. External confinement could, of course, be omitted, and various combinations of internal pressure, axial load and torsion be applied; however, the range of stress variations would be limited due to the low tensile strength of the rock.

If one attempts to use hollow cylinders in an investigation of rock strength, there are several problems of considerable importance which must be solved. One is that of specimen production. In order to produce stresses of sufficient magnitude, the cylinder walls should be relatively thin. In addition, the wall thickness should be uniform around the circumference (i.e., a right circular cylinder) and there should be no variation along the length. In order to produce reasonably uniform stress conditions, the mineral grain or crystal size of the rock should not be too large with respect to cylinder wall thickness. A reasonable minimum wall thickness might be about two times the nominal maximum crystal diameter; however, smaller ratios between thickness and crystal diameter may be feasible.

Due to the brittle nature of rock, the preparation of hollow cylinders according to the preceding criteria will demand quality equipment, skill and considerable care.

The jacketing material used with the specimens is critical. The membranes should be inexpensive, easily prepared and easy to apply

as well as to be impervious to the confining fluid at high pressures. Additionally, the membranes should have relatively small effects on the specimen behavior, both with respect to stress distribution, and with respect to deformation. Previously, for solid specimens subjected to pressures on the order of 15,000 psi, membranes have been made of rubber and vinyl as well as of thin metal foil. Metal foil liners for thin-walled rock specimens under such pressures and meeting the preceding requirements do not seem realistic.

The technique of sealing the internal membrane while applying high fluid pressures is a major obstacle. The seals must be positive and should allow even fluid pressure over the entire surface of the specimen. In order to allow variation in specimen length, the system should also be completely flexible in this respect.

CHAPTER V

REVIEW OF LITERATURE

Prior Tests

At the present time, very little effort has been directed to the determination of the effect of the intermediate principal stress on the strength of rock and rock-like materials. Most of the experimental work has been performed with conventional high pressure triaxial equipment and solid specimens. Many investigations have produced results which might properly be used together with results from other research on this problem; however, included here are only those (except Von Karman's work) which reported comparative data.

In 1900, A. Foppl (13) reported results of tests on cubic specimens of rock. The cubes were loaded in compression to failure in a special apparatus upon either two or four sides. The conclusion drawn by Foppl was that the intermediate principal stress had no influence on the breaking strength.

Based on the techniques of lateral confinement and specimen jacketing developed by T. von Karman (14) several investigators performed tests on rock materials. With the solid specimens used in these series of tests, only the two aforementioned general states of stress (with respect to the relative value of σ_2) can be attained.

Karman's work included the testing of marble and sandstone by holding the confining pressure constant and increasing the axial load

to failure. This corresponds to the case of $\sigma_1 > \sigma_2 = \sigma_3$ and could, therefore, be used as a basis of comparison for later work where the intermediate principal stress was varied.

In 1915, R. Böker (11) performed a series of tests on marble in an apparatus similar to Karman's in which he first produced a state of hydrostatic stress within the solid cylindrical specimens. By then holding the lateral pressure constant and decreasing the axial pressure, Böker caused the specimens to deform plastically and to neck-down in the central portion. This is commonly called an "extension test" as opposed to a "compression test" in which the lateral pressure is maintained constant and the axial pressure increased. In the "extension test," the stress state is such that $\sigma_3 < \sigma_1 = \sigma_2$. Compared to Karman's results, the "extension tests" by Böker indicated a "Mohr Envelope" which lay above that of the compression tests. Böker apparently did not make any correction for changes in cross-sectional area.

Later Böker performed a series of tests on solid marble cylinders in which the specimens were subjected to the combined effects of lateral fluid pressure, axial load and torsion. All of the specimens were jacketed with a very thin metal foil in order to prevent penetration of the confining fluid into the rock pores.

In these tests, Böker primarily demonstrated the ability to vary the failure plane from a normal 45-degree helix under torsion only, to other angles dependent upon the particular stress state. The results of this series have not been utilized to determine the effect on the strength of varying the intermediate principal stress; however, it is believed that calculations based on such a complicated application of

stresses would be subject to considerable criticism.

In 1912, F. D. Adams (3) reported on a series of tests wherein the viscous flow of rocks under conditions approximating those at great depths below the ground surface was studied. The purpose of his work was to investigate the stability of open cavities and to determine the depths below ground at which open cavities could probably exist. Cylinders of rock were prepared with two holes drilled through each. One hole passed through the vertical axis of the column from top to bottom. The other passed transversely through the middle of the column, at right angles to the other hole but a little to one side of it, so that the holes did not intersect.

The rock columns were encased in a thick-walled tube, shrunk-fitted onto the rock. Hardened steel pistons extended into the tube, bearing against the rock column ends. Loads were then applied to the pistons and held constant for various time increments, from 70 seconds up to 2-1/2 months. After the desired time period, the specimens were carefully removed from the tubes and examined for residual deformation and/or collapse. A series of tests were made similarly but with the test temperature elevated to 450° Centigrade. The results of the tests showed that the confinement afforded by the steel tubing caused the rock columns to withstand between 160,000 psi and 200,000 psi axial load before failure. This compares with an average unconfined cube strength of about 27,000 psi. In addition, the "failure" occurred not by a shearing phenomena, but by flaking of very small fragments from the inner walls. The flaking occurred over a range of pressures and at the highest pressures utilized, completely filled the original holes. Oddly

enough, no attempt was made to calculate the stresses which caused the flaking, however, it has been generally conceded that the effects of the shrunk-on steel jackets were sufficient to cloud the results.

In 1918, Bridgeman (2) repeated the experiments of Adams under conditions such that the stresses could be "precisely specified." Rock cylinders containing cavities were jacketed and submerged in a liquid and subjected to high hydrostatic pressure. Both individual, mineral crystals as well as rocks were tested. According to Bridgeman, the outside surfaces of the cylinders were polished and not quite circular. Also, the inner holes were not exactly coaxial with the outer surface and were almost but not quite round. Soft rubber tubing was used for membranes. Changes in internal diametral distances were measured by the use of a close-fitting solder disc placed in the inner hole which deformed permanently during the test. A total of ten specimens were tested including both individual crystals and rock.

Generally, the results indicated lower "collapse" pressures than as reported by Adams but the "failures" were of the same type, i.e., flaking of the inner surface. There was apparently no permanent change of outside dimensions under external confining pressures up to 12,000 kg per sq. cm. A significant conclusion with regard to the flaking-off was that it had no particular connection with structure since, for the rocks, there was no tendency for the flakes to be composed of a single mineral composition. The sand-sized particles formed by the flaking were most irregular in shape and of a "great range" in size. Bridgeman concluded that the phenomenon of rupture by flaking-off is independent of other phenomena accompanying high stress such as cracks or flow.

A "rock-like" material, concrete, was used in a series of biaxial and triaxial tests in 1928 by Richart, Brandtzaeg and Brown (15). The stress states included both "compression" and "tension" tests and, in this case, the results indicated just the opposite effect from that found by earlier experimenters. The Mohr envelope for the "compression" tests fell well above the corresponding curve for the "tension" tests. It was noted by the authors that the differences were within the limits of experimental error and the conclusion was reached that the results were inconclusive regarding the validity of the Mohr criterion. It should be realized, however, that the man-made material, concrete, has not been subjected to the tremendous pressures and temperatures as has the natural rocks and, as a consequence, the behavior of the concrete under stress should not be expected to be completely compatible with the behavior of the rock with its residual internal stresses.

Ros and Eichinger (16) experimented with marble specimens under "compression" and "tension" states of stress and repeated Karman and Böker's tests. These results were comparable to the earlier test results and, in fact, the discrepancies were increased from about 10 per cent to about 25 per cent when the stresses were based on a corrected cross-sectional area rather than on the original area. In general, however, Ros and Eichinger concluded that the Mohr failure criterion was the most satisfactory general theory for non-metals.

In 1937, W. Schmidt (17) presented results of some tests on rock salt. According to Topping (18), all tests (except one "tension" test) were of the "compression" type, and the shear stress corresponding to the "tension" test falls well above the Mohr "compression" failure

envelope.

Several investigations have been made of the strength of concrete under various combinations of applied stresses other than by means of the "standard" triaxial test equipment.

Bresler and Pister (12), 1955, reported the results of tests on hollow concrete specimens under combined axial compression and torsion. They indicated a linear relationship between octahedral shearing stress and octahedral normal stress at failure.

In 1951, A. M. Freudenthal (19), tested solid concrete specimens 4 inches by 10 inches into which "notches" had been formed. Under axial compressive loads, the 0.5-inch deep, circumferential hyperbolic notches caused nonhomogeneous stresses. The results were analyzed on an elastic basis and an "effective stress" failure criterion was assumed. The "effective stress" was defined as being equal to $3I_2$, where:

$$I_2 = 1/6[(\sigma_1 - \sigma_2)^2 + (\sigma_2 - \sigma_3)^2 + (\sigma_3 - \sigma_1)^2] .$$

Robertson (20) reported in 1955, the results of a few hollow cylinder tests on rock subjected to hydrostatic pressures. He used specimens of several limestones, marbles and granites. The diameters of the specimens varied from 3/16-inch to 1 1/4-inch, with most being 5/8-inch O.D. The inside diameter was varied. Failure occurred by either spalling internally or by a shear fracture. Those specimens with radius ratios less than 3 failed in shear while those with radius ratios greater than 3 failed by spalling. The results were presented in the form of curves of the pressure at failure versus the ratio of

radii. The 1 1/4-inch and the 5/8-inch cylinders had the same strengths while the 3/16-inch specimens were of higher strength. Robertson attributed the greater strength of the smaller cylinders to fewer gross inperfections. The typical "trap-door" type of failure occurred and even with the cylinders cut into at various angles to simulate planes of weakness, the same type of failure occurred.

McHenry and Karni (21), 1958 used hollow concrete cylinders and applied compressive axial loads, together with internal fluid pressure. This technique produced, in the cylinder wall, axial compression, variable radial compression and variable circumferential tension. The conclusions reached were that the tensile strength is reduced by an orthogonal compressive stress, and vice versa; that the Mohr failure criterion is not applicable in the range of stresses used; that an essentially linear relationship was found between the octahedral normal and the octahedral shearing stress at failure except for data near the conditions of simple compressive and simple tensile failure.

Bellamy (22) 1961, tested sand-cement mortar hollow cylinders under combined compressive axial load and external fluid pressure. He indicated that the effect of the intermediate principal stress was to increase the major principal stress by a minimum of 0.750_2.

Recently (1963-1966), a series of tests has been performed by Handin and Heard (23) in which they used very small hollow cylinders of Solenhofen Limestone exposed to combined internal pressure, external pressure, axial load and torsion. The specimens used were of the following size: (1) Outside radius = 0.635 cm; (2) Inside radius = 0.565 cm., and (3) Length effective during the test = 1.7 cm. (approx.).

The outer jacketing material was "thin," seamless, annealed copper. The inner "jacket" consisted of a hollowed-out solid copper rod with one end left closed and with a solid cap cemented to the drilled-out end. Fluid pressure was then introduced to the inside of the copper jacket.

Handin and Heard presented a plot of octahedral shear stress versus octahedral normal stress at failure for the results available at the present time. This curve, according to the authors, "seemed to lie between the triaxial compression and extension curves for this rock."

Summary of the Present State of Knowledge

There has been very little work done with respect to the effect of the intermediate principal stress on the strength of rock. In general, that work which imposed high stresses on the specimens was accomplished in some type of triaxial apparatus which utilized a fluid confining medium. In most cases, only confinement together with axial load was used. By such an arrangement, only two cases of stress states are possible and there is some doubt in the mind of this author that the two cases may properly be compared, due to the difference in the manner of arriving at the failure state. Some recent work has been done (and is still continuing) where high confining pressures, axial load and torsional loads were used. Results from these tests are, at present, inconclusive with respect to the effect of σ_2.

Adams and Bridgeman's works with the hollow cylinders were properly in the scope of effect of intermediate principal stress; however, they made no attempt to so analyze their results. The failure

mode, rupture by flaking-off, appears significant under conditions where two principal stresses are reasonably close to the same value and greater than the minor principal stress. Mathematically, such failures are not treated; however, an examination of possible failure planes indicates the feasibility of such occurrences.

Some low pressure work has been done utilizing rather large, hollow cylinder specimens of concrete under combined axial load, internal pressure or torsion. From this work, no definite conclusions have been reached.

The representation of the failure of the materials has largely been with the two-dimensional Mohr diagram, a comparison made between the results obtained from "compression" and "tension" tests. In some investigations, the envelope for the "compression" tests falls above that for the "tension" tests and vice versa. The relation between the octahedral shearing stress and the octahedral normal stress at failure has been used as a representation of the strength of rock and rock-like materials. There is reasonable agreement in that the slope of a graph of the octahedral shearing stress vs. the octahedral normal stress at failure is not constant and the variation appears to form an S-shaped curve.

In addition to the differences noted, there remains all of the problems associated with strength testing in general, such as determination of the failure point for various materials, and the validity of the elastic theory to determine stresses, as well as many others.

CHAPTER VI

THE TRIAXIAL SPECIMEN

Selection of Specimen Type

The general considerations with respect to specimen type were presented in Chapter III. On the basis of those factors, it was decided that the loading system for the direct application of force to cubes, or similar shapes, was not practical. With respect to the variety of stress paths afforded, the hollow cylinder specimen (to be subjected to individually controlled internal and external fluid pressures together with axial load) would offer more versatility than the solid specimen-torsional loading system. In addition, it is believed that the hollow cylinder test more closely approaches real conditions. Therefore, it was decided to use the hollow cylinder specimen.

Specimen Size

The maximum outside diameter was limited by the size of the existing high pressure chambers since the equipment being developed for this project was to be compatible with the existing equipment. This indicated an outer diameter on the order of 2 inches or less, and since membrane material (of the type contemplated) was available in an appropriate size to accommodate an inside diameter of 1.2 inches, and an outside diameter of 1.5 inches, these dimensions were tentatively specified. Due to difficulties in the production of such thin-walled specimens, the outer diameter was increased to 1.60 inches, making the wall

thickness 0.20 inches.

Since no information was available with regard to the appropriate length of a specimen such as this, it was decided to use a length about two times the outside diameter.

Specimen Production

Initial attempts to produce the specimens consisted of a double coring procedure in which the inside diameter was cored with a thin-walled diamond coring bit and then overcored. Reasonably uniform specimens were produced in this manner; however, the procedure was time consuming and, in anticipation of a large-scale testing program, other methods were deemed desirable. The solution to production of regular, uniform specimens was found to be a double-tube core bit which cut both the inner and the outer surfaces at the same time. The bit is of the impregnated diamond-type and was made to produce a hollow core 4 inches in length in order to allow for trim on each end.

It was found necessary to use a heavy-duty precision drill press in order to cut cores from Granite and from similar, hard drilling rock. Penetration rates of about 2 inches per minute are possible in granite when using a 3-hp, radial drill press at 700 rpm and with very poorly controlled drilling water. In order to reduce the possibility of bit damage, drilling was begun at 75 rpm until the bit was seated, after which time the vertical alignment was checked and the 700 rpm rate of revolution was utilized until the drilling was complete. It is necessary to maintain a constant bit pressure to produce a smooth-sided, straight specimen.

The cores were cut to the approximate final length of 3.2 inches with a diamond blade trim saw. The ends of the trimmed cores were then ground plane and perpendicular to the long axis by the use of a rotary carborundum wheel and a special holding jig mounted on a feed table. Since the testing equipment accepts varied specimen lengths, no attempt was made to produce a uniform length since this would require additional time in the grinding operations. The cores were allowed to air-dry for a period of at least one week prior to testing.

Description of the Rock Samples

Two rocks were utilized in this investigation. These were Indiana Limestone and Stone Mountain Granite. Descriptions of these two rocks follow.

Indiana Limestone

Indiana limestone is found in an area around Salem, Indiana. The rock is composed of linestone "sand" grains cemented together by the interlocking action of calcite crystals. The "sand" grains are the result of deposition of calcium carbonate on small, partially broken shells, often in a series of concentric layers. Due to their roughly-spherical shape resembling fish eggs, the grains have been designated "oolitic." Dark spots sprinkled throughout the rock, apparently of a bituminous nature, are organic residue of the original inhabitants of the shells.

The stone varies in color tone from buff (above the ground level) to a grayish or blue-gray shade below ground. The change in color apparently results from oxidation of some of the organic material.

The main constituent of the limestone is calcium carbonate which varies between 95.5 and 98.5 per cent. The magnesium carbonate content runs from 0.2 to 1 per cent. The structure is porous (15 per cent by volume) and quite uniform in all directions. Consequently, the stone is readily machined, working almost equally well in all directions. Generally, the strength parallel to the grain is almost as great as that perpendicular to the grain with an unconfined compressive strength varying from 4000 to about 12,000 psi, averaging around 6000 psi.

Stone Mountain Granite

Microscopically, the rock appears to be an even-textured, medium-grained, light gray, muscovite granite. In mass, there is observed practically no variation in color, texture or composition, although the rock is cut by pegmatitic veins which exhibit no definite directions. The veins are primarily quartz and feldspar with some inclusions of tourmaline, biotite, muscovite and garnet. In hand specimens, the individual mineral components are readily discernable by eye.

The following description of the granite, on a microscopic basis, is given by Watson (24):

> Microscopically, the rock is a medium-grained, allotriomorphic-granular granite, composed of an aggregate of complexly interlocking quartz and feldspar grains, with numerous grouped plates and shreds of muscovite, and some biotite. The quartz is of the usual granitic kind, irregular in outline, and displays evidence of some stress in wavy extinction and lines of fracture. The feldspar constituent consists of irregular, varying-sized crystals of orthoclase with microperthitic structure; microcline, the larger grains of which show some tendency to tabular habit; and scattered, lath-shaped individuals of polysynthetically twinned plagioclase. The orthoclase usually shows good cleavage, while the microcline exhibits, in a typical degree, the characteristic gridiron or grating structure. The plagioclase individuals give small extinction angles measured on the twinning-plane, in basal sections, which indicates a feldspar near oligoclase. The larger

feldspare individuals generally contain rounded drop-like inclusions of quartz and other feldspar species. Muscovite is the predominating accessory present. It occurs, for the most part, as grouped shreds, with good basal cleavage and strong double-refraction, and always appears perfectly fresh. Biotite is more sparingly present as single shreds and filaments, with marked basal cleavage, deep color and strong absorption, partially altered, in some cases, to a reddish-brown chlorite. The biotite shows a tendency to segregate into small bunches, in places. A part of the muscovite is of secondary origin, derived from feldspathic decomposition. Prismatic inclusions of apatite and zircon complete the list of minerals present in the rock.

CHAPTER VII

THE HOLLOW CYLINDER TRIAXIAL APPARATUS

Major Design Criteria

The major problems to be solved in the design of the hollow cylinder triaxial apparatus were:

1. The jacketing of the inner surface of the specimens against pressures up to 15,000 psi differential between the inside and the outside.

2. The utilization of inexpensive and relatively flexible membrane material.

3. The design of equipment which would accommodate specimens of widely different lengths.

4. The design of a simple apparatus, easily assembled and disassembled and relatively fool-proof with respect to malfunctions.

5. The equipment should necessitate relatively minor modifications to the existing high pressure triaxial cells and allow easy change-over from hollow cylinder apparatus to solid cylinder apparatus.

Membranes

Polyvinyl chloride (PVC) electrical sleeving was selected for membranes, inside and outside. This material is readily available in a wide range of sizes from very small diameter up to about 4 inches. It is stock material with many plastic supply houses as well as with electrical insulation suppliers. The quality of the finished product

may vary with respect to freedom from pin holes as well as variation in diameter. It has been found that a product of Suflex Corporation, Woodside, New York, Astra 105 Extruded Vinyl Insulation Tubing, is of good quality and can be used with confidence. The tubing is available in clear plastic as well as opaque. The cost of the PVC tubing is approximately 25 to 40 cents per foot, depending on the diameter required.

One disadvantage of the tubing is that the membrane wall is rather thick and stiff for lower pressure work. The stock thickness for 1-inch ID tubing is 0.035-inch and for the 1.5-inch ID, it is 0.04 inches.

Another minor disconcerting factor is that some of the plasticizer will be squeezed-out of the plastic under pressures of about 2000 psi or more. Although the amount of squeezed-out plasticizer is small, it can stain the specimens and give the appearance of confining fluid leakage.

Prior to the selection of the regular PVC as the membrane material, several other materials were investigated and some were given serious consideration. Among these were:

1. Liquid PVC compounds (plastisols) which cure rather quickly at temperatures of about 400° F. Closed-end, thick "balloons" were formed from this material and fluid was introduced through a tube in one end. The equipment used with this device had an adjustable end cap in order to compensate for differences in specimen length.

2. A family of "heat shrinkable" plastic and rubber materials. These include PVC, NT (Neoprene Tubing) and RNF (Modified polyolefin compound). These designations are those of Rayclad Tubes, Inc. The

molecules in these materials have been cross-linked by high-energy electron beam radiation, producing compounds possessing "elastic memory." The material is first extruded in the form of tubing, then irradiated, and finally expanded by a special process to twice its original diameter. When exposed to temperatures on the order of 400° F. for a few seconds, the radiation-induced elastic memory causes an instantaneous shrinkage to the original diameter. Lengthwise shrinkage is held to less than 10 per cent.

3. Room temperature vulcanizing (RTV) silicone rubber compounds. This group of synthetic rubbers is available in a wide variety of forms including potting, filling, encapsulating and impregnating materials. They are very heat stable, chemically inert and cure at temperatures ranging from 70° F. to 150° C. Several companies (including General Electric and Dow Corning) produce a wide variety of compounds made from this basic material.

The Triaxial Apparatus

The design of an apparatus which met the preceding requirements is shown in Figure 3. It consists basically of two end caps, or loading platens, internal and external jacketing membranes and end plungers for effecting a seal between the internal fluid and the inner surface of the specimen.

The two loading platens, here called a top cap and a bottom cap, have "ring" bearing surfaces of the same dimensions as the specimen. The top cap and the base are machined to obtain a fluid seal on the inside when an "O-ring" is forced downward (or upward as the case may

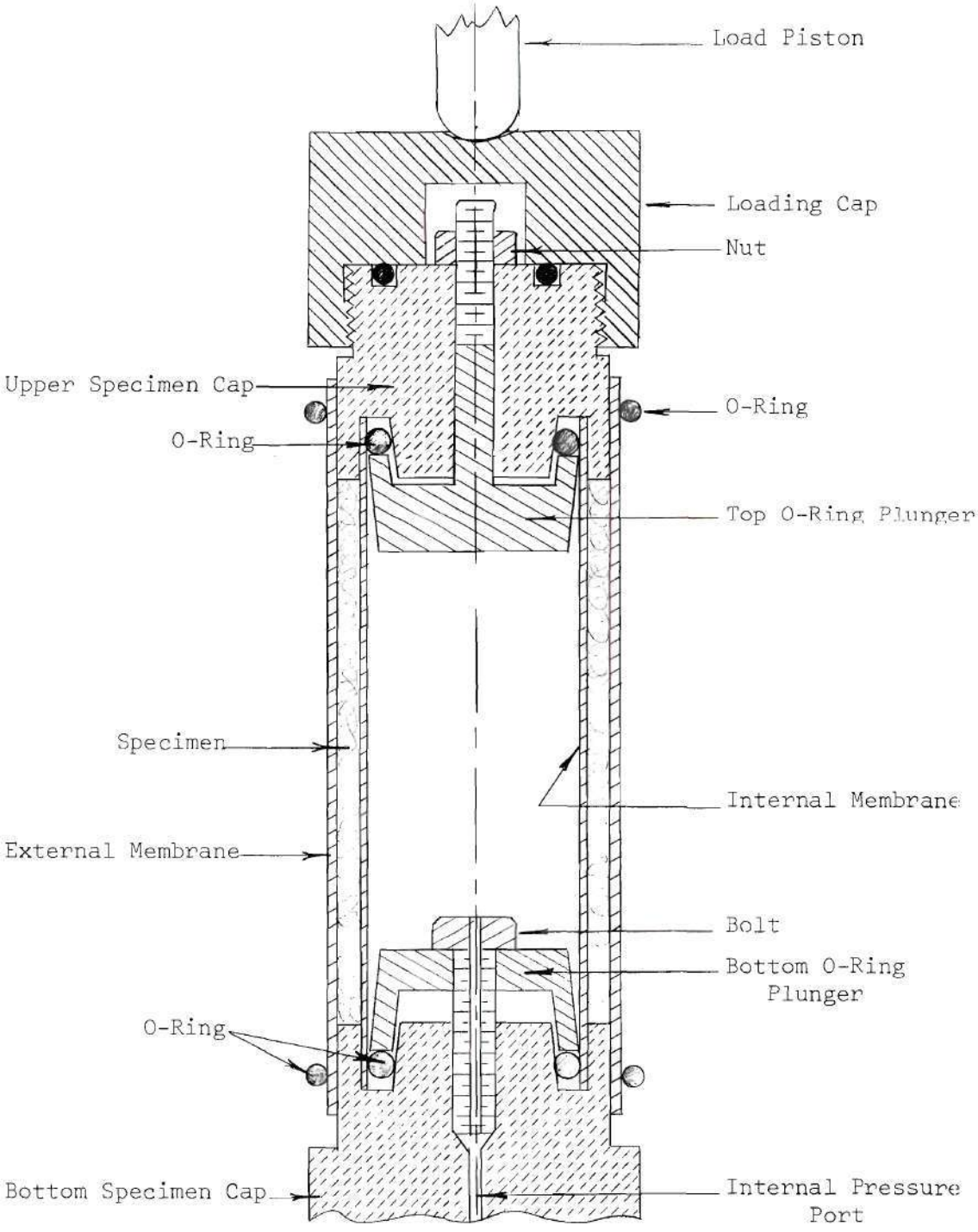

Figure 3. Hollow Cylinder Triaxial Apparatus

be) along an inclined surface which causes the O-ring to press the membrane against the inner surface of the "ring." The bottom O-ring is forced downward by the plunger as a bolt is tightened in threads in the base. The top O-ring is actuated by a plunger arrangement pulled against the top cap by a nut tightened on the plunger stem which extends through the top cap. In order to assure a positive seal between the inner and outer fluids, the top cap contains an O-ring which seats against the loading head. The outer membrane is sealed simply by the fluid pressure forcing it against the caps, although O-rings are used as safety devices to insure sealing at low external confinement.

The bottom cap or platen design is shown in detail in Figure 4. This member has been made to screw into the base of the triaxial cells. This is an interchangeable feature designed to make the cells more versatile with respect to the use of different size and shaped specimens since the same equipment is used for soils testing also. This arrangement includes a stem which fits into mating surfaces machined into the cell base. The bottom cap is held in position by threads which screw into the base. The cap seats (metal to metal) against the base and bears against an O'ring to insure no leakage between external and internal fluids. At the tip of the stem, a second, small diameter O-ring provides against air entrapment in the internal fluid space, and the "dished-in" portion of the stem further reduces air entrapment. This is of importance in testing when making pore pressure measurements since extraneous volume changes must be held to a minimum in such tests.

The internal fluid is introduced through a 1/8-inch bore in the bottom cap.

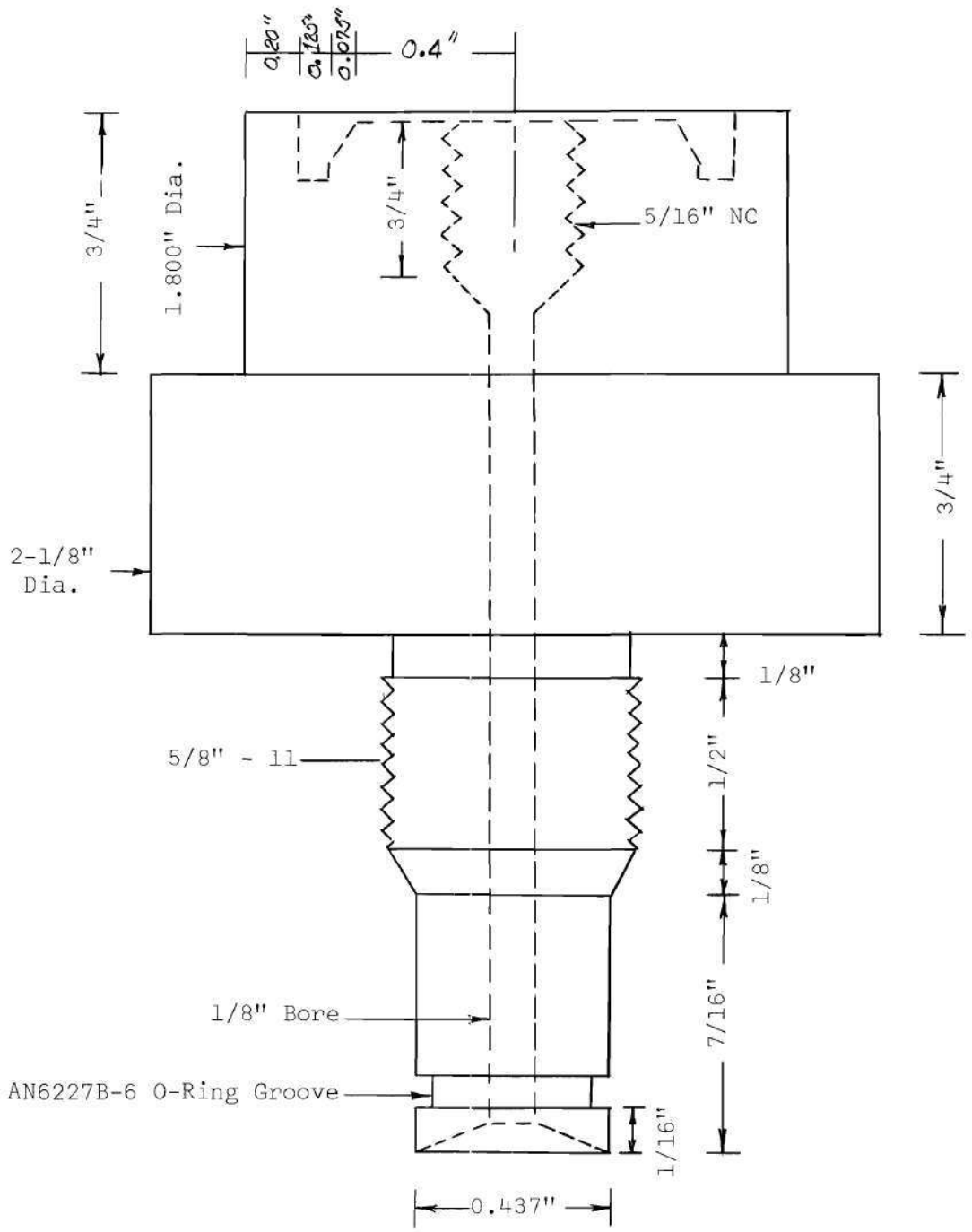

Figure 4. Hollow Cylinder Bottom Platen

The material for the caps is high-strength steel. Since the bearing surfaces between the specimen and the caps is only 0.88 square inches, very high stresses are generated during the testing. The strength of steel is affected much less by confinement than is rock, with the result that mild steel or a similar strength material will fail during the test.

Although not included in the present design, pore pressure measurement can be accomplished through a hole passing through the bottom cap from the specimen seat and extending to the cell base. This would necessitate a port within the cell base which could mate with that in the bottom cap.

Pressure Generating Systems

The confining pressure is controlled by one of several systems, dependent upon the manner in which the test is to be conducted.

One system consists of a high pressure hand pump with valved lines connected to the fluid inlet ports on the triaxial cell. Included in each line is a piston-cylinder arrangement where the pistons are positioned by a bolt reaction member. The adjustment of the bolt either forces the piston into the cylinder or allows it to move outward, thus causing the pressure in the line to increase or decrease, respectively. Since the pressure changes in either the external or the internal confining fluid will normally cause corresponding changes in the other confining pressure, it is necessary that both lines be completely and precisely controllable.

A second, rather convenient system consists of an air-operated, hydraulic pump which can be used to control a continuously increasing pressure. These pumps are essentially pressure intensifiers which are valved so that they are capable of re-cycling when the stroke limit is reached. The type being used utilizes low-pressure air (up to 100 psi) to generate outlet fluid pressures (under conditions of no flow) up to 15,000 psi. Higher pressure output pumps are available. The major disadvantage of the pumps is that they can "unload" only a negligible amount under downstream pressure build-up. This can be overcome by the use of either manually controlled piston-cylinder arrangements or self-relieving fluid pressure regulators.

The confining pressures are measured by the use of hydraulic gauges accurate to ± 0.5 per cent of full scale. The gauges are periodically recalibrated by checking against a precision, standard gauge which, itself, has been calibrated against a dead weight loading device.

CHAPTER VIII

TEST PROCEDURES

Preparation of Specimens

The previously cored, trimmed and ground rock specimens are either sprayed with a Teflon spray or rubbed with a powdered teflon in order to reduce friction between the membranes and the specimens, both during the jacketing operations as well as during the testing. Both of the two preparations have been found satisfactory, but the powdered material produces the smoother surface, probably due to a thicker layer of the Teflon deposited on the specimen.

Jacketing and Sealing

The steps involved in the placement of the specimen in the loading apparatus are as follows:

1. The inner membrane is trimmed to approximate length and inserted in the bottom cap with the bottom O-ring plunger and O-ring contained in the membrane about 1/2 inch from the membrane end.

2. The bottom O-ring plunger is forced downward by the bottom pull-down bolt and the bottom seal is effected.

3. The inner membrane is trimmed to exact length by placing the specimen in position with a metal spacer on the top surface and trimming with a sharp knife.

4. The "inner pressure" fluid line is then purged of air by pumping until hydraulic fluid partially fills the inner membrane.

5. The upper O-ring plunger and O-ring are placed in the top of the inner membrane and the trapped air removed by manipulating the plunger downward and allowing the air to bypass the plunger.

6. The specimen is placed in position on the bottom cap, the outer membrane slipped over the specimen, and the top cap fitted into place.

7. The top O-ring plunger is drawn into position, the loading cap screwed on and the installation is complete.

Deformation Measurement

Only axial deformations were measured during the testing, and for this purpose a linear variable differential transformer (LVDT) was used. The load-deformation curve was traced on a drum recorder, with the axial load indication being actuated by a push-rod arrangement from the testing machine load indication unit. Since a considerable amount of deformation occurs in the test equipment itself, the cell has been calibrated with no specimen between the end caps and this "correction" is applied to the recorded total deformation in order to determine the deformation of the specimen.

Triaxial Cell Preliminaries

With the specimen in position and jacketed, the cell cylinder is screwed to the base. Next, the top packing gland is screwed into the cylinder and the piston then installed in the packing gland and brought into contact with the loading cap. The cylinder is filled with hydraulic fluid and the air is purged through the port at the top of the cylinder. Prior to any pressurization operations, an "axial

seating load" of 200 pounds is placed on the piston in order to assure solid contact between the specimen and the end caps. This is a safety precaution to prevent the possibility of a membrane being squeezed between the specimen and the caps. An effective compressive force is then maintained between top cap and specimen throughout the pressurization and testing procedures, either by the external confining pressure or by axial load on the piston.

Test Modes

The testing procedure is quite similar to any other type of triaxial test with the exception that there are two fluid pressures to be kept in adjustment. In addition, considerable versatility is afforded with this equipment with respect to the direction of the principal stresses. That is, any one of the principal stresses may be applied in the axial, circumferential or radial direction.

Although the majority of the tests have been carried out so that the major principal stress was in the axial direction, the intermediate principal stress in the tangential direction and the minor in the radial, other conditions have been utilized. Also, the stress path to failure has been varied. The different test modes will be discussed individually.

1. Standard Triaxial Tests--The standard triaxial test (compression test) consists of applying a confining pressure to the specimen and then increasing the axial pressure to failure. In this test $\sigma_1 > \sigma_2 = \sigma_3$ throughout the test.

With this equipment, such tests are quite easy to perform since

the proper stress state can be produced by applying equal internal and external confining pressures, maintaining these constant and increasing the axial stress to failure. In this case, $\sigma_1 = \sigma_z$, the axial stress; $\sigma_2 = \sigma_3 = \sigma_\theta = \sigma_r$. ($\sigma_\theta$ = tangential stress; σ_r = radial stress). Although the principal stresses corresponding to this stress state can be induced in other directions, this is by far the easier test method, particularly since there is no continuous changing of pressures and axial loads. Also, the minor and the intermediate principal stresses have the same value as the confining fluid pressures. The most homogeneous stress state within this specimen is produced by this technique.

2. "Extension" Tests--The extension test ($\sigma_1 = \sigma_2 > \sigma_3$) can be conducted by holding σ_3 constant and increasing σ_1 and σ_2, or by holding $\sigma_1 = \sigma_2$ constant and decreasing σ_3. This type of test is most easily performed with this equipment by inducing hydrostatic compression equal to the desired value of $\sigma_1 = \sigma_2$, then maintaining the inner and the outer fluid pressures constant and reducing the axial load to failure. The present equipment is seriously limited in its capabilities for this stress state due to the high-strength characteristics of rock. For example, the relatively weak Indiana Limestone has failure values of about 12,000 psi for $\sigma_3 = 0$ (for σ_3 = constant and for σ_2 and σ_1 increased together to failure). The design capacity of the triaxial chamber is 10,000 psi which means that only a limited number of tests can be performed on a given rock in which the failure stresses are all compressive. Lower fluid confining pressures could induce failure if σ_3 is caused to become less than zero. This could be accomplished by cementing the specimen ends to the loading caps and allowing the

internal confining pressure to exert the necessary upward force.

3. Constant σ_2/σ_1 Tests--In this test, the specimen is subjected to a hydrostatic state of stress equal to the desired value of minor principal stress and subsequently failed by increasing the major and the intermediate principal stresses together in a pre-selected ratio. This is most easily accomplished by maintaining a constant internal pressure and increasing the external pressure, together with the axial load. In order to produce the required high failure stresses, it is usually necessary to make the axial stress the major principal stress.

With the weaker rocks, some tests are possible with the tangential stress as the major, and the axial stress, the intermediate.

4. Constant σ_2/σ_3 Tests--By increasing the external pressure over the internal pressure, the tangential stress (σ_2) is greater than the radial stress (σ_3). This state is maintained while the axial load is increased to failure.

5. Tensile Tests--Tensile stresses are induced in the tangential direction when the internal pressure is greater than the external pressure. In addition to the ability to place the specimen in pure tension, it is possible to evaluate the tensile strength under any combination of compressive stresses in the axial and the radial directions.

CHAPTER IX

RESULTS AND CONCLUSIONS

Strength Analysis

This investigation included testing of specimens under confining pressures of magnitudes such that the material would behave in a brittle manner. For this condition, the failure was in the form of a complete rupture or fracture occurring at the maximum stress level. Thus, the "strength" of the material utilized was the fracture or rupture strength in all cases.

Elastic Analysis of Stresses

The stresses at failure were calculated on the basis of the behavior of a homogeneous, isotropic and elastic material up to and including the time of failure. The stresses induced in the specimens under the three-directional loading are:*

$$\text{Radial Stress, } \sigma_r = \frac{a^2 b^2 (p_i - p_o)}{b^2 - a^2} \cdot \frac{1}{r^2} - \frac{a^2 p_i - b^2 p_o}{b^2 - a^2} \qquad (9.1)$$

$$\text{Tangential Stress, } \sigma_\theta = \frac{a^2 b^2 (p_i - p_o)}{b^2 - a^2} \cdot \frac{1}{r^2} + \frac{a^2 p_i - b^2 p_o}{b^2 - a^2} \qquad (9.2)$$

$$\text{Axial Stress, } \sigma_z = P/A \qquad (9.3)$$

---

*See Appendix for derivation of stress relations.

where: a = inside radius

b = outside radius

p_i = inside fluid pressure

p_o = outside fluid pressure

r = radial distance from cylinder axis to point considered

P = net axial force

A = original cross-sectional area under the axial load

The choice of an elastic analysis rather than another was based on the axial load, axial deformation characteristics, and the type of fracture which occurred. It was recognized that the materials do not, in fact, behave in a completely elastic manner up to fracture and, as a consequence, the assumption of elasticity is not strictly valid. However, the axial strains at which failure occurred were very low, on the order of 1 per cent or less, with the major portion of the strain being linear.

Stress Calculations

The stresses used in analyzing the results were calculated on two bases. One set of stresses are those which acted at the point where failure was considered most likely to occur. This point was where the largest stress difference was located and for these tests, it was at the inside surface of the cylinders. At this point, the principal stresses are determined from the following relations:

$$\sigma_1 = \sigma_z = P/A \tag{9.4}$$

$$\sigma_2 = \sigma_\theta = (4.571)p_o - (3.571)p_i \tag{9.5}$$

$$\sigma_3 = \sigma_r = p_i \tag{9.6}$$

Stresses calculated by these relations will be designated as "inside" stresses.

The second set of stresses were "average" stresses. These were calculated in the following manner:

1. σ_z--the average axial stress was taken as being equal to P/A.

2. σ_θ--the average tangential stress was taken as the "elastic" tangential stress acting close to the mid-point of the wall thickness. The stress at the mid-point is:

$$\sigma_\theta = (3.9650)\ p_o - (2.9650)\ p_i \tag{9.7}$$

For convenience, the expression was modified to:

$$\sigma_\theta = 4\ p_o - 3\ p_i \tag{9.8}$$

3. σ_r--the average radial stress was taken as being the numerical average of the "elastic" stresses acting at the inner surface and at the outer surface. This produces:

$$\sigma_r = (p_o - p_i)/2 \tag{9.9}$$

Octahedral Stresses

Octahedral stresses were calculated for both sets of principal stresses. The octahedral stress relations are:*

$$\sigma_o \text{ (Octahedral Normal Stress)} = \frac{1}{3}(\sigma_1 + \sigma_2 + \sigma_3) \qquad (9.10)$$

$$\tau_o \text{ (Octahedral Shear Stress)} = \qquad (9.11)$$

$$\frac{1}{3}[(\sigma_1 - \sigma_2)^2 + (\sigma_2 - \sigma_3)^2 + (\sigma_3 - \sigma_1)^2]^{\frac{1}{2}}$$

For comparison purposes, the octahedral stresses were normalized to the "unit plane," i.e., where $\sigma_o = 1.00$. This was accomplished by graphing the values of τ_o vs. σ_o for solid cylinders tested under various confining pressures such that $\sigma_2 = \sigma_3 =$ constant for a given test. The points were analyzed by the "method of least squares" and the resulting straight line was projected to intersect the σ_o axis and to determine a locus for the projection of the other octahedral shear stresses to the unit plane. The increment of stress ($\Delta \sigma_o$) from the point of intersection to the τ_o axis was used to adjust the octahedral normal stress, and the value of the normalized octahedral shear stresses then became:

$$\tau_o \text{ (On Unit Plane)} = \tau_o/(\sigma_o + \Delta \sigma_o) \qquad (9.12)$$

---

*See Appendix for derivations.

Discussion of Results

Strength of Hollow Cylinders vs. Solid Cylinders

It is well known that the "strength" of a material is dependent upon specimen size and shape, as well as on other factors. The "standard" shape of specimen for tests of rock strength (in the United States) is a solid cylinder and the ratio of height to diameter is commonly chosen as between 2 and 2-1/2. The actual diameter will vary, dependent upon the capabilities of the testing apparatus. Since the shape of the specimens utilized in this investigation are different from the "standard," it is of interest to compare strength results from the hollow cylinder tests with results from solid cylinder tests conducted under comparable stress states. One such state is for the condition of $\sigma_2 = \sigma_3 = \text{Constant}$, and with σ_1 increased to failure.

The results from several series of such tests on both Indiana Limestone and Stone Mountain Granite are presented in Figures 5 through 10.

Typical stress-strain curves for the Indiana Limestone for both the solid and the hollow cylinder tests are shown in Figure 5. The differences between these curves are minor in comparison to the usual differences obtained from tests on similarly shaped specimens. As an example of the variation in the rock itself, the strength results of several test series are listed in Table 1.

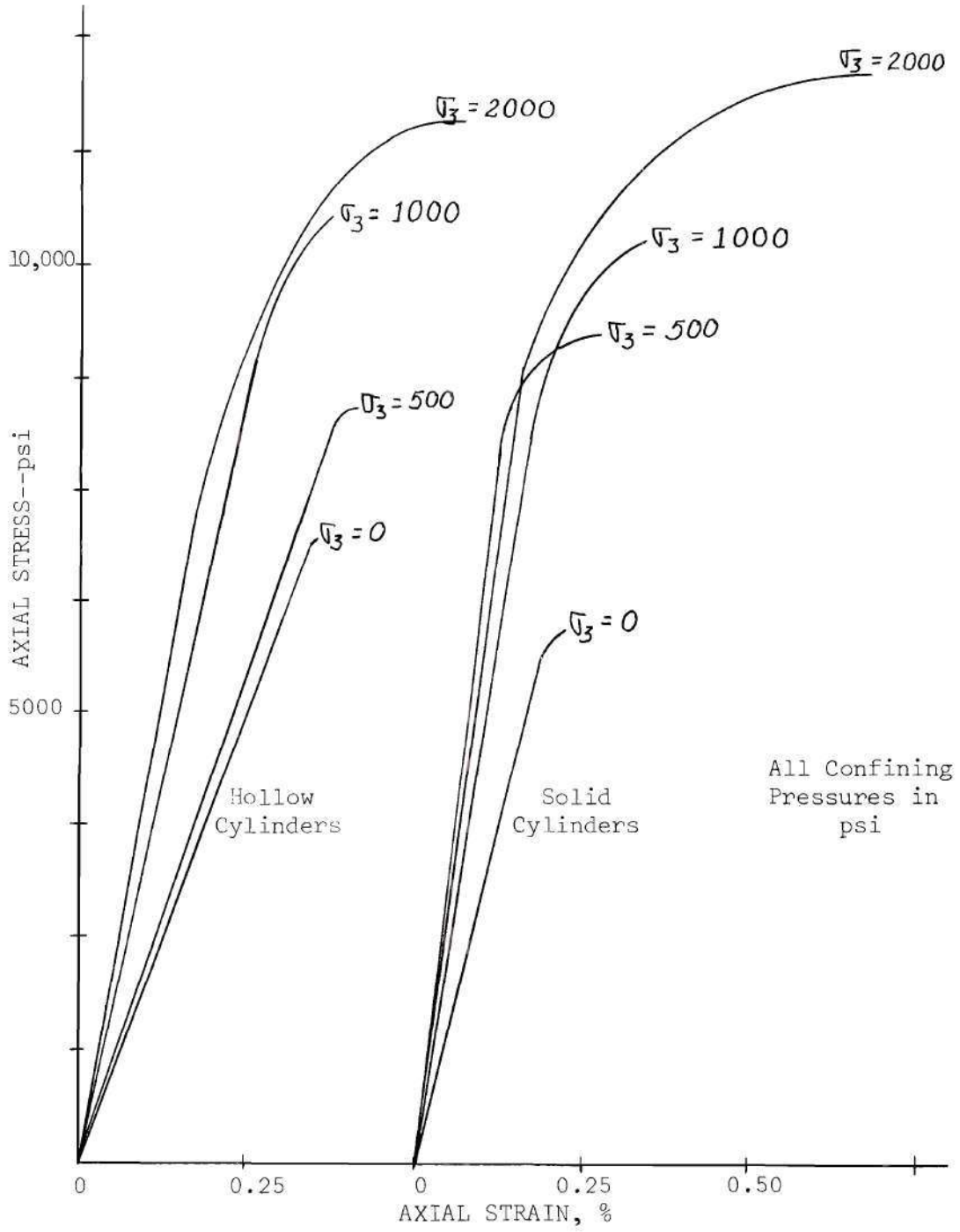

Figure 5. Typical Axial Stress--Axial Strain Curves for Indiana Limestone, Solid and Hollow Cylinders

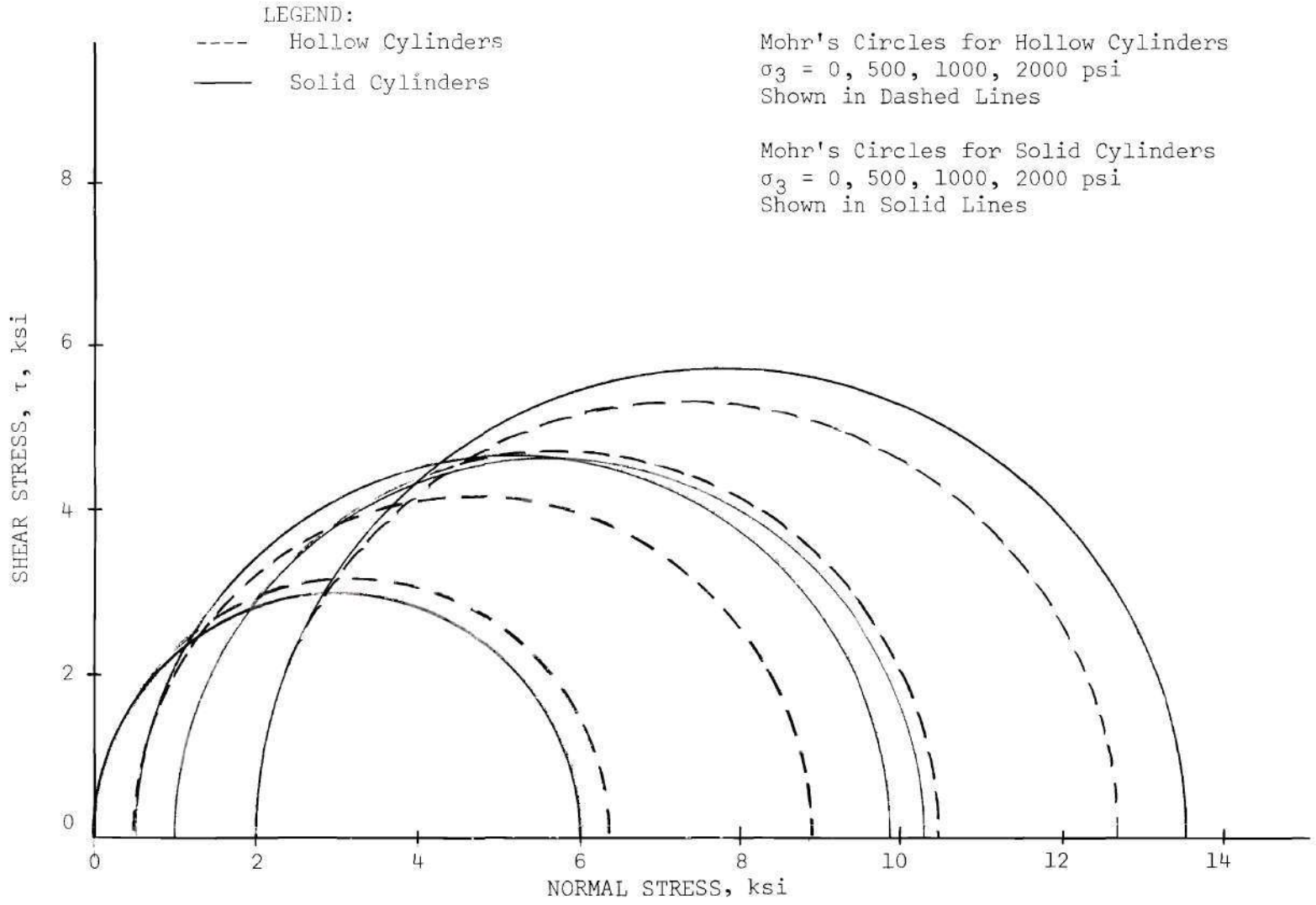

Figure 6. Mohr Diagrams for Indiana Limestone, Solid and Hollow Cylinders

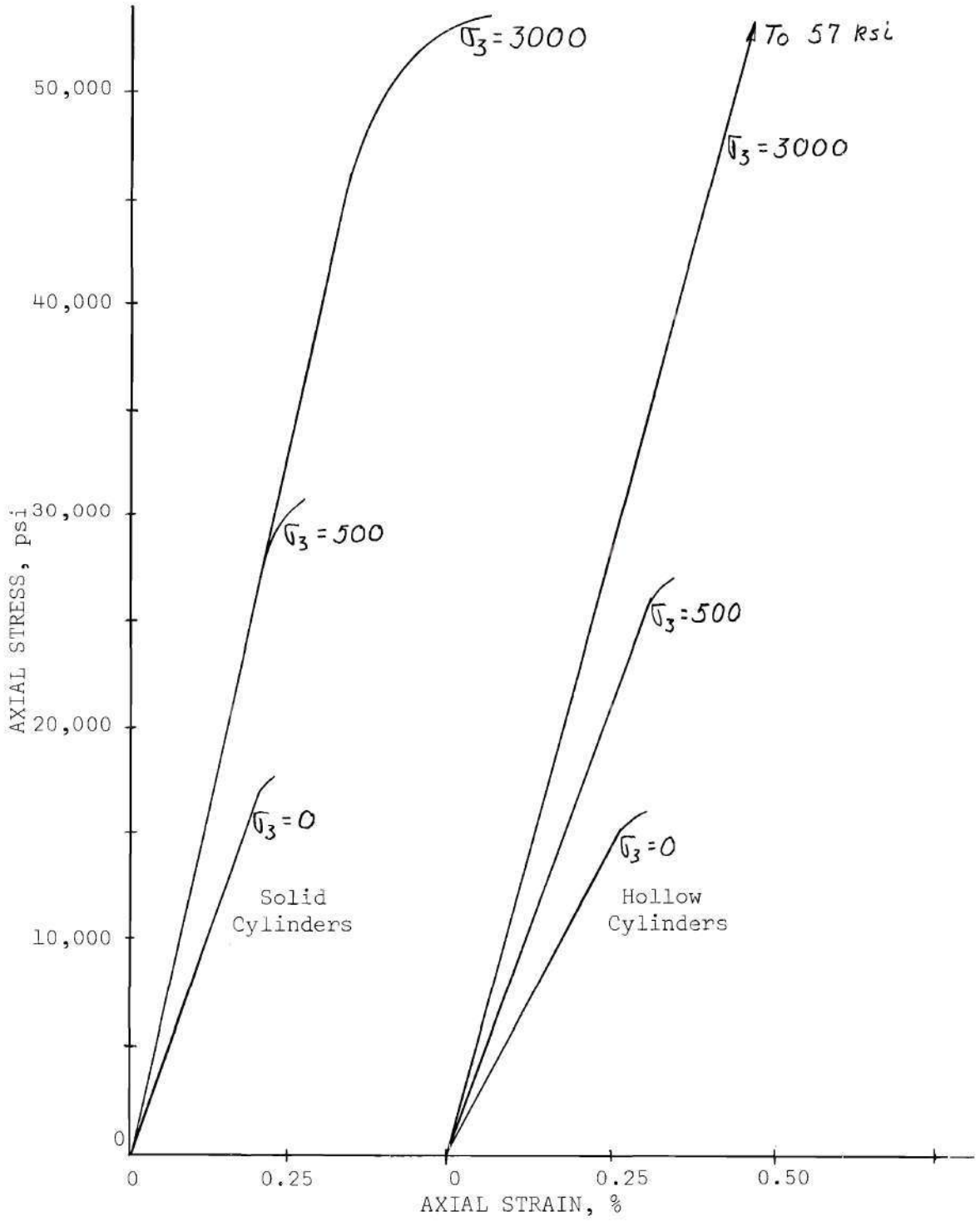

Figure 7. Typical Axial Stress--Axial Strain Curves for Stone Mountain Granite, Solid and Hollow Cylinders

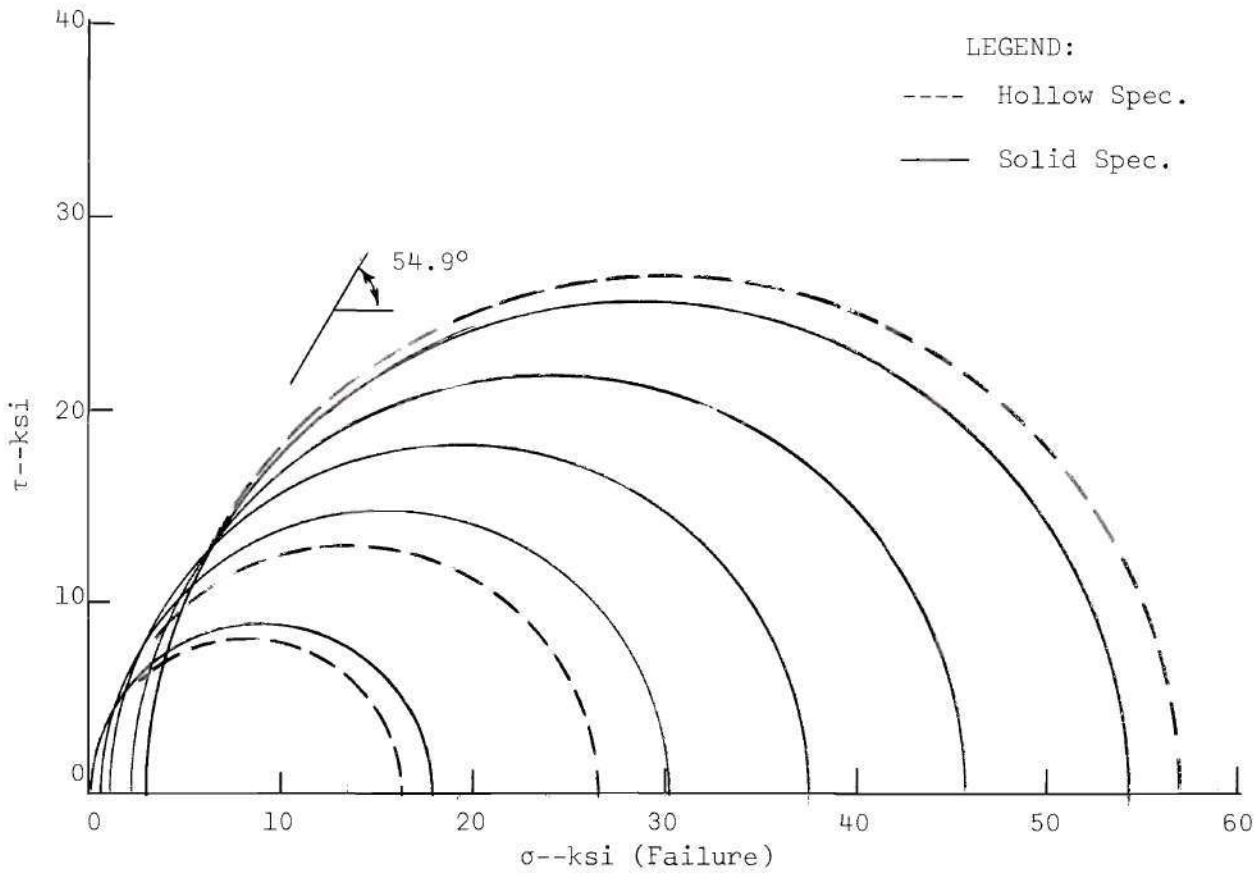

Figure 8. Mohr Diagram for Granite Tested with $\sigma_2 = \sigma_3$ and σ_1 Increased to Failure

Table 1. Indiana Limestone Strength

SERIES S STANDARD TRIAXIAL CONDITIONS			
Specimen Type	Principal Stresses at Failure		
	σ_3	σ_1	Average σ_1
Hollow	0	7070	
	0	5850	6370
	0	6200	
Solid	0	5970	
	0	5730	6010
	0	6340	
Hollow	1000	10,010	10,440
	1000	10,870	
Solid	1000	11,620	
	1000	9,850	10,300
	1000	9,440	
Hollow	2000	11,440	12,690
	2000	13,940	
Solid	2000	13,000	13,510
	2000	14,020	

Mohr diagrams for the Indiana Limestone are presented in Figure 6. The plotted circles are for the averaged values from the entire series which consisted of two or three test specimens per test condition.

On the basis of these data, a Mohr failure envelope can be determined. In order to compare the hollow cylinder results with the solid cylinder results, straight-line envelopes have been developed, although actually the envelopes are slightly concave downward for this range of

confining pressures. The results are as follows:

Type Specimen	ϕ	c
Solid	35.1 degrees	1.74 ksi
Hollow	31.1	1.93

It is evident that, for practical purposes, the strength envelopes are identical.

Comparable test results for the Granite are shown in Figure 7 and in Figure 8. As in the case of the Limestone, the Mohr envelope for the Granite solid cylinders is essentially the same as for the hollow cylinders.

Under "conventional triaxial stress states" ($\sigma_1 > \sigma_2 = \sigma_3$), the hollow cylinders fail in a manner quite similar to that of the solid cylinders. Failure planes are formed in both tests at about the same angles and extend completely through the walls of the hollow cylinders so that a side view of the hollow cylinder looks like that of a solid cylinder. A comparison of failure surfaces for Granite is shown in Figure 9.

It is well known (see, for example, Schwartz (25), that Indiana limestone behaves in a "plastic" manner when subjected to confining pressures above about 4000 psi in a standard traixial test. Another comparison between the results of hollow cylinder tests and those of solid cylinders can be made in this respect. A hollow cylinder was subjected to a stress state of hydrostatic pressure equal to 5000 psi and then failed by increasing the axial pressure while maintaining the radial

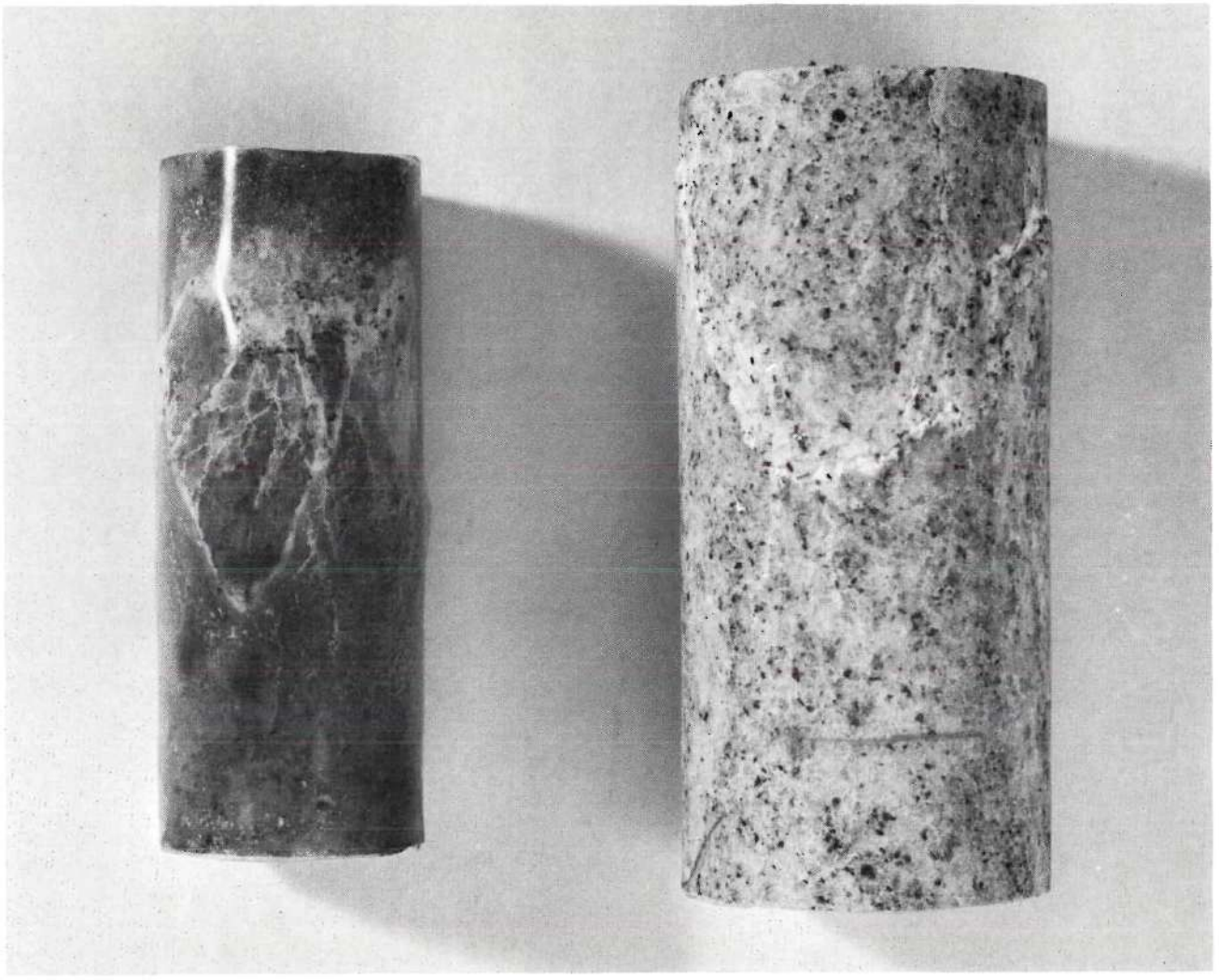

Figure 9. Comparison of Fracture Planes for Granite Under Standard Triaxial Conditions.

and tangential stresses at 5000 psi. The cylinder "failed" by bulging, with two bulges being produced, at approximately each of the 1/3 points of the axial lengths. The value of σ_1 at failure for the hollow cylinder was 20,600 psi, as compared to 20,100 psi for solid cylinders tested at the same confining pressure.

The Effect of the Intermediate Principal Stress

Effects Based on Inside Stresses. The effect of the intermediate principal stress, σ_2, on the strength can be illustrated by Mohr circles for a series of tests where the minor principal stress, σ_3, is held constant and σ_2 is increased with σ_1 (at a constant ratio) until failure occurs. The results from several test series, both for limestone and for granite, are shown in Figures 10 through 12.

In all cases shown for the limestone, irrespective of the value of the minor principal stress, there is a general increase in the diameters of the circles with increasing values of σ_2/σ_1, tending towards a limiting value at higher values of σ_3. For the granite, the circle diameters reach a maximum and then decrease from that maximum as the ratio σ_2/σ_1 approaches unity. The same results are shown in Figures 13 and 15 in the form of curves of $(\sigma_1 - \sigma_3)$ vs. σ_2/σ_1. Quite apparent is the general increase and leveling-off of the principal stress difference for the limestone curves, as well as the increase and subsequent decrease for the granite.

For constant σ_3, up to the maximum value of σ_3 used in the limestone tests, there is an increase in the deviator stress for all values of σ_2/σ_1. This is shown in Figure 13. Such is not the case for the granite. The individual granite curves (Figure 15) reach a maximum,

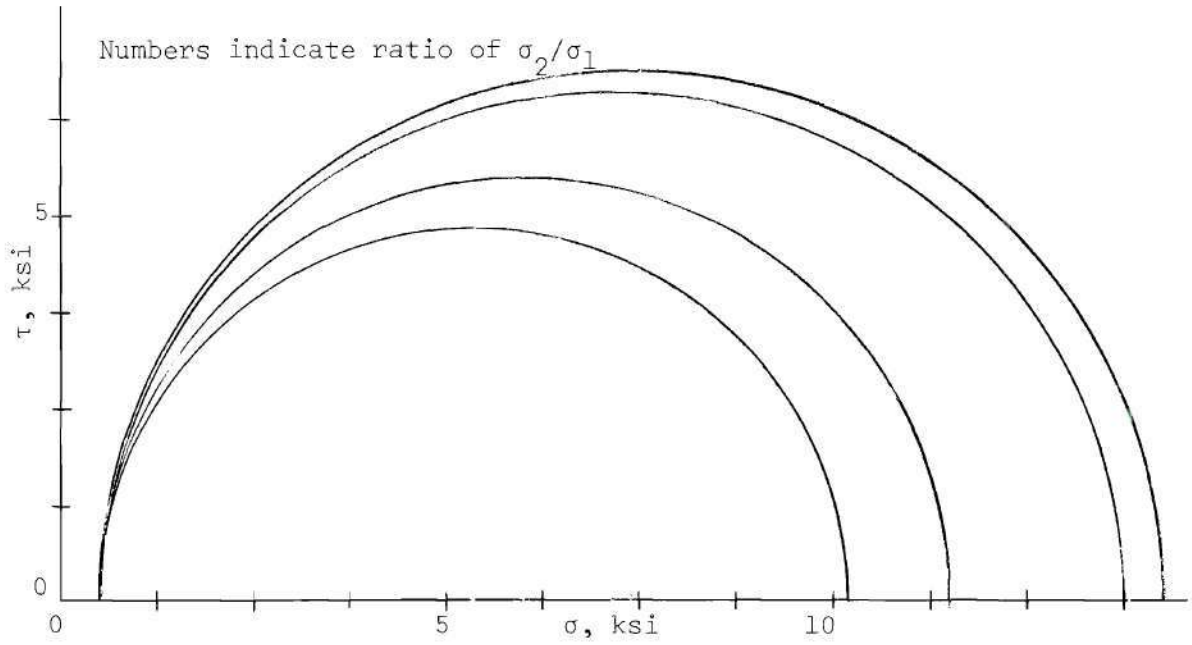

Figure 10. Mohr Circles for Indiana Limestone Hollow Cylinders for σ_3 = 500 psi and Varying σ_2/σ_1 Ratios

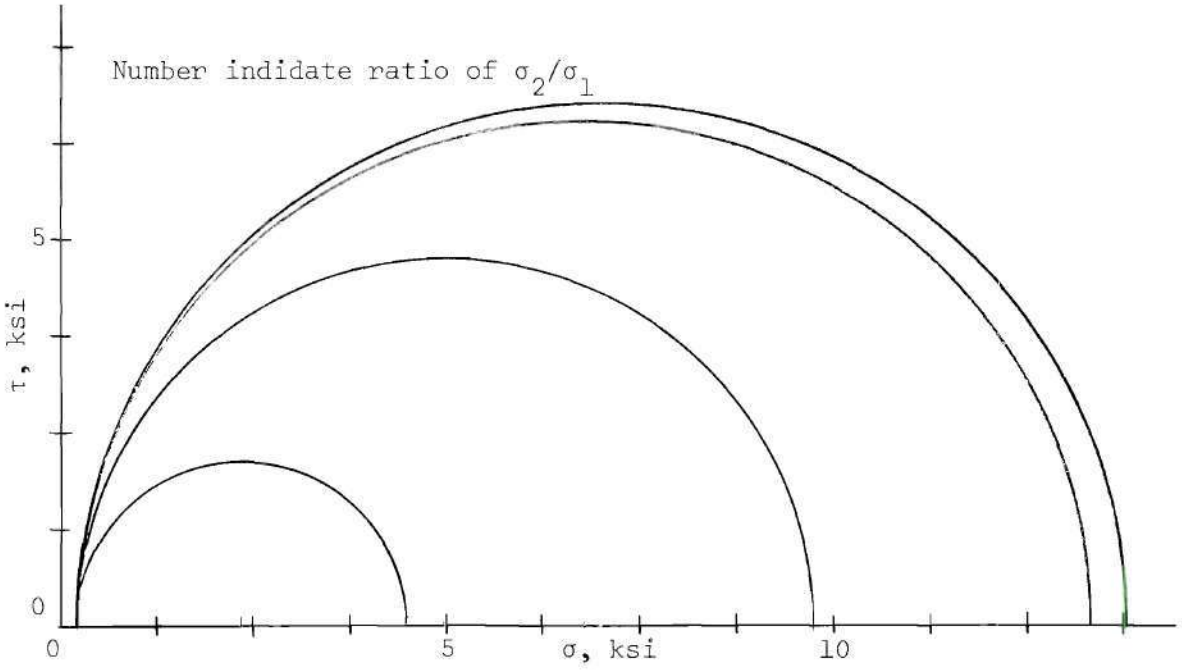

Figure 11. Mohr Circles for Indiana Limestone Hollow Cylinders for σ_3 = 250 psi and Varying σ_2/σ_1 Ratios

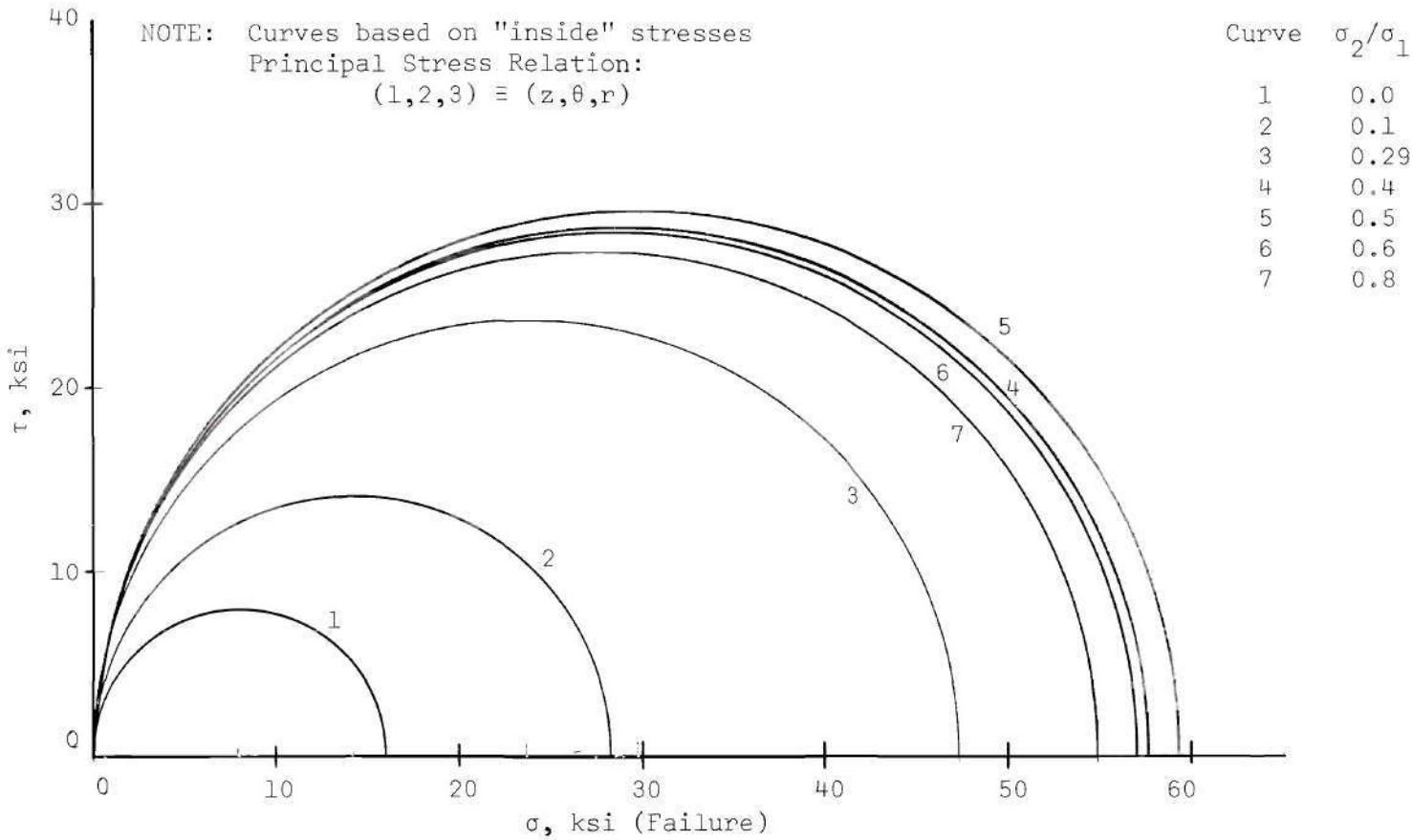

Figure 12. Mohr Circles for Granite Hollow Cylinders for $\sigma_3 = 0$ and Varying σ_2/σ_1 Ratios

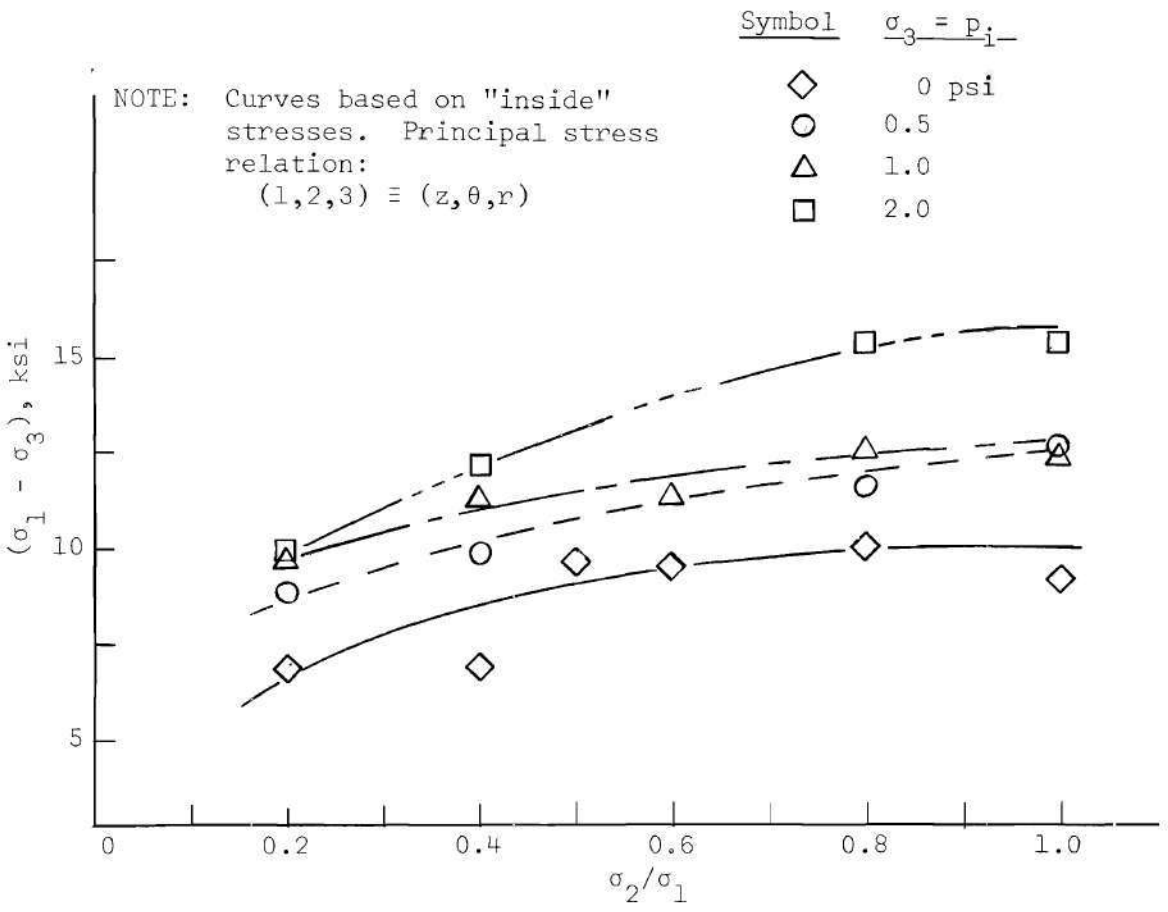

Figure 13. Variation of Principal Stress Difference with σ_2/σ_1 Ratio, Indiana Limestone Series A

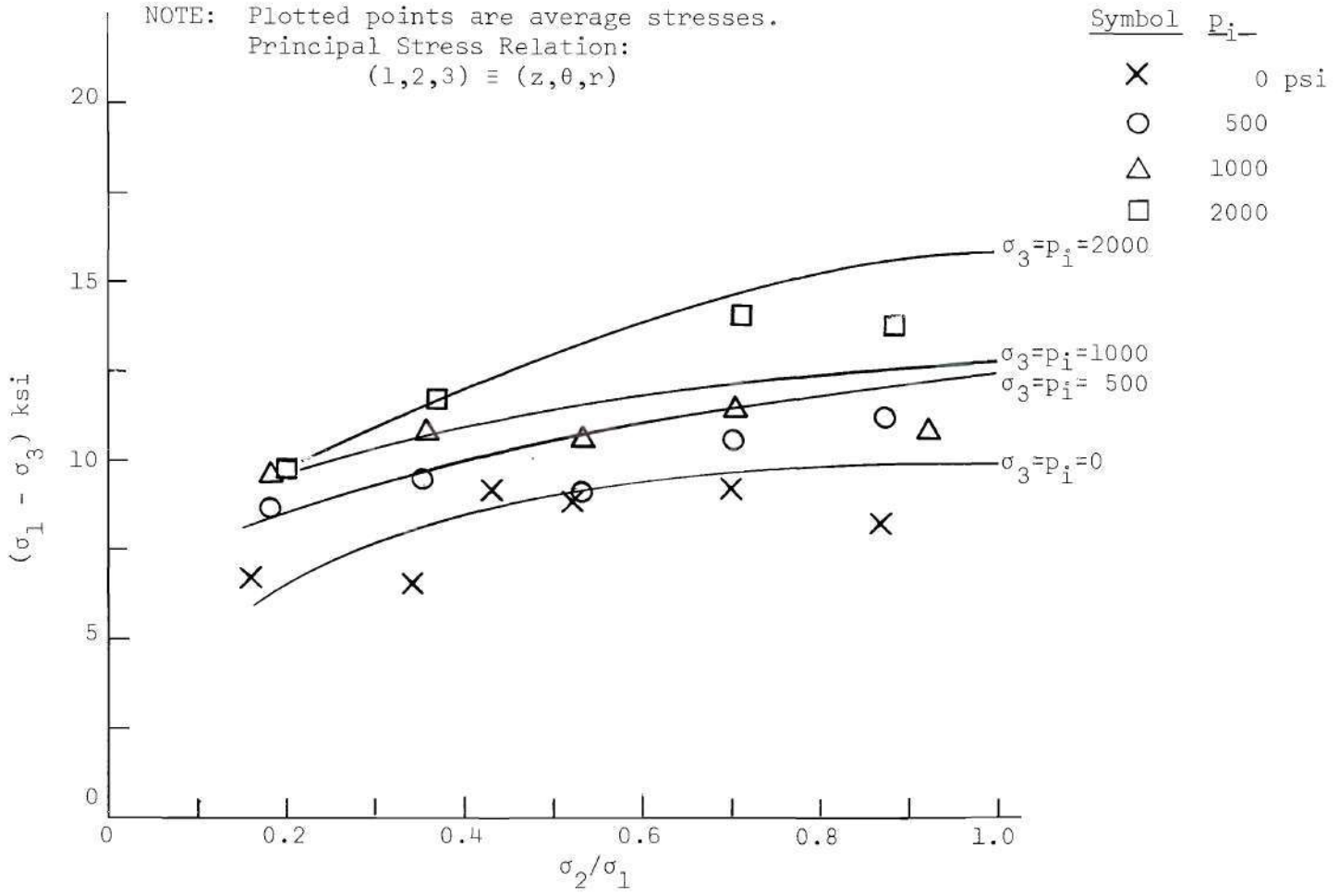

Figure 14. Variation of Principal Stress Difference with σ_2/σ_1 Ratio, Indiana Limestone Series A, Average Stresses

NOTE: Inside stresses utilized
Principal Stress Relation:
(1,2,3) ≡ (z,θ,r)

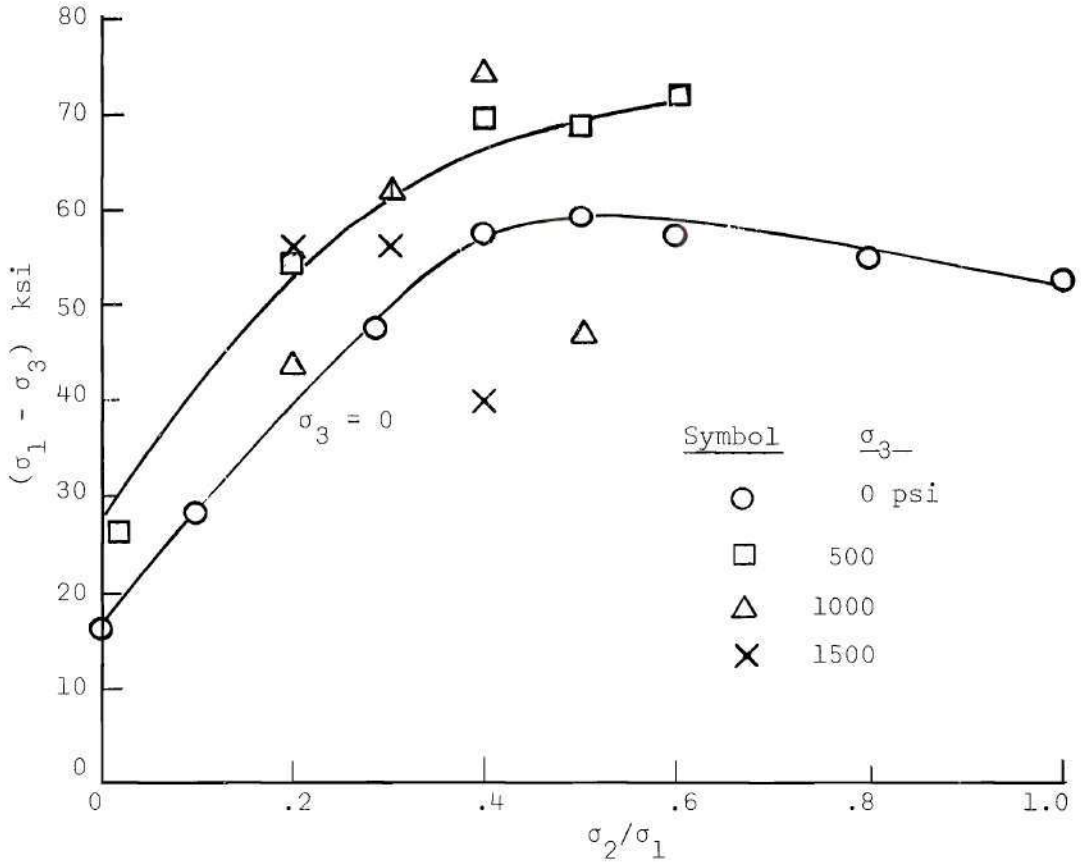

Figure 15. Variation of Principal Stress Difference with σ_2/σ_1 Ratio for Granite Hollow Cylinders for Inside Stresses

after which a decrease is noted. The value of σ_2/σ_1 at which the maximum is reached decreases with increasing values of σ_3. Also, the shape of the curve changes somewhat, in general becoming steeper on both sides of the maximum and having more of a "peaked" shape.

Curves of Principal Stress Difference ($\sigma_1 - \sigma_3$) vs. Confining Pressure (σ_3) are often used to indicate the influence of confinement on the strength of a material. A typical shape for such curves is concave downward. Figure 17 presents the results of some limestone tests in the form of families of such curves. There is a general increase in principal stress difference for a given σ_3 with increasing values of σ_2/σ_1 but there is a distinct separation of the curves for different σ_3 values. Figure 18 shows the same type of plot for granite. Here the points are considerably irregular and no attempt was made to define curves. There does appear to be some increase in ($\sigma_1 - \sigma_3$) with increasing σ_2/σ_1 at low values of σ_3 but the data for σ_3 = 1.5 ksi are completely irrational.

Comparison of the Mohr "ϕ" angles for limestone for varying values of σ_2/σ_1 are shown in Figure 19. An approximate straight-line relation exists, increasing with increasing values of σ_2/σ_1, based on the "inside" stresses. The total change is approximately 12°. The values of "ϕ" used in Figure 19 were determined from plots of ($\sigma_1 - \sigma_3$) vs. ($\sigma_1 + \sigma_3$) for the various ratios of σ_2/σ_1. The slopes (δ) of the ($\sigma_1 - \sigma_3$) vs. ($\sigma_1 + \sigma_3$) curves are related to the Mohr "ϕ" by the relation:

$$\text{Sin } \phi = \text{Tan } \delta \ . \qquad (9.13)$$

NOTE: Plotted points are average stresses.
Principal Stress Relation: (1,2,3) ≡ (z,θ,r)

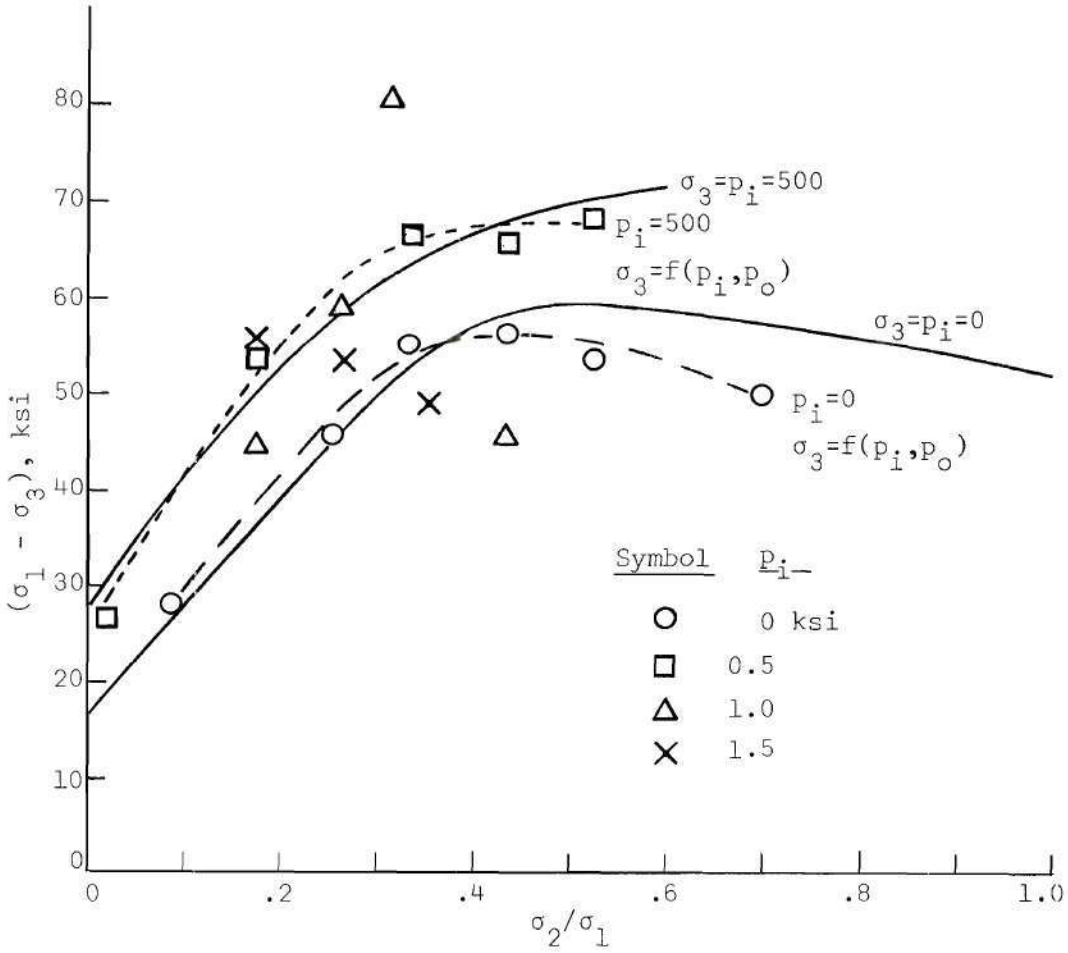

Figure 16. Variation of Principal Stress Difference with σ_2/σ_1 Ratio for Granite Hollow Cylinders for Average Stresses

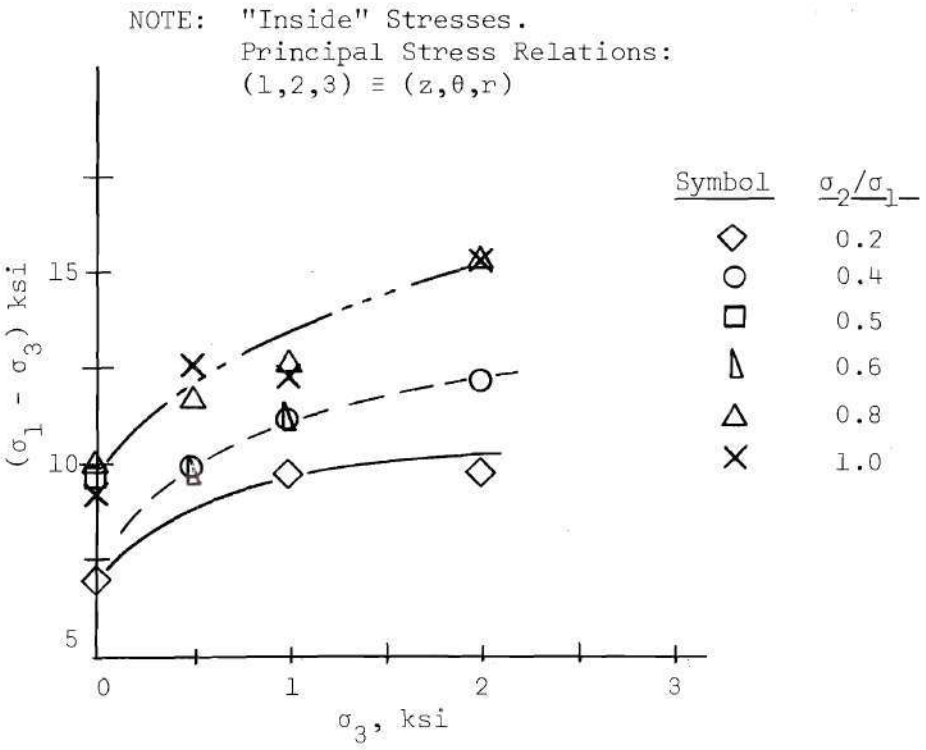

Figure 17. Variation of Principal Stress Difference with Minor Principal Stress, Indiana Limestone Hollow Cylinders, Series A

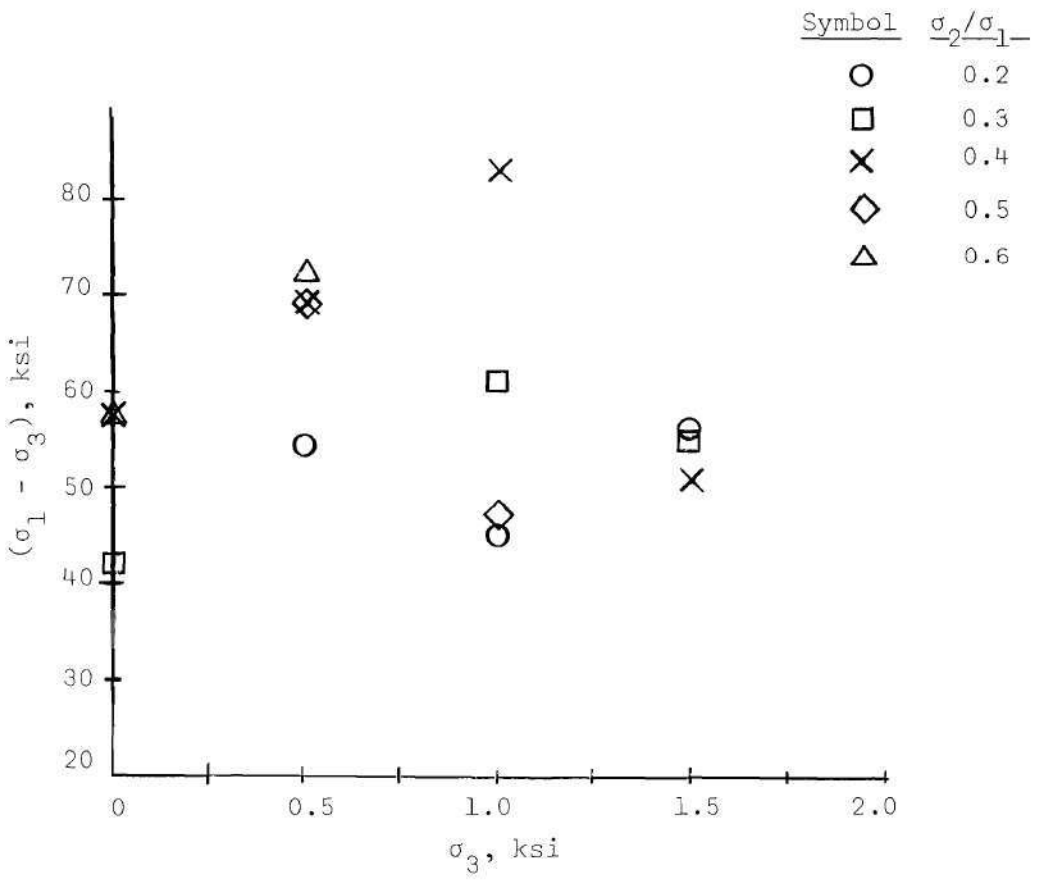

Figure 18. Variation of Principal Stress Difference with Minor Principal Stress, Granite Hollow Cylinders

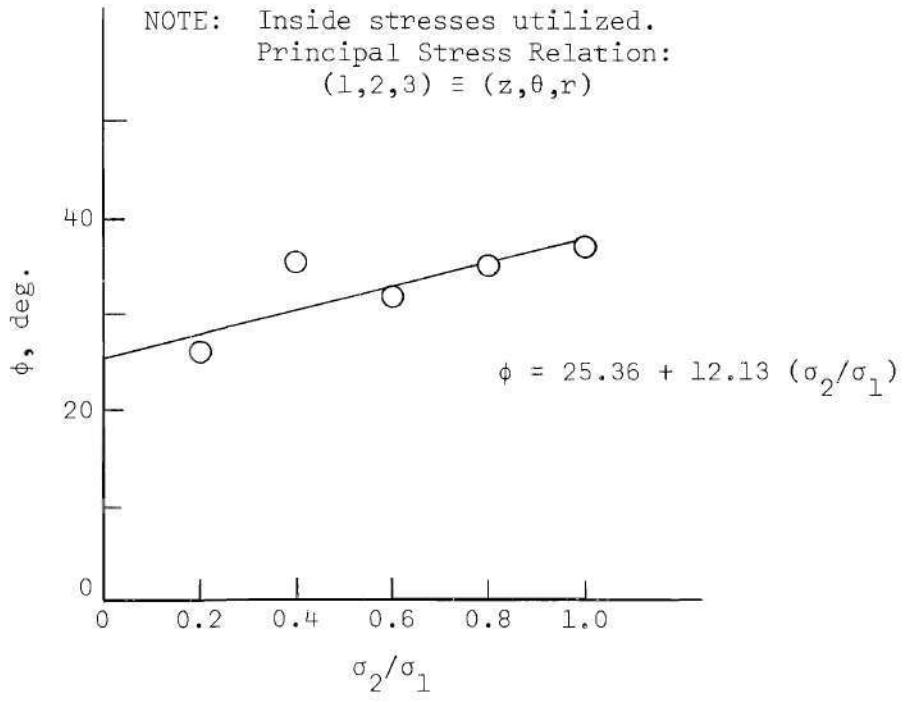

Figure 19. Variation of Angle of Internal Friction with σ_2/σ_1 Ratio, Indiana Limestone, Series A

Curves of $(\sigma_1 - \sigma_3)$ vs. $(\sigma_1 + \sigma_3)$ are shown in Figure 20 for σ_2/σ_1 equal to 0.2 and 1.0. Table 2 presents the results for all values of σ_2/σ_1 for test series A.

Table 2. Principal Stress Difference vs. Principal Stress Sum Values for Indiana Limestone, Series A

Sample	σ_2/σ_1	$\sigma_1 - \sigma_3$ ksi	$\sigma_2 + \sigma_3$ ksi	Intercept	Slope
A-1	0.2	6.890	6.890		
A-6	0.2	8.900	9.900	4.205	0.437
A-12	0.2	9.750	11.750		
A-18	0.2	9.750	13.750		
A-2	0.4	6.870	6.870		
A-7	0.4	9.900	10.900	3.212	0.579
A-13	0.4	11.250	13.250		
A-17	0.4	12.150	16.150		
A-4	0.6	9.550	9.550		
A-9	0.6	9.500	10.500	4.350	0.510
A-14	0.6	11.350	13.350		
A-5	0.8	10.000	10.000		
A-8	0.8	11.570	12.570	4.342	0.569
A-15	0.8	12.550	14.550		
A-20	0.8	15.350	19.350		
A-11	1.0	9.160	9.160		
A-10	1.0	12.610	13.610	3.900	0.600
A-16	1.0	12.290	14.290		
A-19	1.0	15.340	19.340		

NOTE: "Inside" stresses utilized.

Effects Based on Average Stresses. The same general effects are apparent for the average stresses as for the inside stresses. Figures 14 and 16 illustrate the effects of the average stresses as compared to the inside stresses. It can be seen that there is a general shift of

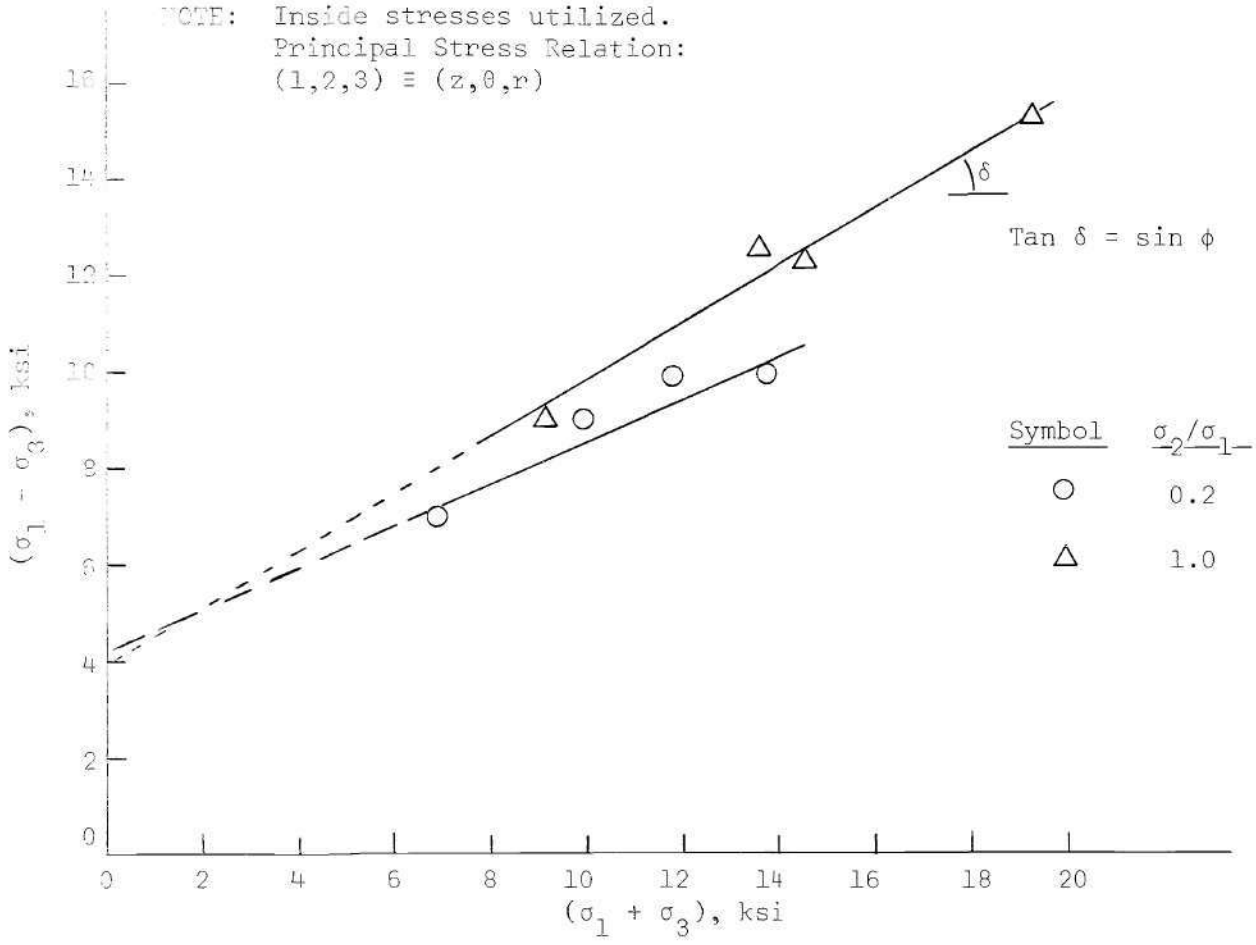

Figure 20. Principal Stress Difference vs. Principal Stress Sum, Indiana Limestone, Series A

the curves towards lower values of σ_2/σ_1 and $(\sigma_1 - \sigma_3)$ but retaining the same general shape, i.e., concave downward. There appears to be no better or worse correlation of the data when using the average stresses than with inside stresses.

Conclusions. Based on the results presented in these forms, it is concluded that there are no general relationships of the type considered which are valid for both materials under consideration. For the limestone, the relations are much better defined and fairly consistent with respect to the variables. Such is not true for the granite. It is true that the limestone is a much more homogeneous material when compared to the granite and it is possible that much of the erratic behavior of the granite could be attributed to the structural variation in the specimens. Also, the range of confining pressures was much greater for the limestone than that for the granite when compared to the value of σ_1 at failure. The confining pressure capacity of the cell, together with the inherent behavior of the granite with increasing confinement, were responsible for the relatively low confining pressures used in the study of this material. Although these results indicate otherwise, it is therefore possible that general relationships for granite, comparable in uniformity to those for limestone, may exist if considerably higher values of σ_3 are used.

The fact that there is an influence on the strength characteristics of a given rock from the intermediate principal stress is quite apparent from even a cursory examination of the results.

Results in Terms of Octahedral Stresses

The test data expressed in terms of Octahedral stresses are shown

in Figures 21 through 28.

Plots of τ_o vs. σ_o for the Limestone are presented in Figures 21 and 22. Figure 21 indicates a general increase in τ_o with increasing σ_o. This is consistent with results of other investigations of strength of marble and as reported by Topping (14). See Figure 29. There is a rather broad scatter-band at the lower values of σ_o which apparently diminishes in size as σ_o increases, although this could be due to a scarcity of test data for higher values of σ_o. When distinctions between the values of τ_o are made with respect to σ_3, there appears to be rather distinct separations between such data at lower values of σ_o (Figure 22). The separations become smaller as σ_o increases and become indistinguishable at the higher values of σ_o.

Figure 23 presents the data for Granite and a general increase in τ_o with increase in σ_o is indicated. There is considerable scatter in the values of τ_o at the higher values of σ_o and there appears to be a downward concavity to the curve. This suggests a continuous decrease in slope of τ_o vs. σ_o for this material as the confining pressure is increased and a possible maximum or limiting value of τ_o; however, this is probably due to absence of data at higher σ_o values.

A useful relation for illustrating the effect of σ_2 on strength develops when the octahedral shearing stress is normalized with respect to σ_o and plotted versus σ_2/σ_1. For the case of $\sigma_3 = 0$, the relation reduces to

$$\tau_o/\sigma_o = \frac{\sqrt{2}\ \sqrt{1 + \sigma_2^2/\sigma_1^2 + \sigma_2/\sigma_1}}{1 + \sigma_2/\sigma_1} \qquad (9.14)$$

This case is purely mathematical since no material properties are included, and this case is shown in the following figures without data points with the individual values presented in Table 3.

Table 3. Octahedral Stress Ratio for $\sigma_3 = 0$

σ_2/σ_1	τ_o/σ_o
0	1.414
0.2	1.080
0.4	0.881
0.6	0.771
0.8	0.720
1.0	0.707

For cases other than when $\sigma_3 = 0$, the effect of an increasing value of σ_3 is to decrease the value of τ_o/σ_o, and for limestone, Figure 24 shows that a regular family of curves is formed, with the value of τ_o/σ_o decreasing rapidly at the lower values of σ_2/σ_1, and approaching a constant for each value of σ_3 as σ_2/σ_1 approaches 1.0.

For the granite, Figure 25 shows the same trends, but the values of σ_3 used in this study were of insufficient magnitude to delineate families of curves, if such exist. This is due to the very large increase in σ_1 with small increases in σ_3 which obscures the effect of σ_3 in the relations.

The regularity of the families of curves is shown by Figure 26

in terms of a plot of Log τ_o/σ_o vs. σ_3. Families of curves in terms of σ_2/σ_1 are straight lines decreasing in value of τ_o/σ_o with increasing minor principal stress. The mathematical expression for the limestone curves is of the form:

$$\text{Log}_{10}\left[\frac{(\tau_o/\sigma_o)_1 + \Delta(\tau_o/\sigma_o)}{(\tau_o/\sigma_o)_1}\right] = -k \cdot \Delta\sigma_3 \qquad (9.15)$$

The preceding curves indicate the slope of lines drawn from the τ_o, σ_o origin to the value of the point under consideration. The significance of the curves is therefore phenomenological, and not a generalized relation for all rocks. Although this does not invalidate the use of such plots, it suggests that a more general relation could be obtained by utilizing the τ_o values normalized to $\sigma_o = 1.0$. This amounts to the determination of the slopes of lines drawn from the "failure envelope" locus to the point under consideration. The results in such forms are shown in Figure 27.

The adjusted values produce curves, which, for the limestone, are only slightly concave upward and which exhibit little distinction with respect to the inside confining pressure. The granite curves, while being shifted downward and to the left, reflect the relatively small σ_o adjustment in that the resultant curves still have a large slope. This is particularly true at the lower values of σ_2/σ_1.

On this type of plot, the von Mises failure criterion is a straight, horizontal line. The Tresca is similar in *shape* to the experimental curves, being slightly concave upward with a minimum occurring at

approximately $\sigma_2/\sigma_1 = 0.5$. The minimum value of the Tresca will be 0.886 of the maximum (which occurs at $\sigma_2/\sigma_1 = 1.0$) and at a position greater than zero, but dependent upon both the value of σ_2 and the material properties. The Mohr criteria will also plot as a concave upward curve, except that the minimum would occur at $\sigma_2 = \sigma_1$, and the exact trace of the curve would depend upon the material properties.

It can be seen that the correlation utilizing adjusted σ_o values is no better, if not worse, than that with the unadjusted σ_o values.

The results of this investigation can be expressed in the following manner:

$$\tau_o/\tau_o = \left(\frac{\sqrt{2}\,[1 - (\sigma_2/\sigma_1) + (\sigma_2/\sigma_1)^2]^{1/2}}{1 + (\sigma_2/\sigma_1)} \right) e^{-a\,\sigma_3} \qquad (9.16)$$

where: a = material constant.

For the limestone, the expression is plotted for the cases of $\sigma_3 = 0.0$, 0.5, 1.0 and 2.0 ksi in Figure 28. The value of "a" is 0.10674. The experimental data for $\sigma_3 = 0.5$ and 1.0 ksi (using inside stresses) are extremely close to the plotted curves. For $\sigma_3 = 2.0$ ksi, there is good correlation at low values of σ_2/σ_1, but considerable deviation at higher values. The maximum deviation is on the order of 8 per cent. It may be recalled that the limestone will, in fact, behave in a "ductile" manner when subjected to confining pressures somewhat above 2 ksi in a standard triaxial test. It is likely, therefore, that the deviation from the curves at the higher σ_2/σ_1 values is due to such "ductile" behavior which would cause the failure stresses to be quite

different from the "inside" stresses.

In the case of the granite, while there definitely appears to be the same general behavior as for the limestone, there is insufficient data to determine the value of the constant, a. Since the effect of σ_3 is very small up to the maximum value utilized, a value of 0.0 for the constant "a" could be used.

Conclusions. The results of this investigation, presented in the form of τ_o vs. σ_o curves, indicate reasonable correlation for the range of stresses considered, even though the granite results appeared erratic. The implications of this are either that the behavior can be properly represented in terms of the octahedral stresses, or that the octahedral stress relations are not sufficiently sensitive to detect major deviations from an apparent trend. The relations shown in Figures 24, 25, and 28 appear to have the most value. It is concluded that the strength of both the limestone and the granite can be represented by Equation (9.16), utilizing, for the limestone, a = 0.10674, and for the granite, a = 0.0. Curves of this type could provide the necessary relations to calculate strength under conditions where certain principal stress ratios exist and where one or more of the principal stresses are then deduced. This type of relation could also be used to determine the magnitude of applied minor principal stress necessary to maintain stability under conditions where changes in the principal stresses are sufficient to cause failure.

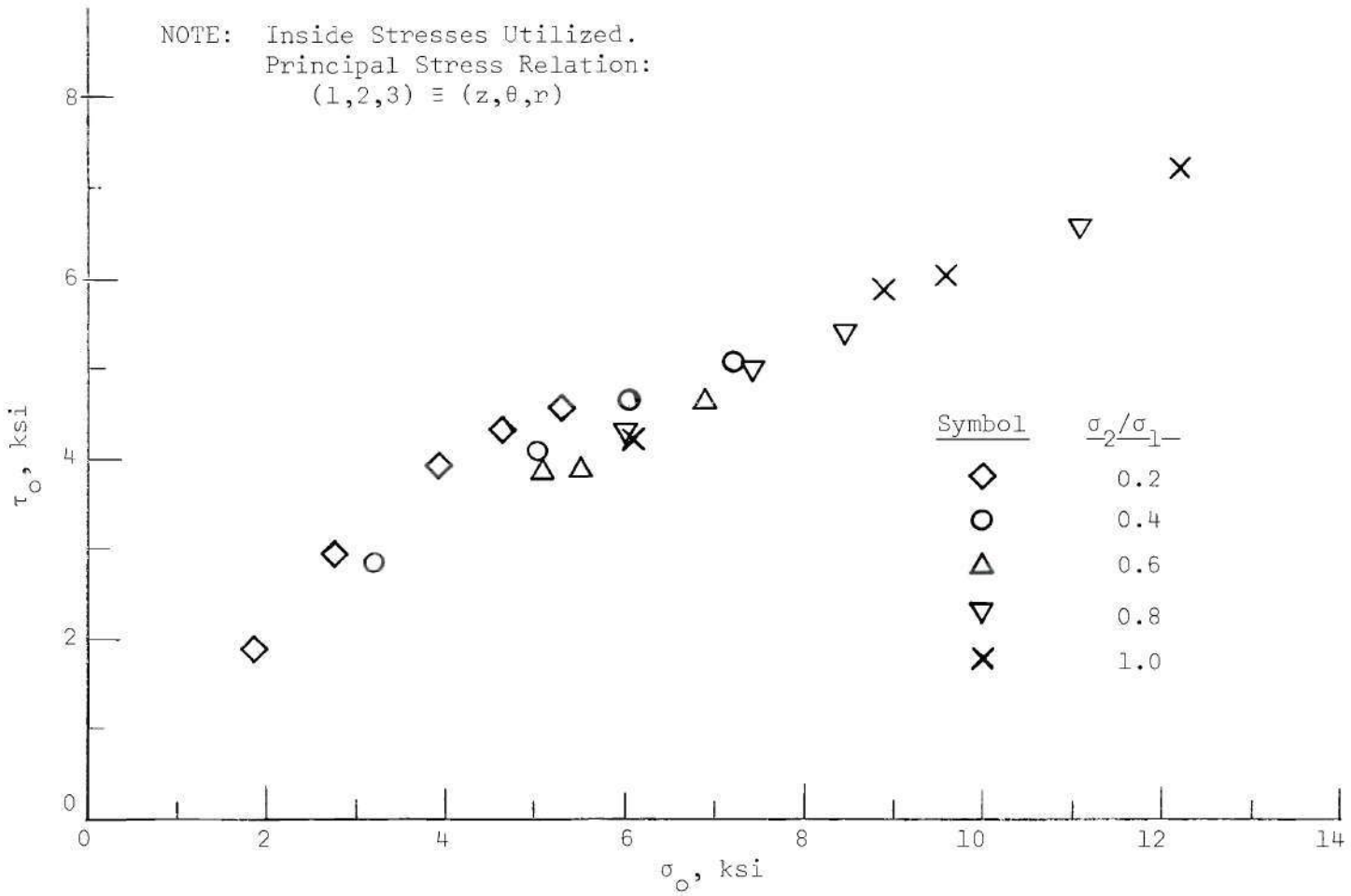

Figure 21. Variation of Octahedral Shear Stress with Octahedral Normal Stress, as Influenced by σ_2/σ_1, Indiana Limestone, Series A

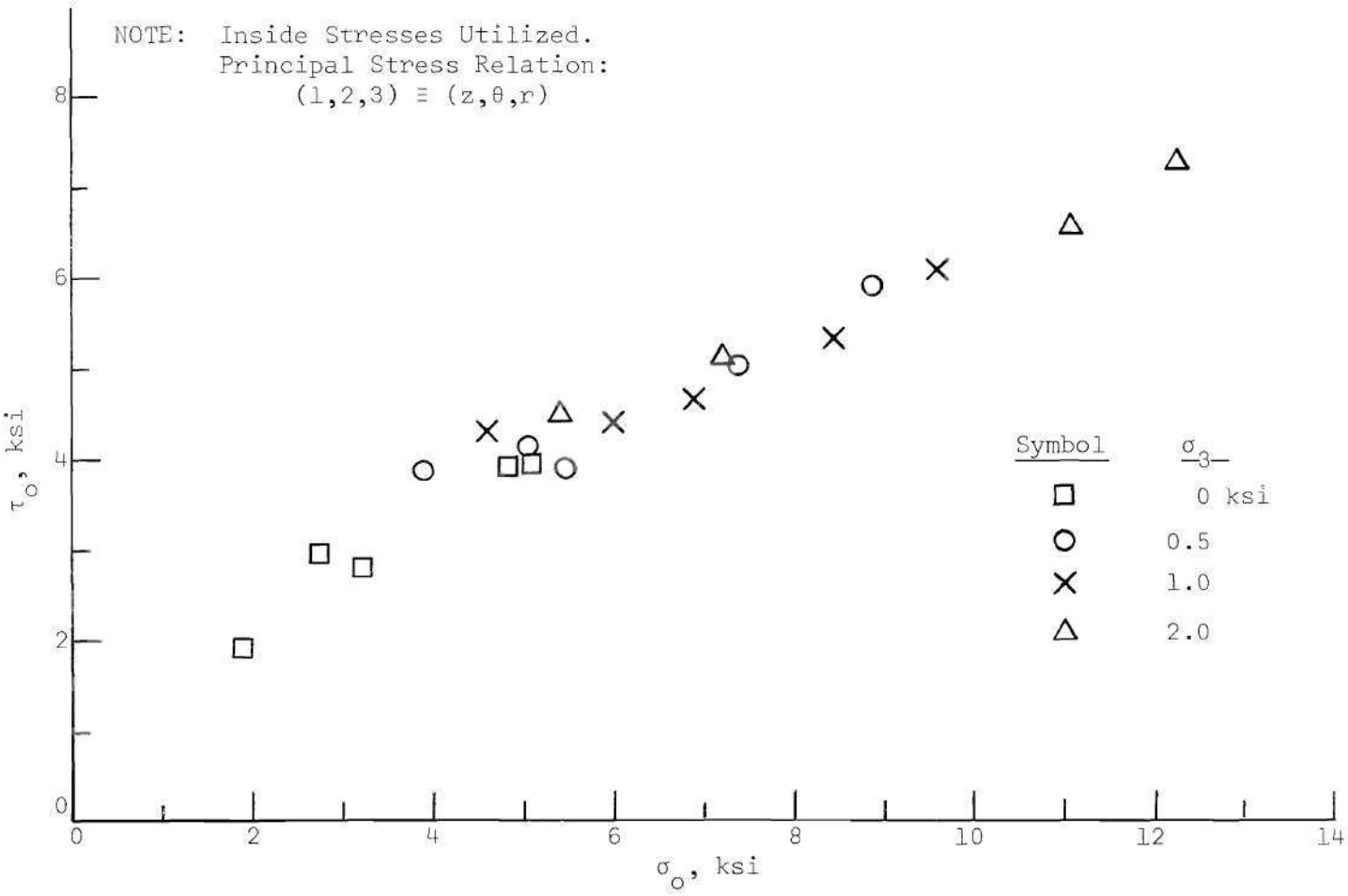

Figure 22. Variation of Octahedral Shear Stress with Octahedral Normal Stress, as Influenced by σ_3, Indiana Limestone, Series A

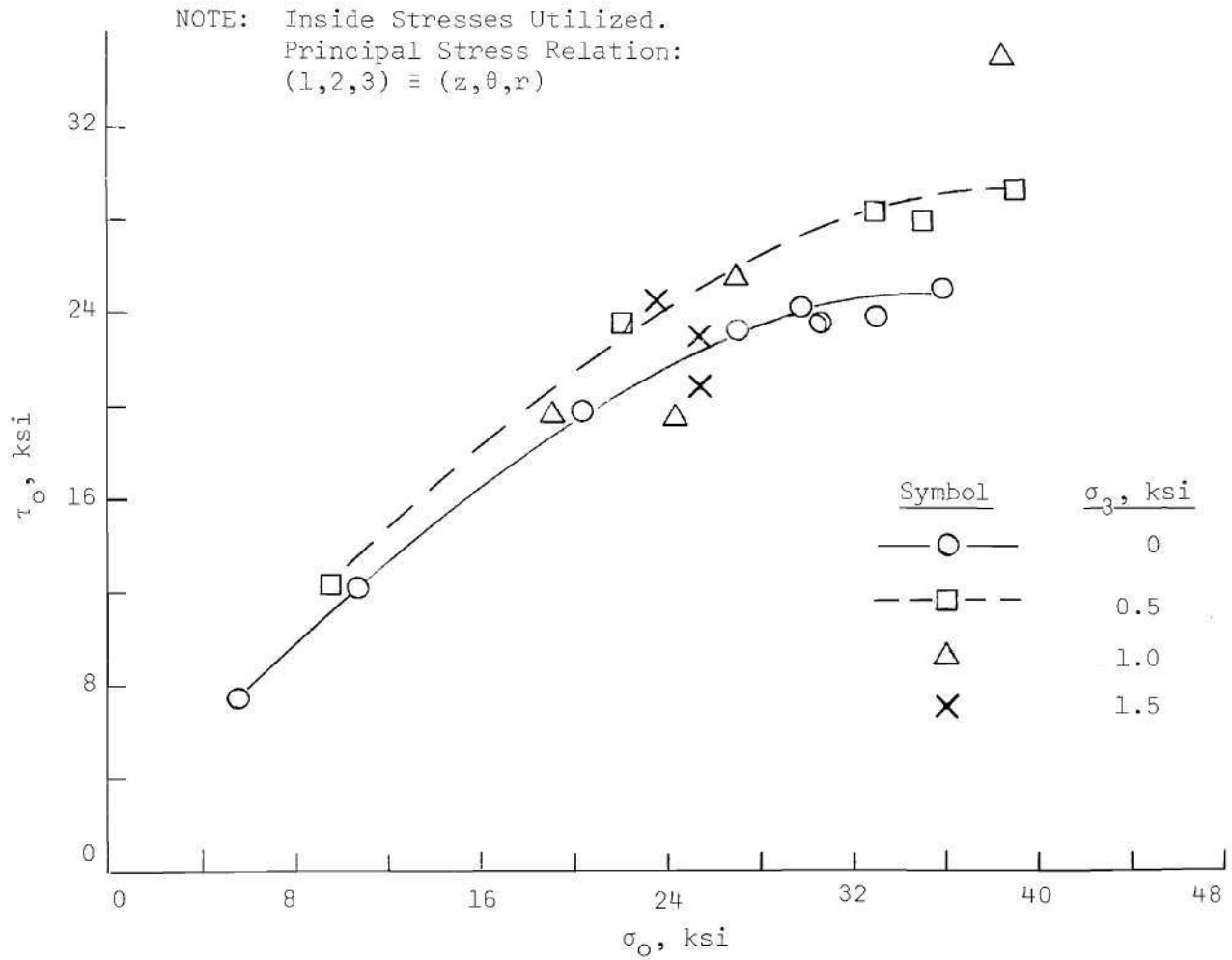

Figure 23. Variation of Octahedral Shear Stress with Octahedral Normal Stress, as Influenced by σ_3, Granite

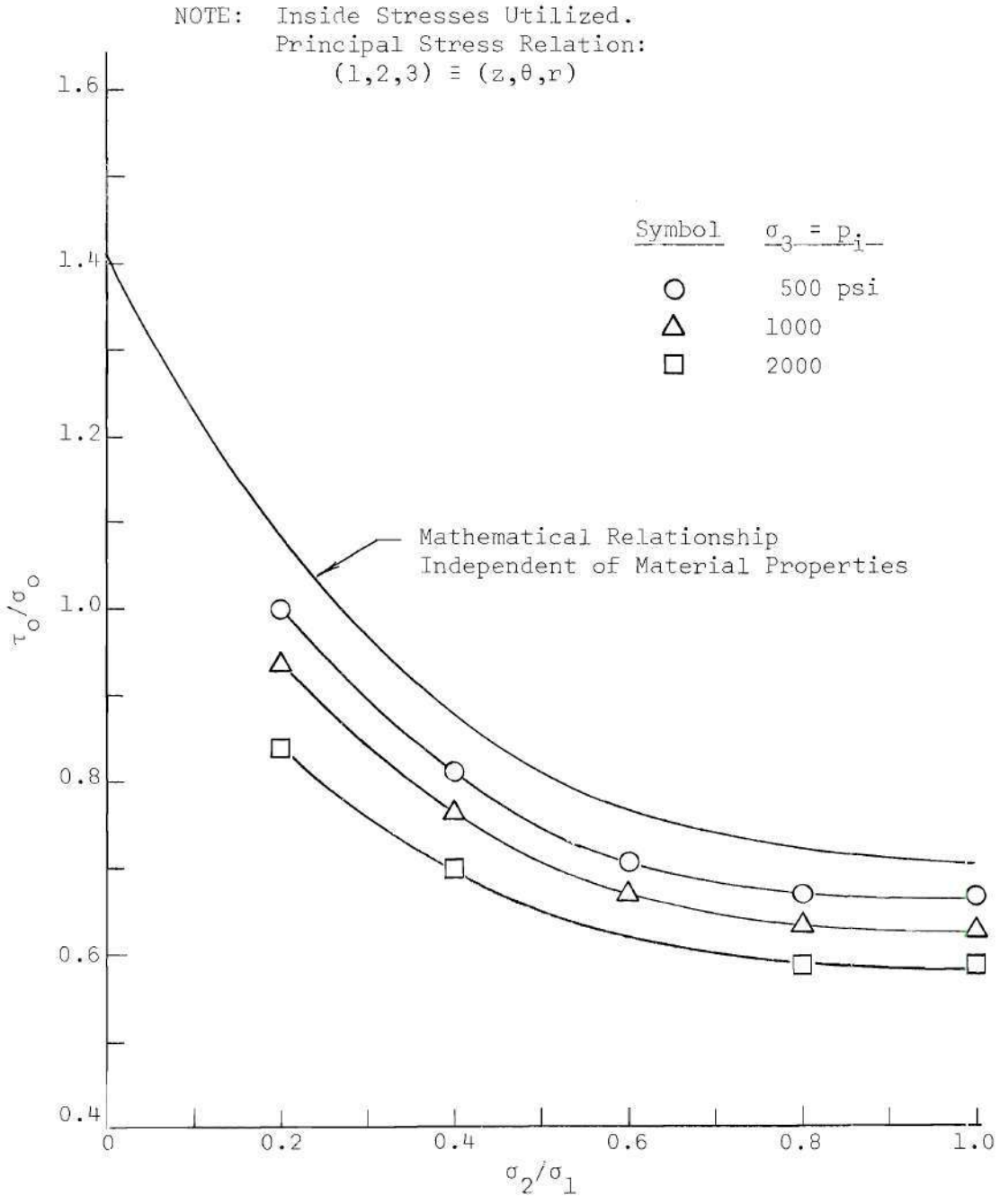

Figure 24. Octahedral Stress Ratio vs. σ_2/σ_1 Ratio, Indiana Limestone, Series A

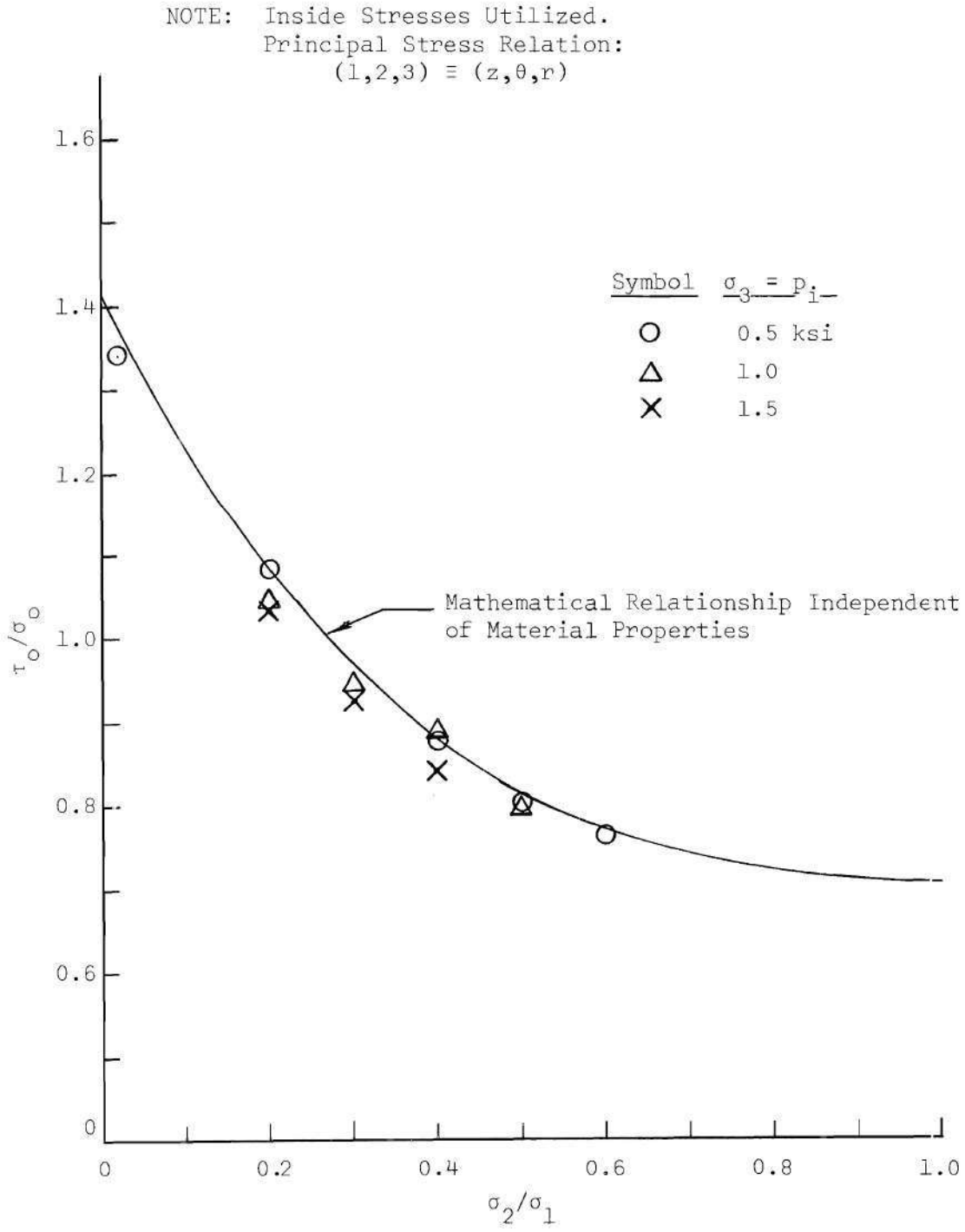

Figure 25. Octahedral Stress Ratio vs. σ_2/σ_1 Ratio, Granite

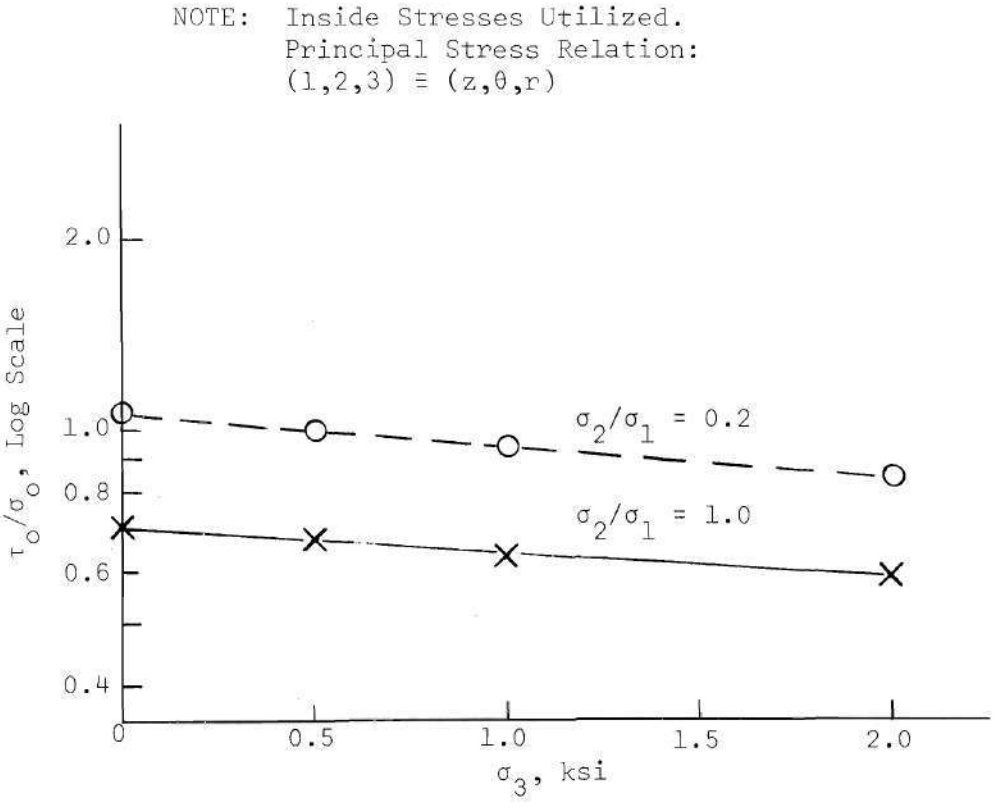

Figure 26. Effects of Principal Stresses on Octahedral Stress Ratio for Indiana Limestone

NOTE: Principal Stress Relation:
(1,2,3) ≡ (z,θ,r)

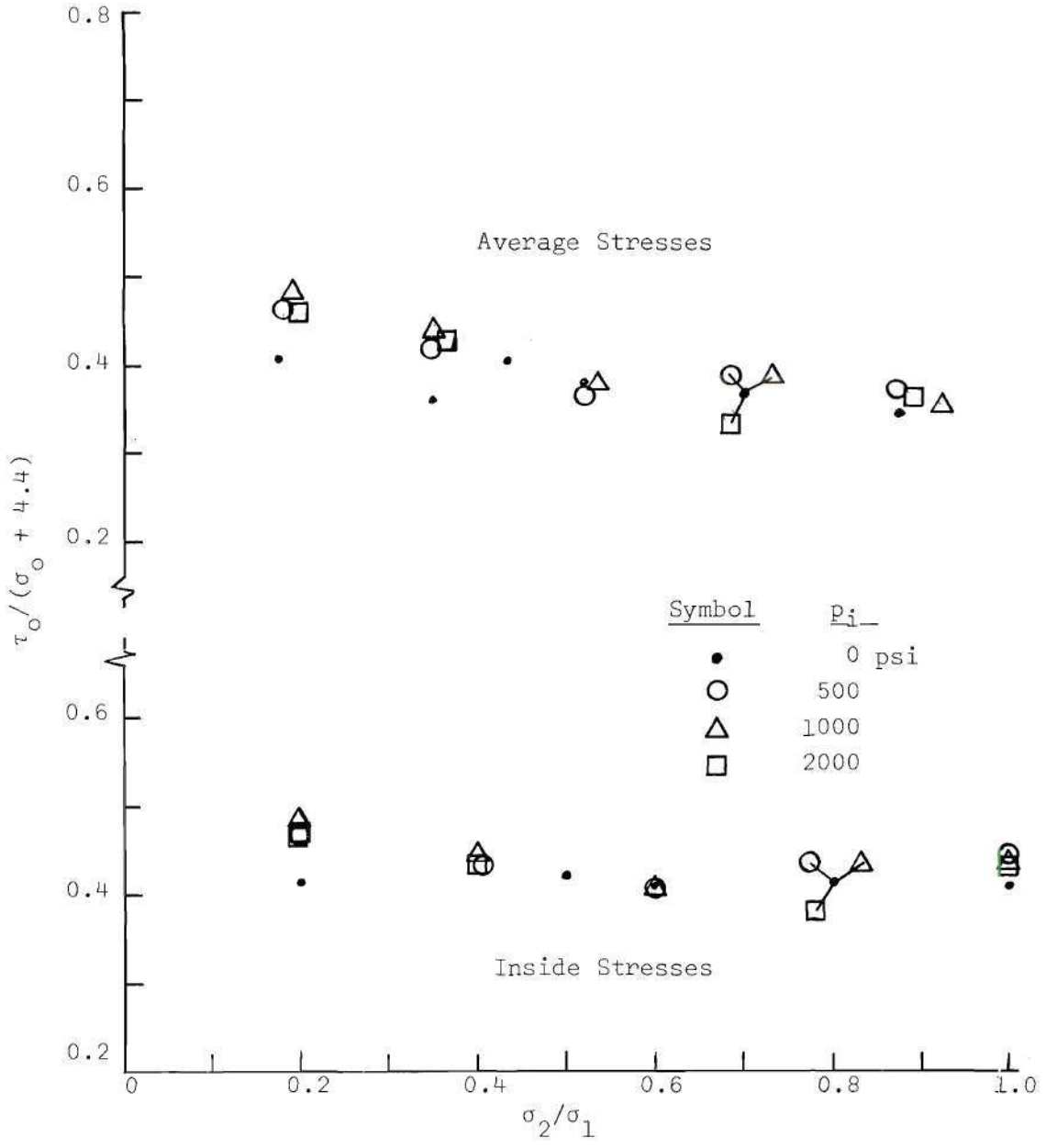

Figure 27. Variation of Adjusted τ_o/σ_o Ratio vs. σ_2/σ_1, For Indiana Limestone, Series A

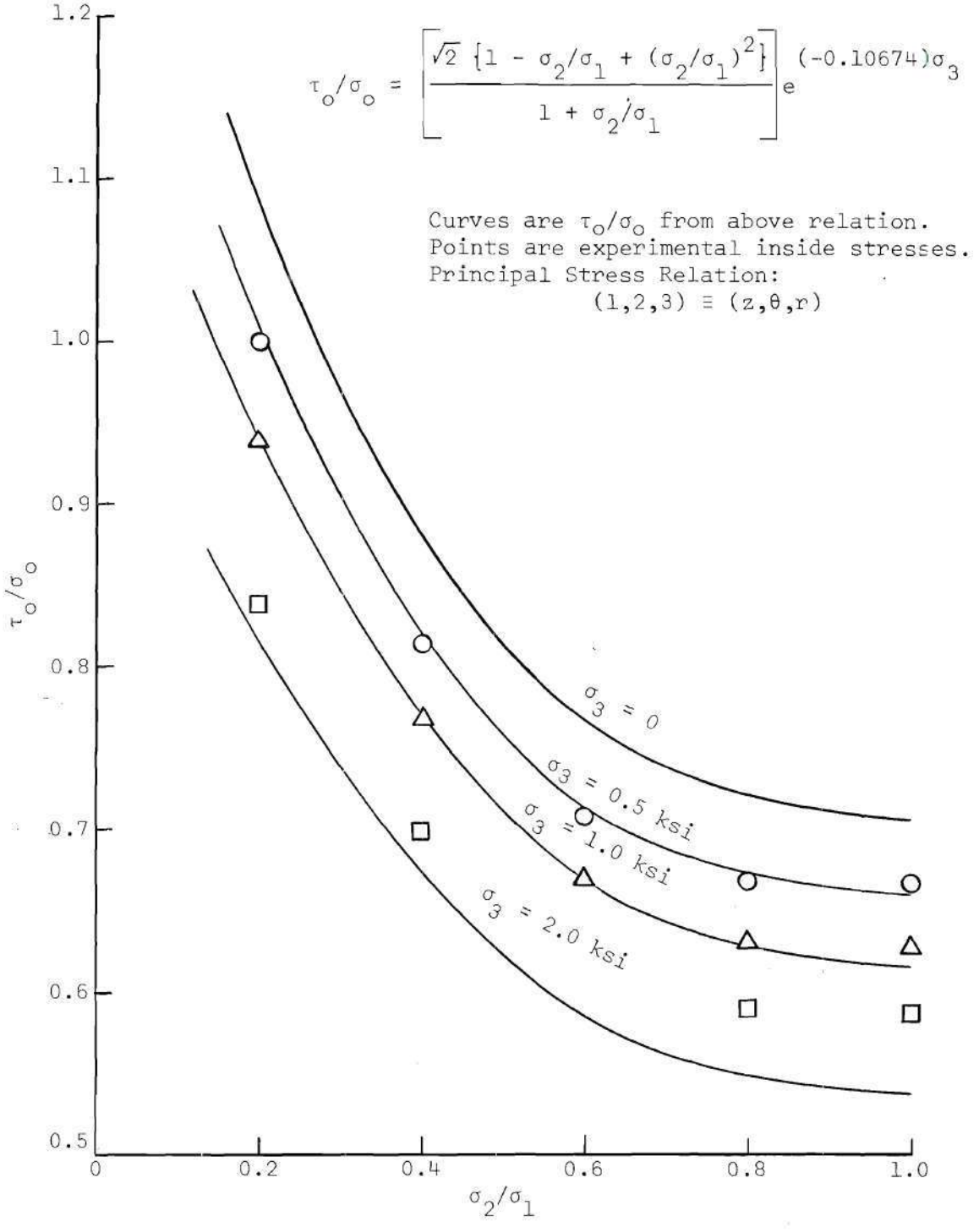

Figure 28. Strength Criterion in Terms of τ_o/σ_o, Indiana Limestone

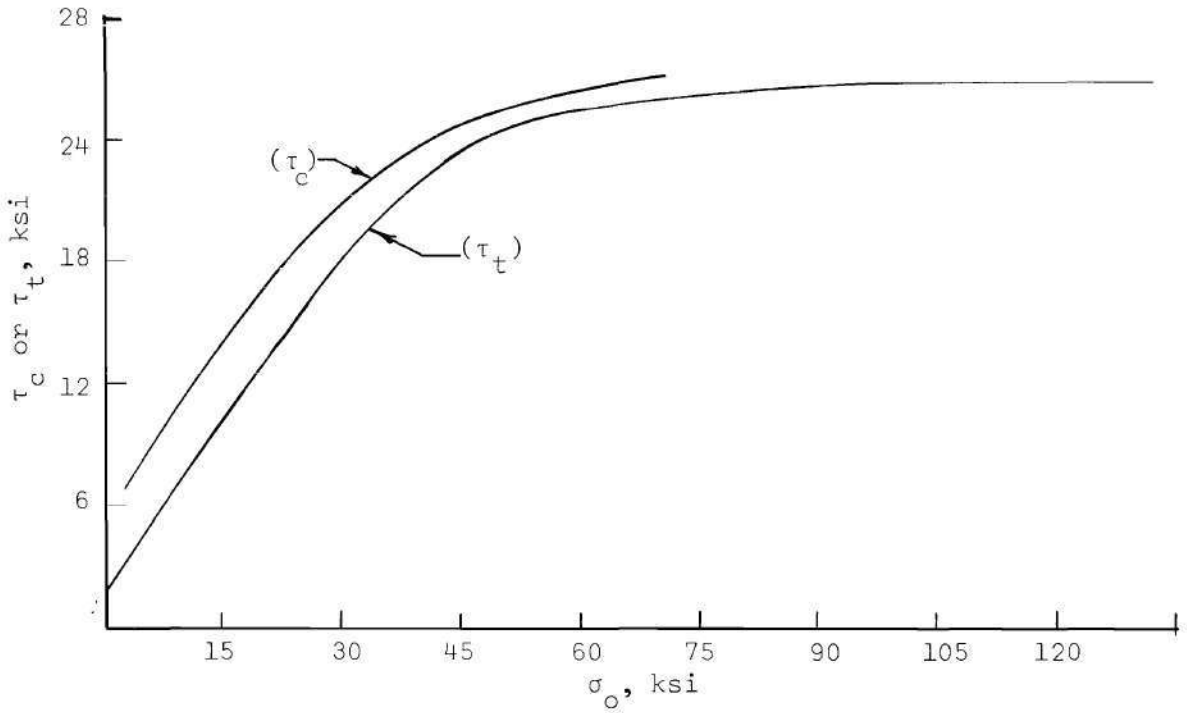

Figure 29. General Relation Between Octahedral Shear and Octahedral Normal Stresses for Marble, After Topping

Representation in Principal Stress Coordinates

The representation of results in principal stress coordinates is developed in the appendix. Failure envelopes in principal stress space for limestone and granite are shown in Figures 30, 31, and 32. The experimentally-determined values are contrasted with the von Mises, the Tresca and the Mohr relations. In the case of the Mohr diagram, it is assumed the "ϕ" is a constant for all values of σ_2/σ_1.

In order to analyze experimental data on this basis, it is necessary to either normalize the data to a particular value of σ_o or to use the contour method of presentation. The contour method is preferable if there is sufficient data with respect to various values of σ_o; however, this study did not include the control of octahedral stresses and, consequently, there are insufficient results for given values of σ_o to develop contours with respect to σ_o. Thus, it is expedient to use the normalization technique. The values of τ_o were normalized to the "unit plane" in the manner indicated previously (and as illustrated in the appendix).

For both the limestone and the granite, the normalized values of τ_o can be approximated by straight lines. In all cases, the "average" stress curves lie below the "inside" stress curves.

For the granite, the "average" stress curve falls considerably below the Mohr relation, while the "inside" stresses curve practically coincides with the Mohr relation.

For the limestone, the "average" stress curves more closely approximate the Mohr relation than do the "inside" stresses. The relative position of the curves can be demonstrated by determining the Mohr

ϕ which would be necessary to produce the experimental curves and contrasting it with the actual Mohr ϕ for the material. This is shown in Table 4.

Table 4. Contrast of Mohr ϕ Angles

Rock	Actual Mohr ϕ Deg.	Mohr ϕ to Generate Experimental Curve, Deg.	
		Inside Stresses	Average Stresses
Limestone (Series A)	26.5	13.5	29.5
Limestone (Series S)	31.1	10	26
Granite	54.9	56	> 90

A more reasonable comparison is on the basis of the ratio of the experimental value of τ_o to the Mohr τ_o for the case of $\sigma_2/\sigma_1 = 1.0$. This is shown in Table 5.

Table 5. Comparison of τ_o at $\sigma_2/\sigma_1 = 1.0$

Rock	Ratio of Experimental τ_o to Mohr τ_o	
	Inside Stresses	Average Stresses
Limestone (Series A)	1.158	0.974
Limestone (Series S)	1.288	1.082
Granite	0.988	0.814

These results clearly indicate that the materials do not behave as "Mohr materials." However, the granite, on the basis of the "inside" stresses, and the limestone, on the basis of average stresses, are clearly close to such behavior. The implications of this are: if one accepts the validity of the Mohr criterion, then stress calculations for weaker rocks such as the limestone should be based on average stresses, and for stronger rocks like the granite, the stress calculations should be based on "inside" stresses. In general, however, these results indicate that none of the three criteria considered can correctly predict the behavior of all rocks. For the less competent rocks, such as the limestone, the Mohr relation will be conservative. This is contrary to what might be expected, since the ϕ angle actually increases with increasing values of σ_2/σ_1. The Tresca and the von Mises relations overestimate the strength of the limestone.

For the more competent rocks, such as the granite, the Mohr relation can be considered a valid representation of the strength, while Tresca and Mises overestimate by a factor of at least 2 in the extreme case when $\sigma_2/\sigma_1 = 1.0$. The closeness of the experimental data to the Mohr plot probably reflects the insensitivity of the octahedral stresses to the relatively small σ_3 values used. It is possible that much larger values of σ_3 would result in an experimental curve which lies above the Mohr relation.

The stresses within a mass of rock in-situ are difficult to predict. Geologic disturbances have produced highly complex structures, and, in so doing, have induced states of stress which can not be calculated directly. Experimental techniques are available which provide

estimates of the magnitudes and directions of the in-situ principal stresses. Part of the uncertainty in the determination of the stresses is due to the necessity for complete stress relief in the mass very close to the point at which the stresses are determined. In addition, the rock mass is normally inhomogeneous, non-isotropic and non-intact.

Some of the same problems arise in connection with the determination of the strength parameters by means of laboratory tests. It is necessary to excavate masses of the rock from which smaller specimens are then procured. Thus, the rock specimen under test is subjected to almost complete stress relief prior to the testing operations. By the imposition of the confining pressures during the testing, we hope to either approximate the stress conditions in-situ or to generate stress states which provide a basis for a generalization of the strength parameters. Although considerable data has been collected by these means, there still exists uncertainties with respect to the influence of the stress history during the sampling and testing operations.

An approximation of the stresses existing within the earth can be made by assuming an increase in vertical stress of 1 psi per foot of depth below the ground surface. Thus, the confining pressures used in this work represent vertical stresses at depths from zero to 2000 feet below ground surface for the limestone and to 1500 feet in the case of the granite. In addition, the minimum stress in an excavation below ground is generally atmospheric or only slightly greater. Therefore, these results can apply to excavations much deeper, as well as to situations nearer the ground surface where, due to geologic disturbances, there exist lateral stresses greater than the vertical.

NOTE: x — Inside Stresses
● — Average Stresses
Principal Stress Relation: (1,2,3) = ≡ (z,θ,r)

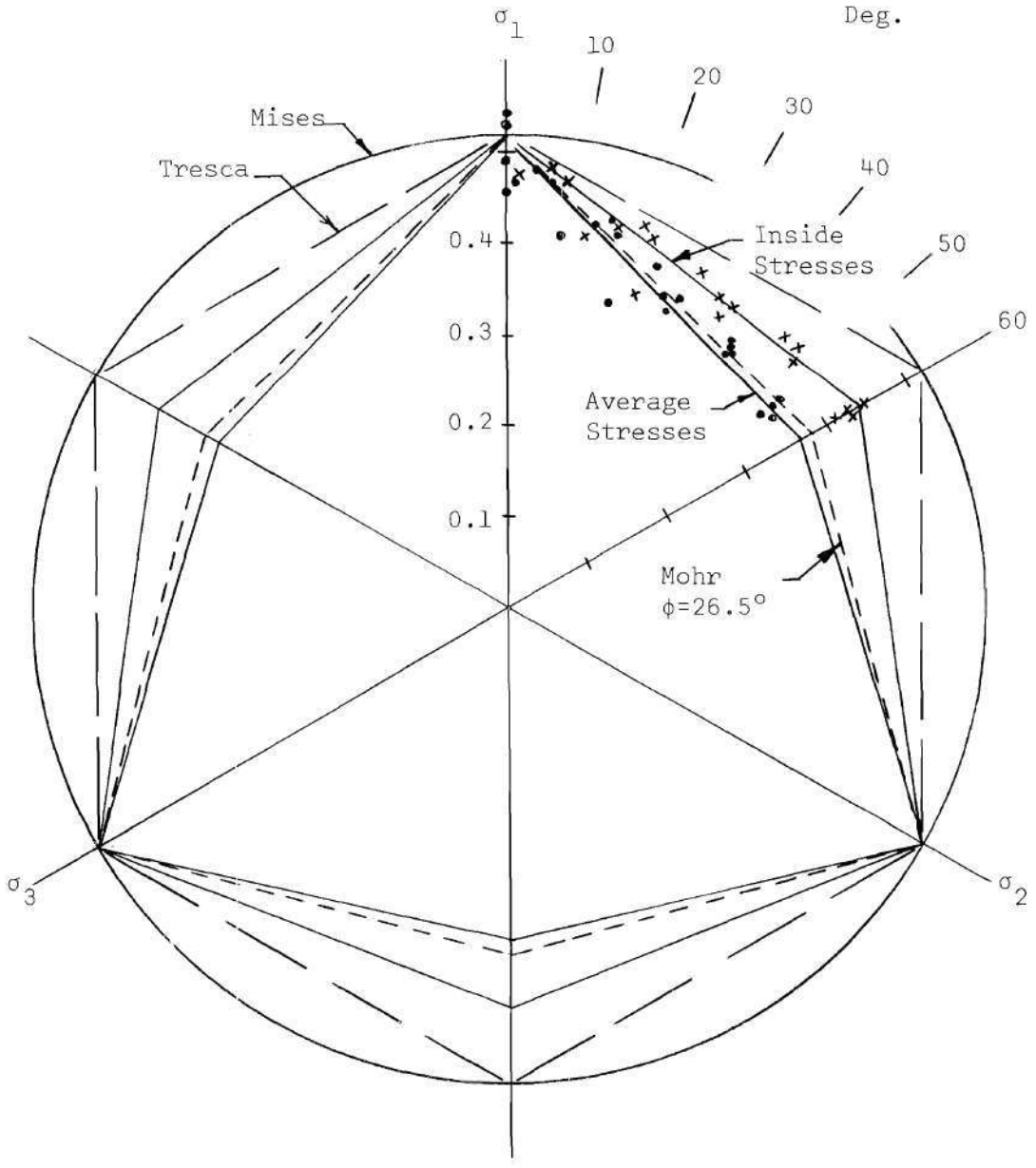

Figure 30. Indiana Limestone Test Results in Principal Stress Coordinates, Series A

NOTE: x — Inside Stresses
o — Average Stresses
Principal Stress Relation: (1,2,3) ≡ (z,θ,r)

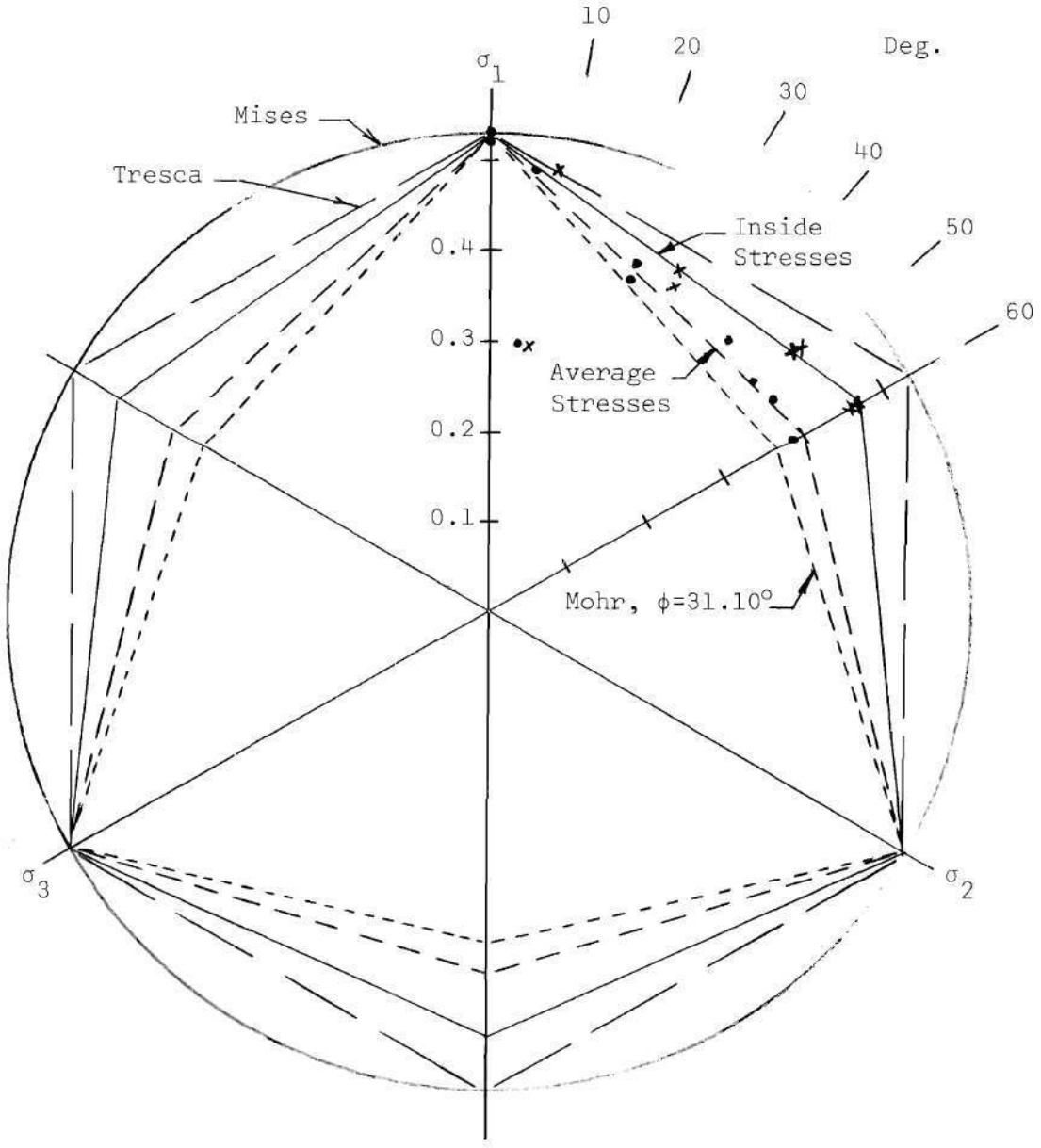

Figure 31. Indiana Limestone Test Results in Principal Stress Coordinates, Series S

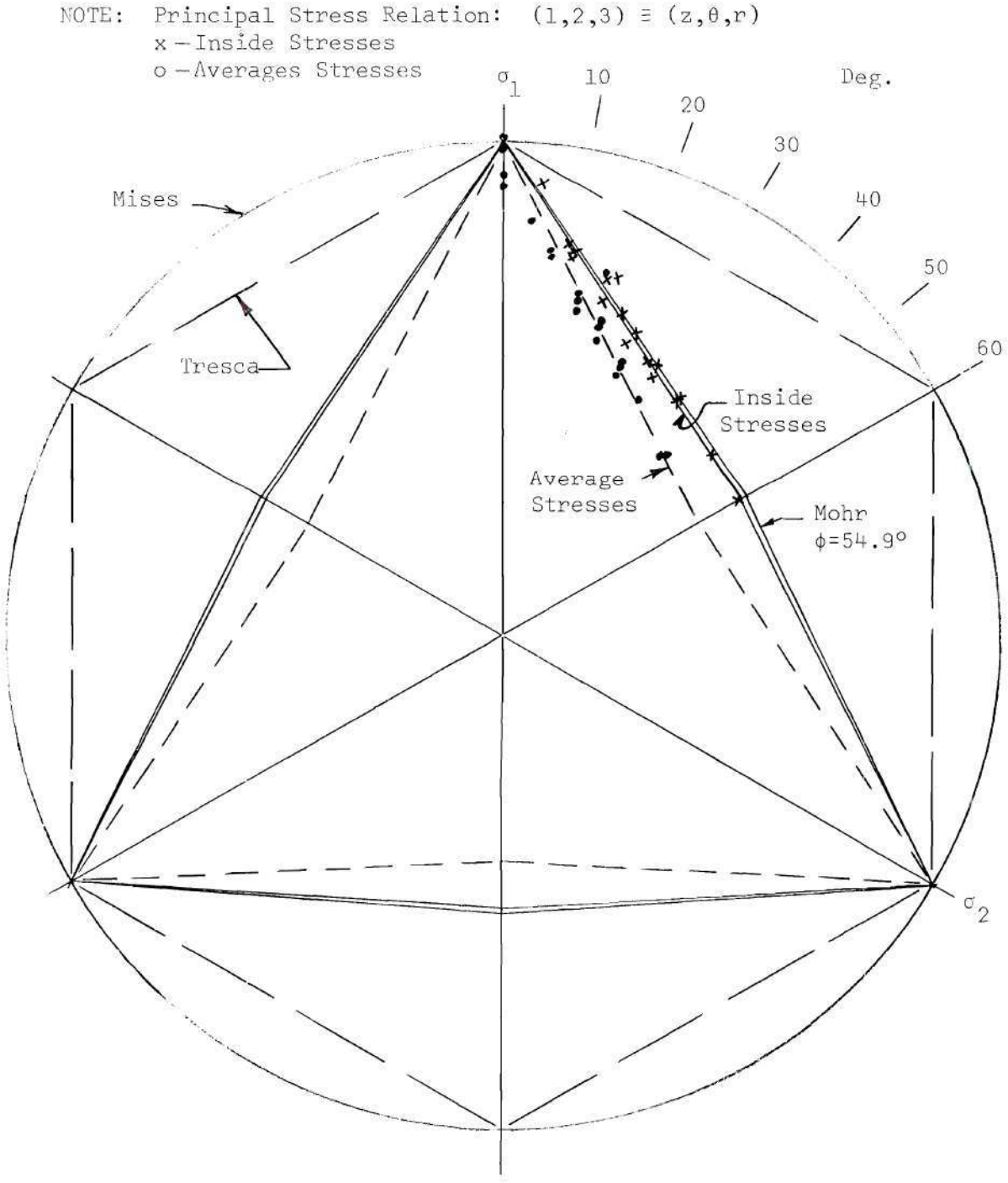

Figure 32. Granite Test Results in Principal Stress Coordinates

Rock Spalling

In a hollow cylinder, subjected to a combination of internal pressure, external pressure and axial load, there are stresses imposed in the axial, the radial and the tangential directions. Neglecting surface shearing stresses and assuming an elastic distribution of stresses, the radial (σ_r), the tangential (σ_θ) and the axial (σ_z) stresses are the principal stresses.

It has been amply demonstrated that rock (or other similar materials) will fail or rupture along some surface which generally bears some relation to the relative values of the principal stresses as well as to certain inherent properties or characteristics of the material. There will be an infinite number of potential failure surfaces, and the actual rupture surface will depend upon local irregularities or imperfections in the material which tend to either intensity the stresses or to cause a decrease in the strength, and, as a consequence, allow the formation of a rupture surface to develop.

For the usual type of triaxial specimen (a solid cylinder), two of the principal stresses are equal in value and there is no way to determine whether the rupture surface is developed perpendicular to a σ_2 plane or to a σ_3 plane. It seems reasonable, however, that if a specimen and a loading system combination is used which would allow the intermediate principal stress (σ_2) to be at some value between the major (σ_1) and the minor (σ_3) principal stresses, then the failure surface should be formed perpendicular to σ_2, all other factors being equal.

The hollow cylinder specimen with the previously described loading

conditions lends itself rather well to a study of the rupture phenomenon. Under such conditions, we may show the general failure pattern tendency between each pair of the principal stresses.

1. For the stress-pair, σ_z -- σ_r, there will be generated two systems of cones cutting each other at angles which are dependent upon the particular material properties and stress values. See Figure 32a. This type of failure is typified by the familiar "twin-cones" formed in an unconfined compression test of concrete or rock.

2. For the stress-pair, σ_θ -- σ_r, the stress differences produce two systems of curved surfaces which have spiral traces on a plane perpendicular to the axis of the cylinder cutting the radii at angles consistent with the material properties and stress state (Figure 33b).

3. The stress-pair, σ_θ -- σ_z, give rise to two families of helicoidal failure surfaces (Figure 33c). The pitch angle of the surfaces, and, consequently, the angle of intersection will be dependent on the material characteristics and the state of stress. This set of surfaces are recognized as Leuder's lines on the surface of cylindrical specimens.

The general character of the surfaces described in 1, 2, and 3 above are shown in Figure 33. The cracks are shown on the outer surface, a section through the axis and over a cross-section perpendicular to the axis as developed by failure in each case.

The surface of shear which actually develops will depend upon the relative values of the three principal stresses, and the shape may be influenced by the other sets of stress-pairs. On the assumption of no effect from other stress-pairs, a single type of failure surface

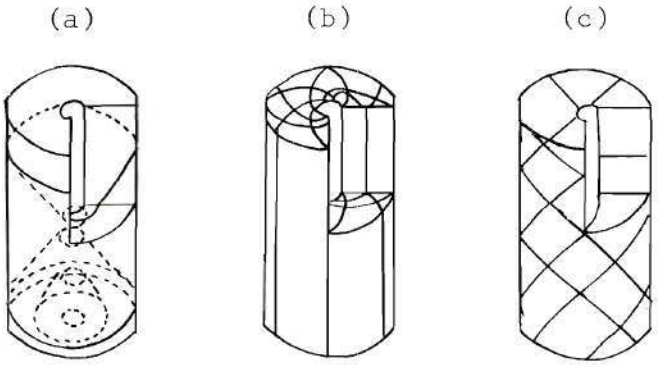

a. Axial-Radial $\sigma_z > \sigma_\theta > \sigma_r$

b. Tangential-Radial $\sigma_\theta > \sigma_z > \sigma_r$

c. Tangential-Axial $\sigma_\theta > \sigma_r > \sigma_z$

Figure 33. Failure Patterns for Pairs of Principal Stresses

would develop. Consider, for example, a case where failure is due to the σ_z -- σ_r system. The tendency would be to the formation of a single slip surface, but there exists a distinct possibility of narrow "rings" being broken off the interior surface (for the case where σ_r varies from a minimum at the interior surface to a maximum at the exterior). Next, consider the σ_θ -- σ_r system with σ_r = minimum and σ_θ = maximum at the interior. This *could* cause long "splinters" to chip from the interior surface.

If one considers the two systems, σ_z -- σ_r and σ_θ -- σ_r, together, it appears that the spalled-off rings or splinters could be broken into small splinters or individual "grains." Stress differences between the σ_z -- σ_θ pair would aggravate the tendency toward the formation of fine grains, or powder.

This situation has been observed by several investigators. Adams (3), working with hollowed-out cylinders of Solenhofen Limestone and Westerly Granite, subjected the cylinders to combined stresses by loading the cylinders axially while the specimens were constrained in a thick, steel, shrunk-fit jacket. Bridgeman (2) studied several rocks, as well as individual crystals of quartz, tourmaline, calcite, barite, feldspar and glass. The method of loading was by immersion of rubber-jacketed specimens in a fluid under pressure.

Both of the above hypothetical-failure-produced particle types were observed. Bridgeman noted, for andesite, "minute splinters" which were "projected with such violence when they had flaked off as to penetrate some distance into the solid brass and stick themselves in position." (The "solid brass" referred to a brass rod in the cavity which

supported a lead washer.) Both Adams and Bridgeman reported that ultimate failures were in the form of erosion of fine sand-sized particles, rather than by the development of a shear plane or even flow of the rock. Apparently there was sufficient erosion to completely fill the voids and thereby to prevent further deterioration of the specimen.

Similar behavior was observed by Robertson (20). He reported that spalling occurred for hollow cylinders subjected to hydrostatic pressure when the ratio of the outer to the inner radius of the specimens was greater than three. He concluded that the spalling was not a release mechanism, and he was able to completely close the specimens with continued application of hydrostatic pressure after the spalling was initiated.

Similar erosion or flaking was noted on specimens of granite in the present investigation. A photograph of one such specimen is shown in Figure 34. This particular specimen was exposed to stress conditions where the ratio of σ_2/σ_1 was approximately 0.88, and the test was terminated prior to complete failure. Similar distress was noted on other specimens even when the failure was complete. In Adams' work, it was not possible to determine the stress conditions with any degree of certainty, but in Bridgeman's experiments, the stress conditions were approximately:

$$\sigma_\theta = 2\,\sigma_z \quad \text{or} \quad \sigma_2/\sigma_1 = 0.50$$

$$\text{and,} \quad \sigma_r = 0 \ .$$

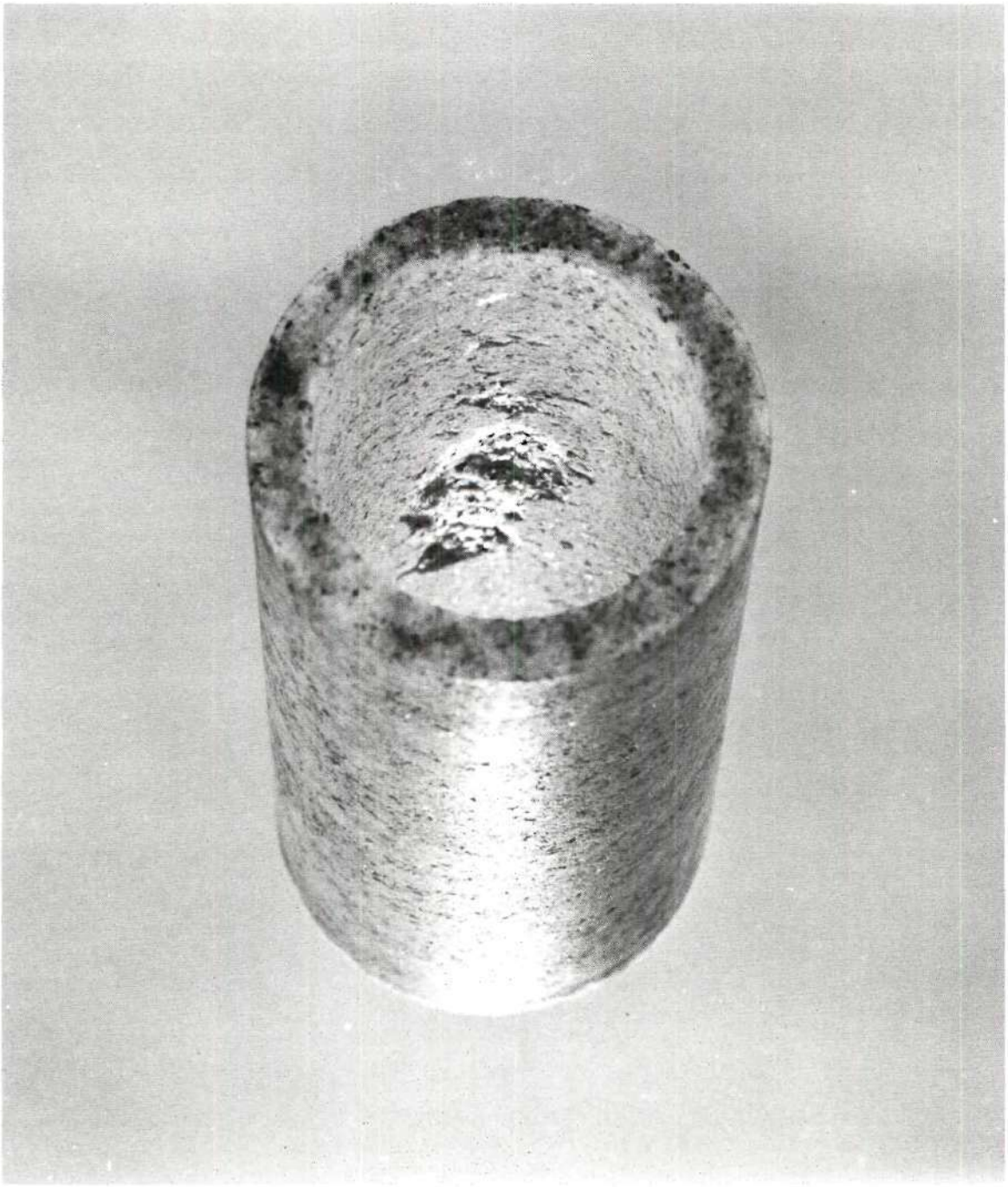

Figure 34. Spalling Inside Granite Cylinder Unloaded Prior to Fracture, $\sigma_3 = 0$ and $\sigma_2/\sigma_1 = 0.88$.

A summary of Bridgeman's results are shown in Table 6.

Table 6. Summary of Bridgeman's Tests on Hollow Rock Crystals

Crystal or Rock	Confining Pressure Kg/CM^2	Duration of Confining Pressure		Comments
Granite	5000	1	Hour	Cavity filled by flaking.
Limestone	5000	1	Hour	Cavity filled by flaking.
Andesite	6000	30	Minutes	Slight flaking.
	7000	9	Hours	Slight flaking.
	8000	5-1/2	Hours	Cavity filled by flaking.
Porphyry	6000	10	Minutes	Slight flaking.
	7000	10	Minutes	Cavity filled by flaking.
Barite	3300	6	Hours	Moderate flaking.
Feldspar	3000	40-1/2	Hours	Slight flaking.
	5000	4	Hours	Cavity filled by flaking.
	3000	15-1/2	Hours	Slight flaking.
Tourmaline	7000	10	Minutes	Minute longitudinal splinters.
	10,000	10	Minutes	Minute longitudinal splinters.
	12,000	2	Hours	Cavity filled by flaking.
Calcite	500	10	Minutes	Tendency to slip along many
	1000	10	Minutes	internal cleavage planes; became
	1500	10	Minutes	translucent; at 1500 some flaking; specimen fell apart prior to 2000 Kg/CM^2 pressure application.
Quartz				
No. 1	7500	10	Minutes	Slight flaking.
No. 2	8000	10	Minutes	Slight flaking.

It can be seen that the flaking phenomenon is dependent upon the material strength characteristics, having started in the calcite at 1500 kg/sq cm confining pressure, and not until 7500 kg/sq cm for the quartz. Bridgeman was at a loss to explain the very high stresses sustained by the hollow specimens as compared to the unconfined compressive strength of the same material. This result is undoubtedly due to the effect of the intermediate principal stress. Although the increase in failure strength in the present investigation is only about 4.5 to 5 times as great as the unconfined compressive strength, where Bridgeman indicates somewhat more of a strength gain. In the case of the granite, something on the order of a 5.0 to 5.5 increase is indicated. This difference might be partly due to specimen size or possibly due simply to the inherent differences in strength.

The degree of polish of the interior surface seems to be an important factor; however, its effect is apparently negligible until the polish is practically complete. Bridgeman found no tendency to flaking with natural, negative crystals of quartz, whereas the artificially formed cavities in the quartz did flake, even after being highly polished.

It seems appropriate, in the face of evidence of such "failures," to comment on the "extension" test with standard triaxial equipment and specimens. The flaking occurs from the σ_3 plane. In the case of hollow cylinders, even when jacketed internally and with internal confining pressure, this phenomenon is free (or relatively so) to take place. In the extension test, the flaking would have to occur from a small surface

area, the specimen end, which is supported by an unyielding surface (the end cap). Under such conditions, it seems reasonable that the flaking would be completely obscured, if not prevented entirely. The flaking "failure" appears to be of considerable importance since it can be compared to "rock bursts" in tunnelling operations and, consequently, additional study of the phenomenon seems in order.

Summary of Conclusions

The objectives of this work were: (1) to develop equipment for the testing of rock under controllable, three-dimensional loading, (2) to develop techniques for the production of specimens, and, (3) to evaluate the effect of the intermediate principal stress on the strength of intact rock.

As a result of this investigation, the following conclusions have been reached with respect to the two rocks tested:

1. The effect of the intermediate principal stress on the strength of intact rock can be evaluated with the use of equipment developed by this investigator and described in this report.

2. Suitable specimens for use with the equipment can be produced from intact rock blocks by coring with specially-designed core bits.

3. Triaxial cell capacity must be increased to at least 20,000 psi and perhaps higher in order to delineate strength parameters of the stronger rock.

4. Within the pressure ranges utilized, the strength can be represented by the following expression:

$$\tau_o/\sigma_o = \left[\frac{\sqrt{2}\ (1 - x + x^2)^{1/2}}{1 + x}\right] e^{-a\ \sigma_3}$$

where: a = 0.10674 for limestone

a = 0.0 for granite

$x = \sigma_2/\sigma_1$

σ_3 is in ksi.

5. In principal-stress coordinates, the failure envelope shape is closely represented by straight lines.

6. The Mohr failure surface criterion in principal stress coordinates is a more reasonable approximation of the actual failure surface than either the Tresca or the von Mises criteria. For rock similar in characteristics to the limestone used, the Mohr criterion will be conservative. For more competent rock, like granite, the Mohr criterion will closely predict the strength.

7. The Mohr ϕ angle is not a constant for rocks similar to the limestone. It is a function of the ratio σ_2/σ_1, and will increase approximately 12 degrees as σ_2 increases from zero up to the value of σ_1.

8. Rocks can "fail" by a mechanism called "spalling." This phenomenon apparently occurs when the ratio of σ_2 to σ_1 is relatively high, i.e., greater than 0.5.

CHAPTER X

RECOMMENDATIONS FOR FURTHER STUDY

There are good indications that the true load-deformation and strength parameters of rock can be determined by the use of equipment, specimens, and techniques like, or similar to, those used in this study. As is the case with all completely new or radically different testing methods, there are numerous questions to be answered before wide-spread usage of the methods can be accomplished. Some of the problems needing attention are:

1. Effects of Specimen Size. Although the results presented here are quite promising, there was no effort made to determine the possible effects of varying the relation between the length, external diameter, and the wall thickness of the hollow cylinders. A systematic study of these variables would be quite appropriate.

2. Effects of Equipment. There is need for an evaluation of the effects produced on the specimens and consequently on the failure strength by the end caps. End-cap configurations other than that utilized at present could be investigated, as well as various lubricants or friction-reducing elements. A photoelastic study would be of considerable value in visualizing the stress distributions within the specimens.

3. Effects of Testing Techniques. A limited amount of work was done with respect to differences in results obtained due to the

variation in the stress paths prior to failure. There is a definite possibility that the stress history could alter the structure and/or the bonding of the rock under study and produce, as a consequence, drastic differences in results obtained by a given method.

4. Analysis of Stresses. The analysis of the stress distribution at failure in the study of rock strength is obviously quite important. Completely irrelevant and misleading conclusions can be drawn on the basis of improper decisions with respect to the stress distribution. The choice of an elastic analysis is an expediency, and it is evident that the stresses at failure may never have corresponding values. Comprehensive studies should be undertaken to explore the usage of other than elastic models for analysis. This could include an experimental program in conjunction with a theoretical analysis.

5. Extension of Equipment Capabilities. The present fluid-pressure capacity is not sufficient to perform exhaustive test programs on even the weak rocks. Fluid pressures of at least 20,000 psi working pressures are necessary. Provision for making pore pressure studies would be of considerable value.

6. Study of Flaking Rupture Phenomena. A detailed investigation of the flaking action seems to be warranted. Such study could possibly be combined with work concerned with time effects at stresses below, but close to, the short-term rupture strength.

7. Study of Fractured Rock. There appears to be a distinct possibility that fractured rock specimens can be successfully tested in the present apparatus. Specimens could contain natural flaws or purposely induced cracks.

APPENDIX

Octahedral Stresses

The state of stress in a solid body may be completely defined in terms of the three principal stresses and their directions. When the body is isotropic, the directions of the individual stresses become redundant and it is sufficient to define the resultant stress by specifying only the three principal stresses. Since the main theme of this paper is related to homogeneous and isotropic solids, the treatment of other conditions will be included only in a superficial manner.

Haigh (26) and Westergaard (27) utilized the three principal stresses as coordinate axes in order to represent the state of stress in a solid body. Each point in this stress space corresponds to a particular state of stress. One such stress state is indicated in Figure 35. For an isotropic body where the three principal stress directions are equivalent, a given state of stress is represented by six different points which are obtained by permutation of the three principal stresses. Using the notation, σ_I, σ_{II}, σ_{III}, for the principal stresses where no distinction is made respecting the relative magnitudes of the stresses, an example of the six points just mentioned is shown in Table 7.

Table 7. Points Illustrating Equivalent Stress States

Point	σ_I	σ_{II}	σ_{III}
1	X	Y	Z
2	X	Z	Y
3	Y	X	Z
4	Y	Z	X
5	Z	X	Y
6	Z	Y	X

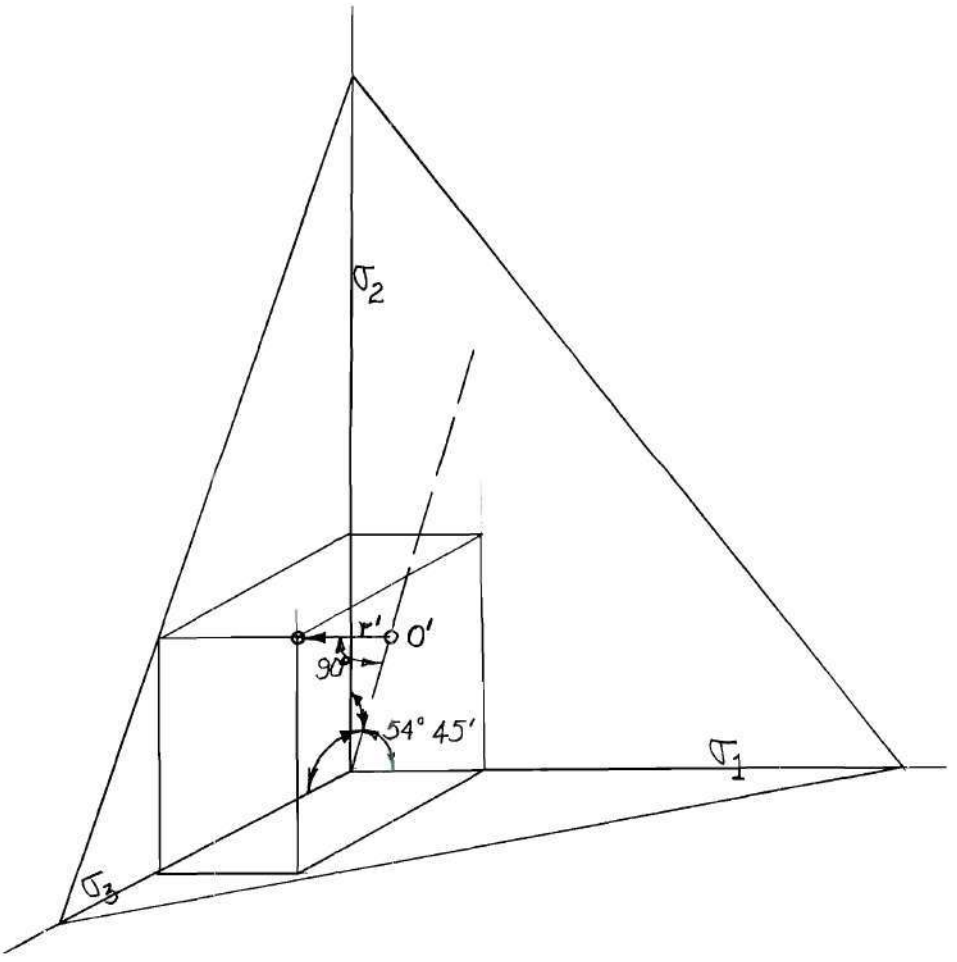

Figure 35. State of Stress Represented in Principal Stress Coordinates

All six points are contained in a plane given by $\sigma_I + \sigma_{II} + \sigma_{III} =$ Constant, which is normal to the space diagonal $\sigma_I = \sigma_{II} = \sigma_{III}$ of the positive octant (Figure 36).

If all possible combinations of the plus and minus signs are considered, there will be eight inclined planes passing through the stress point whose normals, n, have the direction cosines

$$\cos(n, \sigma_I) = \pm 1/\sqrt{3}$$

$$\cos(n, \sigma_{II}) = \pm 1/\sqrt{3}$$

$$\cos(n, \sigma_{III}) = \pm 1/\sqrt{3}$$

These eight planes which pass through the stress point may be visualized better when redrawn in the form of a regular octahedron around the point. The acute angles formed between the normals to the octahedral planes and the coordinate axes are equal to

$$\text{arc cos } 1/\sqrt{3} = 54^\circ\ 45'$$

Referring to Figure 37, it can be seen that the projection onto the octahedral plane of one of the principal stresses, σ_1 for example, produces a vector $O'\ \sigma_1'$. The length of $O'\ \sigma_1'$ is equal to $\sigma_1 \cdot \sqrt{2/3}$. The *direction* of the projection, $O'\ \sigma_1'$, corresponds to the direction of the octahedral shearing stress caused by the application of the principal stress, σ_1, on its principal plane. Obviously, the octahedral

Point	σ_I	σ_{II}	σ_{III}
1	X	Y	Z
2	X	Z	Y
3	Y	X	Z
4	Y	Z	X
5	Z	X	Y
6	Z	Y	X

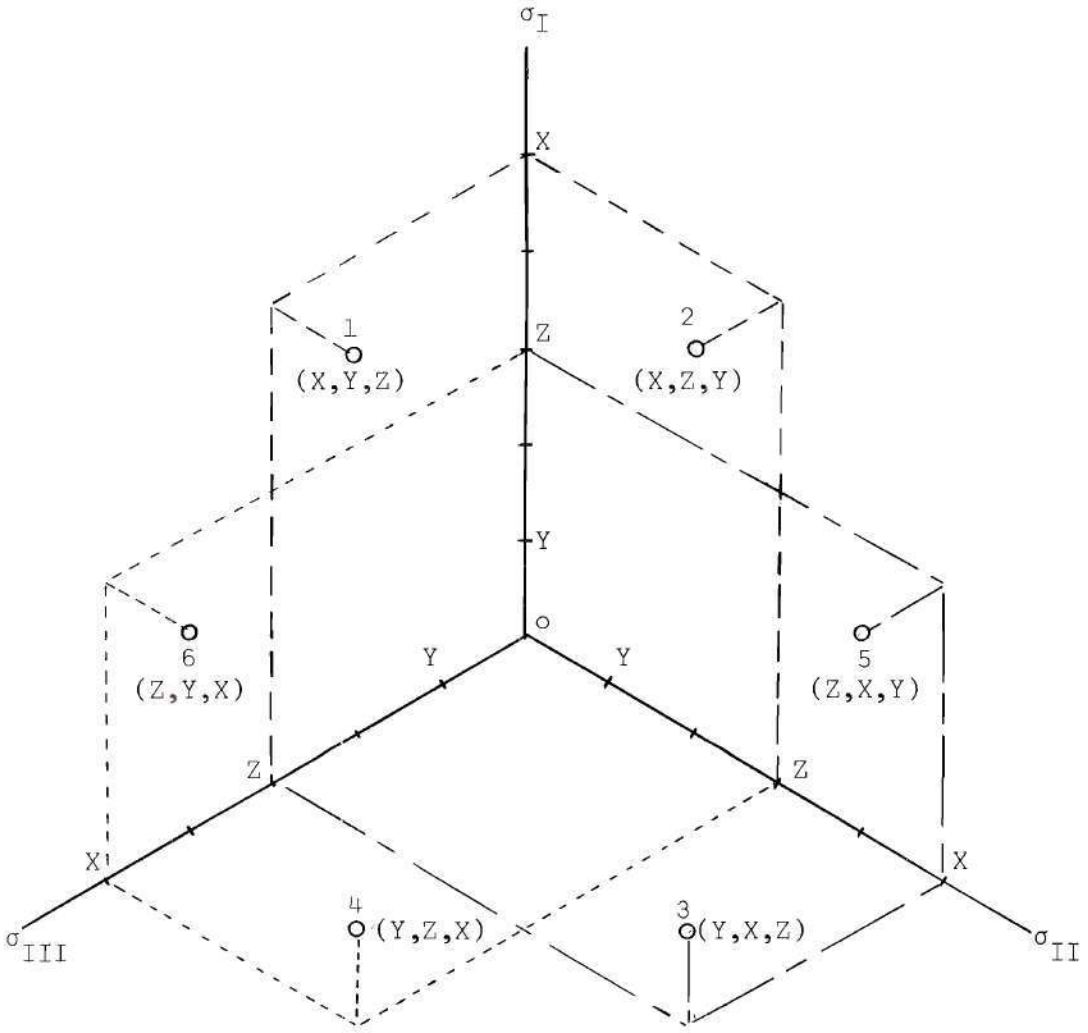

Figure 36. Equivalent States of Stress in an Isotropic Body

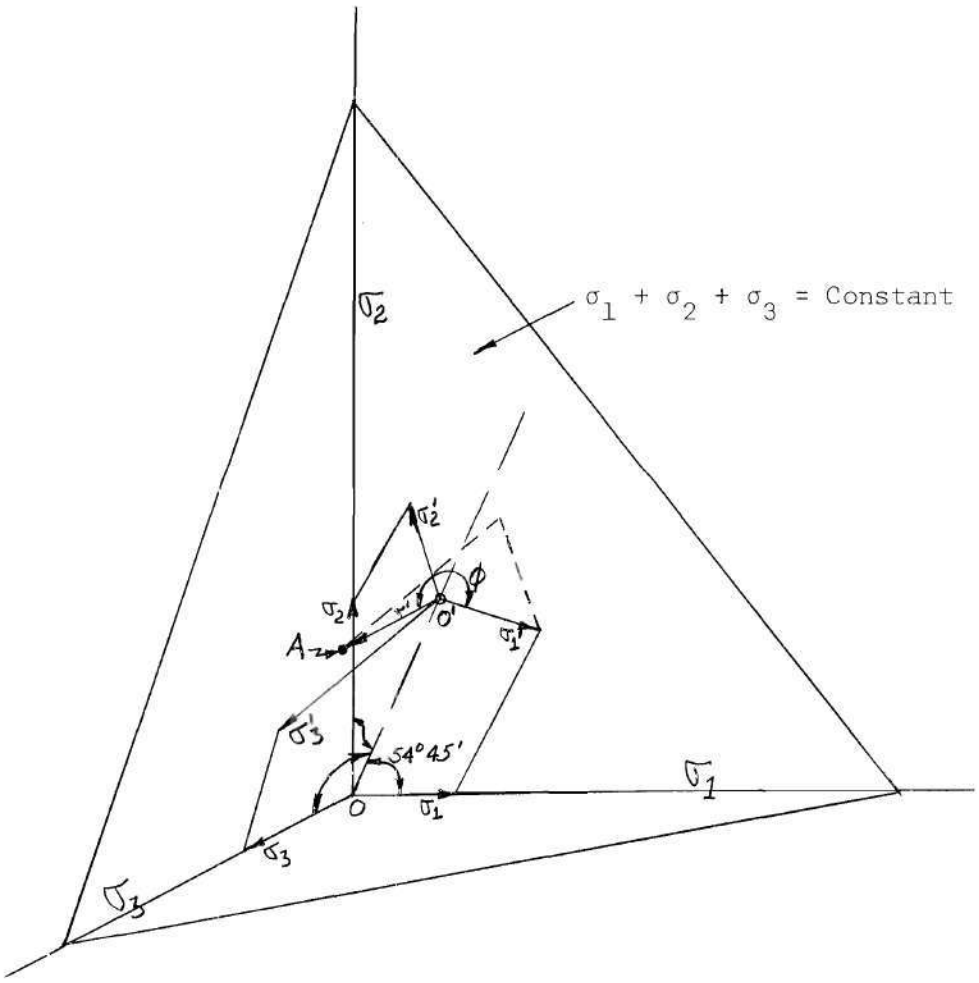

Figure 37. Representation of Octahedral Stresses

normal stress due to σ_1 acts in the direction 0 0' where 0' is the projection of the origin 0 onto the octahedral plane.

The lengths of the lines 00' and 0' σ_1' then can represent, graphically, the octahedral normal stress, σ_o, and the octahedral shear stress, τ_o. The actual values of

$$\sigma_o = \frac{\sigma_1 + \sigma_2 + \sigma_3}{3}$$

and of

$$\tau_o = \frac{1}{3}\left[(\sigma_1 - \sigma_2)^2 + (\sigma_2 - \sigma_3)^2 + (\sigma_3 - \sigma_4)^2\right]^{1/2} .$$

Since, however, the *true* component of the octahedral stress, τ_o, which acts in the direction of the σ_1 axis is $\sigma_1/\sqrt{3}$, rather than σ_1, 00' will actually be equal to $\sigma_0 \cdot \sqrt{3}$ and 0' σ_1' will equal $\tau_o \cdot \sqrt{3}$.

Considering all three principal stresses, the vectorial addition of the stress projections produce the vectors 00' and r', which represent the resultants σ_o and τ_o, each increased by a factor of $\sqrt{3}$. The angle θ indicates the direction, on the octahedral plane, of τ_o. In this representation, the expressions for the polar coordinates of the resultant point can be calculated to be:

$$r' = \frac{1}{\sqrt{3}} \cdot \left[(\sigma_1 - \sigma_2)^2 + (\sigma_2 - \sigma_3)^2 + (\sigma_3 - \sigma_1)^2\right]^{1/2}$$

$$\theta = \arctan \sqrt{3} \cdot \frac{(\sigma_2 - \sigma_3)}{(\sigma_1 - \sigma_2) - (\sigma_3 - \sigma_1)}$$

Mehldahl (27) showed the convenience of representing the coordinates axionometrically, employing the normal isometric projection (Figure 38). In this representation, the space diagonal $\sigma_1 = \sigma_2 = \sigma_3$ is normal to the plane of projection and is, therefore, projected onto the origin. The three positive coordinate axes make angles of 120° with one another and represent projections of the three planes of symmetry, $\sigma_1 - \sigma_2 = 0$, $\sigma_2 - \sigma_3 = 0$ and $\sigma_3 - \sigma_1 = 0$.

In this projection, the length scale of the three principal stresses is shortened in the ratio $\sqrt{2/3}$. Since this shortening is made on all axes, it is convenient to disregard this factor and to set off the three principal stresses directly along the three axes, making angles of 120° with one another. The length, r', is then increased in the ratio $\sqrt{3/2}$ and,

$$r' = \frac{1}{\sqrt{2}} \cdot [(\sigma_1 - \sigma_2)^2 + (\sigma_2 - \sigma_3)^2 + (\sigma_3 - \sigma_1)^2]^{1/2}$$

$$= [\sigma_1^2 + \sigma_2^2 + \sigma_3^2 - \sigma_1 \sigma_2 - \sigma_2 \sigma_3 - \sigma_3 - \sigma_1]^{1/2}$$

If we now utilize axes with scale of $\frac{\sqrt{2}}{3}\sigma_1$, $\frac{\sqrt{2}}{3}\sigma_2$ and $\frac{\sqrt{2}}{3}\sigma_3$, it will be apparent that the new vector

$$r' = \frac{1}{3}[(\sigma_1 - \sigma_2)^2 + (\sigma_2 - \sigma_3)^2 + (\sigma_3 - \sigma_1)^2]^{1/2},$$

which is the true value of τ_o. The angle θ remains the same. It is sometimes convenient to employ the X and Y components of r' which are

$$X = \frac{1}{\sqrt{6}} (\sigma_2 - \sigma_3)$$

$$Y = \frac{1}{3\sqrt{2}} [(\sigma_1 - \sigma_2) - (\sigma_3 - \sigma_1)]$$

It has been found, experimentally, that rock-like materials can behave differently (fail at *different values* of τ_o) for *identical values* of σ_o. Therefore, in order to compare the relationship of the octahedral stresses at failure for different states of stress, it is necessary to consider the *direction* of the resultant failure stresses as well as the relative magnitudes.

The relationship between certain states of stress, as indicated by Mohr stress circles, and the direction of τ_o are shown in Figure 39. Considering the usual designation of σ_1, σ_2, and σ_3, with respect to the absolute value of the three, it is apparent that the curve generated by connecting the terminal points of the τ_o vectors will be symmetrical about a given principal stress axis and, therefore, only a 60° sector of the space need be investigated. If a series of tests are performed on a given material, in which series the state of stress varies (while holding σ_o constant) from test to test so that a 60° sector is covered, a "failure surface" is generated. By other test series, similarly conducted but with σ_o at other values, additional surfaces can be determined. These curves will form a series of "contour lines" about the origin. The separation between the contour lines is an indication of the shape of the failure envelope in Principal Stress space with respect to the distance from the origin. Equal

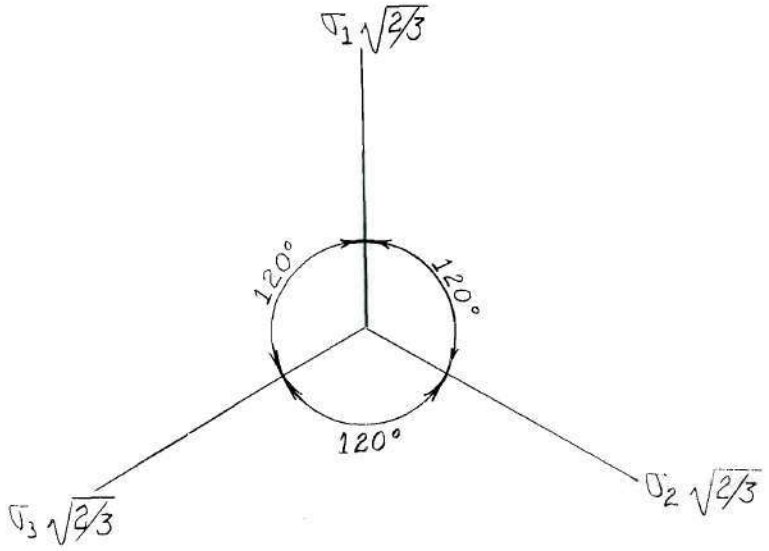

Figure 38. Meldahl's Isometric Projection of Principal Stress Coordinates

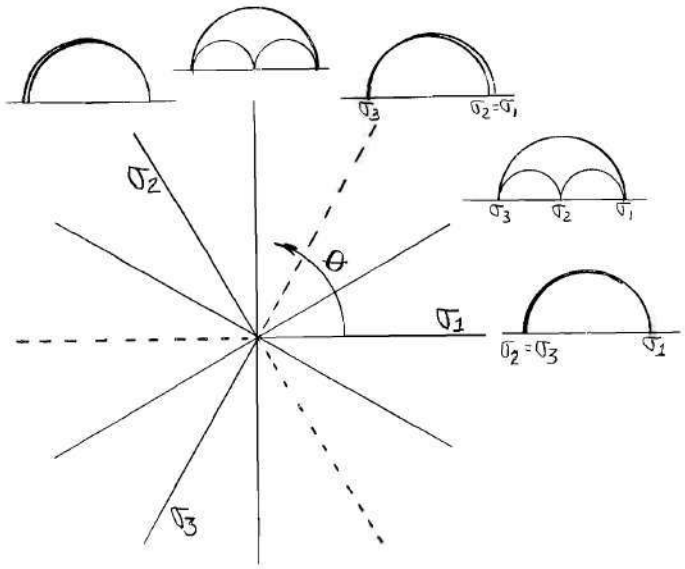

Figure 39. Correlation of Mohr's Circles with Principal Stress Coordinates

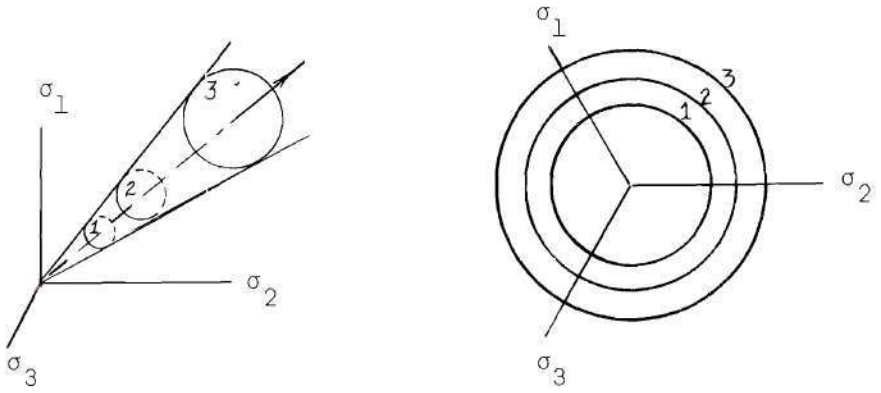

Figure 40. Right, Conical Failure Envelope in Principal Stress Coordinates

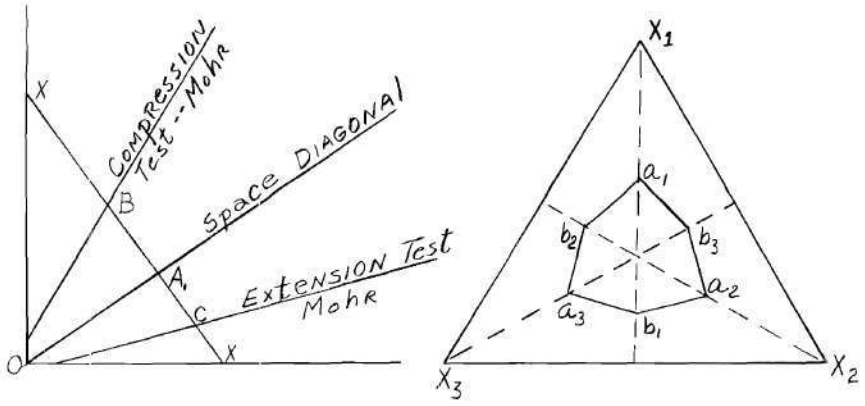

Figure 41. Mohr-Coulomb Failure Criterion in Principal Stress Coordinates

spacing between contour lines (for equal increments of σ_o) would indicate, for example, a straight-line envelope in Principal Stress Coordinates. This is illustrated in Figure 40 for a right, conical envelope.

The τ_o values for different value of σ_o can be represented by a single curve referenced to a specific value of σ_o, provided the proper normalization factor is used.

Failure Criteria

At present, there are three failure criteria which appear to be most useful. These are: (1) the Mohr, (2) the Tresca, and (3) the von Mises.

The Mohr Criterion

The Mohr criterion expressed in terms of principal stresses is

$$(\sigma_1 - \sigma_3) = 2c \cos\phi + (\sigma_1 + \sigma_3) \sin\phi \qquad (x\text{-}1)$$

when the envelope is a straight line with an inclination of ϕ and intercept "c." This implies that the Coulomb failure conditions are valid and Eq. x-1 becomes the Mohr-Coulomb failure condition. The failure lines are shown on a section of symmetry in principal stress space on the basis of no dependency on the value of the intermediate principal stress, i.e., that ϕ and c are constant. It should be noted that the distances AB and AC are not equal and that these distances correspond to τ_o for compression and extension, respectively. The points B and C correspond to points a_1 and b_1 in Figure 41, the right

section X-X. On this "octahedral plane" the points of penetration by the three axes are indicated by x_1, x_2, and x_3. Points a_2, b_2, a_3 and b_3 are obtained in a manner similar to a_1 and b_1. Since, mathematically, straight lines joining points $a_i b_i$ represent failure conditions for intermediate values of σ_2, the complete Mohr-Coulomb failure surface is a pyramid with an irregular hexagonal base. The equation of the surface is

$$[(\sigma_1 - \sigma_2)^2 - \{2c \cos \phi + (\sigma_1 + \sigma_2)\sin \phi\}^2] \times \qquad (x\text{-}2)$$

$$[(\sigma_2 - \sigma_3)^2 - 2c \cos \phi + (\sigma_2 + \sigma_3)\sin \phi\}^2] \times$$

$$[(\sigma_3 - \sigma_1)^2 - \{2c \cos \phi + (\sigma_3 + \sigma_1)\sin \phi\}^2] = 0$$

which is a combination of six equations similar to Eq. (x-1).

The Extended Tresca Criterion

If $\phi = 0$, the Mohr-Coulomb criterion becomes

$$\sigma_1 - \sigma_3 = C' \qquad (x\text{-}3)$$

and five corresponding equations. These, when combined into a single equation produce an equation similar to Eq. (x-2). This generates a regular hexagonal prism in three-space with a corresponding hexagon as the right section.

The Extended Tresca condition is based on the failure condition

$$(\sigma_1 - \sigma_3) = C + \bar{\mu}\,\sigma_o \qquad (x\text{-}4)$$

and the five corresponding equations. These produce a failure surface which is a pyramid with a regular hexagonal right section.

The Extended von Mises Criterion

Based on theoretical and experimental investigations by von Mises and others, the von Mises failure condition

$$(\sigma_1 - \sigma_2)^2 + (\sigma_2 - \sigma_3)^2 + (\sigma_3 - \sigma_1)^2 = \text{Constant} \qquad (x\text{-}5)$$

has been extended and presented in the form

$$(\sigma_1 - \sigma_2)^2 + (\sigma_2 - \sigma_3)^2 + (\sigma_3 - \sigma_1)^2 = [c + \tfrac{\bar{\mu}}{3}\,\sigma_o]^2 \qquad (x\text{-}6)$$

In principal stress space, this produces a cone, symmetrical with the space diagonal, whose right section is a circle which circumscribes the Tresca hexagon.

The three failure surfaces described in the preceding paragraphs are indicated in Figure 2.

Stress Distribution in Hollow Cylinders

The solution of two-dimensional stress problems for homogeneous, isotropic bodies involves the integration of the differential equations of equilibrium together with the compatibility equation and the boundary conditions.

Complete solutions of the general case, as well as for specific

cases, are given in S. Timoshenko and J. Goodier (29).

As shown therein, for an axially symmetric problem, such as that of a hollow cylinder under internal and external pressure, the equilibrium equations reduce to

$$\frac{d\,\sigma_r}{dr} + \frac{1}{r}(\sigma_r - \sigma_\theta) + R = 0, \quad T = 0$$

where: σ_r is the radial stress

σ_θ is the tangential stress

R is the radial body force

T is the tangential body force

the compatibility relation can be simplified to

$$\frac{1}{r}\frac{d}{dr}\{r\frac{d}{dr}[\frac{1}{r}\frac{d}{dr}(r\frac{dF}{dr})]\} = 0$$

where: F is the Airy Stress Function, $F = F(r)$.

Integration of the preceding formula produces

$$F = A \log r + Br^2 \log r + Cr^2 + D$$

where A, B, C, and D are arbitrary constants of integration which are determined by boundary conditions.

The stress components

$$\sigma_r = \frac{1}{4}\frac{dF}{dr}$$

$$\sigma_\theta = \frac{d^2F}{dr^2}$$

then become

$$\sigma_r = \frac{A}{r^2} + B(1 + 2 \log r) + 2C$$

$$\sigma_\theta = -\frac{A}{r^2} + B(3 + 2 \log r) + 2C$$

and for a doubly-connected body, such as a cylindrical ring, the constant $B = 0$ and the stress components reduce to

$$\sigma_r = \frac{A}{r^2} + 2C$$

$$\sigma_\theta = -\frac{A}{r^2} + 2C$$

For a thick-walled cylinder with inner radius, a, outer radius, b, and with internal pressure, P_i, and external pressure, P_o, the boundary conditions are

$$\sigma_r = -P_o \quad \text{for} \quad r = b$$

$$\sigma_r = -P_i \quad \text{for} \quad r = a$$

these yield

$$A = \frac{a^2 b^2 (P_o - P_i)}{b^2 - a^2}$$

$$2C = \frac{P_i a^2 - P_o b^2}{b^2 - a^2}$$

and

$$\sigma_r = \frac{a^2 b^2 (P_i - P_o)}{(b^2 - a^2)} \cdot \frac{1}{r^2} - \frac{(a^2 P_i - b^2 P_o)}{(b^2 - a^2)}$$

$$\sigma_\theta = \frac{a^2 b^2 (P_i - P_o)}{(b^2 - a^2)} \cdot \frac{1}{r^2} + \frac{(a^2 P_i - b^2 P_o)}{(b^2 - a^2)}$$

The derivation was carried out on the basis of tensile stresses being positive. The final form of the relations has been changed so that compressive stresses are positive.

In order to consider the effect of an axial load acting on a right circular cylinder, in addition to the internal and external pressures, it is necessary to utilize the "principle of superposition" (29). This is justified on the basis that the deformations under the loads do not substantially affect the action of the external forces.

Data for Indiana Limestone
Series A
Fluid Pressures and Inside Stresses at Failure (psi)

Test No.	p_o	p_i	σ_1	σ_2	σ_3	σ_o	τ_o
A-1	300	0	6890	1380	0	2760	2980
A-2	600	0	6870	2750	0	3200	2820
A-3	1050	0	9660	4830	0	4830	3940
A-4	1250	0	9550	5730	0	5090	3920
A-5	1750	0	10000	8000	0	6010	4320
A-11	2000	0	9160	9160	0	6110	4320
A-6	800	500	9400	1880	500	3930	3910
A-7	1300	500	10400	4160	500	5020	4100
A-9	1700	500	10000	6000	500	5500	3890
A-8	2500	500	12070	9655	500	7410	4980
A-10	3250	500	13110	13110	500	8910	5950
A-12	1250	1000	10750	2150	1000	4630	4350
A-13	1850	1000	12250	4900	1000	6050	4660
A-14	2400	1000	12350	7410	1000	6920	4650
A-15	3150	1000	13550	10840	1000	8460	5380
A-16	3820	1000	13290	13290	1000	9610	6060
A-18	2070	2000	11750	2350	2000	5370	4570
A-17	2800	2000	14150	5660	2000	7270	5090
A-20	4600	2000	17350	13880	2000	11080	6560
A-19	5350	2000	17340	17340	2000	12230	7240
A-21	0	0	6300	0	0	2100	2970
A-22	2000	2000	14450	2000	2000	6150	5870
A-23	2000	2000	13610	2000	2000	5870	5470
A-24	2000	2000	14610	2000	2000	6000	5670
A-25	3000	3000	16700	3000	3000	8900	6460

Data for Indiana Limestone
Series S
Fluid Pressures and Inside Stresses at Failure (psi)

Test No.	p_o	p_i	σ_1	σ_2	σ_3	σ_o	τ_o
1	393	250	4510	900	250	1890	1880
2	1257	250	9720	4860	250	4940	3870
3	2525	250	13330	10670	250	8080	5650
4	3208	250	13800	13800	250	9610	6390
5	840	500	10290	2060	500	4280	4290
6	1647	500	11500	5750	500	5920	4490
7	3810	500	13840	11070	500	8470	5750
8	3520	500	14320	14320	500	9870	6510
9	0	0	6370	0	0	2120	3000
10	500	500	8880	500	500	3290	3950
11	1000	1000	10440	1000	1000	4150	4450
12	2000	2000	12690	2000	2000	5560	5040
13	Solid	0	6010	0	0	2000	2830
14	Solid	500	9890	500	500	3630	4430
15	Solid	1000	10300	1000	1000	4100	4380
16	Solid	2000	13510	2000	2000	5840	4480

NOTE: Test Nos. 1 through 8 are averages of three tests.

Data for Granite
Fluid Pressures and Inside Stresses at Failure (psi)

Test No.	p_o	p_i	σ_o	σ_o	σ_o	σ_o	τ_o
1	0	0	16000	0	0	5330	7540
27	620	0	28350	2480	300	10380	12740
26	3000	0	47270	12000	1500	20260	18240
23	4800	0	57500	19200	2400	26370	23060
31	6500	0	59400	26000	3250	29550	23055
25	7500	0	57150	30000	3750	30300	21800
24	9600	0	54750	38400	4800	32650	20790
50	9500	0	53430	38000	4750	32060	20310
33	500	500	27300	500	500	9430	12630
29	2800	500	55000	9700	1650	22120	23480
30	6500	500	70000	23500	3500	32330	27860
32	8000	500	69600	30500	4250	34780	26850
43	10000	500	73200	38500	5250	35650	28160
42	2750	1000	46350	8000	1870	18740	19680
39	4840	1000	62100	16360	2920	27130	25340
34	7400	1000	84500	26600	4200	38430	38040
44	6100	1000	48840	21400	3550	24600	18630
46	3700	1500	58150	10300	2600	23680	24570
49	4900	1500	56750	15100	3200	25020	22960
48	5750	1500	52400	18500	3620	24840	20410

REFERENCES

1. Terzaghi, K., "Stress Conditions for the Failure of Saturated Concrete and Rock," *American Society for Testing and Materials Proceedings*, Vol. 45, 1945, pp. 777-801.

2. Bridgeman, "The Failure of Cavities in Crystals and Rocks under Pressure," *American Journal of Science*, Vol. 45, pp. 243-268, 1918.

3. Adams, F. D., "An Experimental Contribution to the Question of the Depth of the Zone of Flow in the Earth's Crust," *The Journal of Geology*, Vol. 20, pp. 97-118, 1912.

4. Nadai, A., *Theory of Flow and Fracture of Solids*, McGraw-Hill Book Company, New York, 1950, pp. 230.

5. Nadai, A., "Theories of Strength," *Journal of Applied Mechanics*, Vol. 1, No. 3, pp. 111-129, 1933.

6. Silverman, I. K., "Behavior of Materials and Theories of Failure," *Second Symposium on Rock Mechanics*, Golden, Colorado, 1957, pp. 3-17.

7. Kjellman, W., "Report on Apparatus for Consummate Investigation of the Mechanical Properties of Soil," *Proceedings International Conference on Soil Mechanics and Foundation Engineering*, Cambridge, Mass., 1936.

8. Wade, N. H., "Plane Strain Failure Characteristics of a Saturated Clay," Ph.D. Thesis, University of London, 1963.

9. Cornforth, D. H., "Plane Strain Failure Characteristics of a Saturated Sand," Ph.D. Thesis, University of London, 1961.

10. Kummeneje, O., "To-dimensjonale varuum-triaxialforsok pa torr sand." *Norwegian Geotechnical Institute Internal Report*, F. 80, 1957 (unpublished).

11. Boker, R., "Die Mechanik der Bleibenden Formanderung in Kristallinisch Aufgebauten Korpern," *Forschungsarbeiten*, No. 175/176, 1915.

12. Bresler and Pister, "Failure of Plain Concrete under Combined Stresses," *Transactions*, American Society of Civil Engineers, Vol. 122, pp. 1049-1060, 1957.

13. Foppl, A., "Die Abhangigkeit der Bruchgefahn von der Art des Spannungszustandes," *Mittheilungen Aus dem Mechnischen-Technischen Laboratorium*, Mundhen, 1900.

14. von Karman, T., "Festigkeitsversuche unter Allseitigem Druck," *Zeitschrift des Vereines deutscher Ingenieure*, Vol. 55, No. 42, 1911, pp. 1749-1757.

15. Richart, F., A. Brandtzaeg and R. Brown, "A Study of the Failure of Concrete under Combined Compressive Stresses," University of Illinois Engineering Experiment Station Bulletin 185, Vol. 26, November, 1928.

16. Ros, M. and A. Eichinger, "Versuche zur Klarung der Frage der Bruchgefahr. II. Nichtmetallische Stoffe," *Eidgenossische Materialpnufungsamstalf an der Eidgenossischen Technischen Hockschule*, Zurich, 1928, p. 57.

17. Schmidt, W., "Festigreit und Verfestigung von Steinsalz," *Zeitschrift fur Angewandte Mineralogie*, Vol. 1, pp. 1-29, 1937.

18. Topping, A. D., "The Use of Experimental Constants in the Application of Theories of Strength to Rock," *Proceedings Second Midwest Conference on Solid Mechanics*, Purdue University, 1955, pp. 178-192.

19. Freudenthal, A. M., "The Inelastic Behavior and Failure of Concrete," *Proceedings of lst U. S. National Congress of Applied Mechanics*, pp. 641-646, 1951.

20. Robertson, E. C., "Experimental Study of the Strength of Rock," *Bulletin of the Geological Society of America*, Vol. 66, 1955, pp. 1275-1314.

21. McHenry, D. and J. Karni, "Strength of Concrete under Combined Tensile and Compressive Stress," *Journal of the American Concrete Institute, Proceedings*, Vol. 54, No. 10, pp. 829-839, April, 1958.

22. Bellamy, "Strength of Concrete under Combined Stress," *Journal of the American Concrete Institute, Proceedings*, Vol. 58, No. 4, pp. 367-380, October, 1961.

23. Handin, J., H. Heard and J. Magouirk, "Effects of the Intermediate Principal Stress on the Failure of Limestone, Dolomite, and Glass at Different Temperatures and Strain Rates," *Journal of Geophysical Research*, Vol. 72, No. 2, pp. 611-640, January, 1967.

24. Watson, T. L., "Granites of Georgia," *State of Georgia Geological Reports*, No. 9A, pp. 114-117.

25. Schwartz, A., "Failure of Rock in the Triaxial Shear Test," *Proceedings of the Sixth Symposium on Rock Mechanics*, Rolla, Missouri, 1964.

26. Haigh, B., "The Strain Energy Function and the Elastic Limit," vol. 109, pp. 1920.

27. Westergaard, H., "On the Resistance of Ductile Materials to Combined Stresses in Two or Three Directions Perpendicular to One Another," *Journal of the Franklin Institute*, Vol. 189, pp. 627-640, May, 1920.

28. Mehldahl, A., "A New Graphical Method of Representing Strength Characteristics," *The Brown Bovari Review*, Vol. 31, No. 8, pp. 260-267, October, 1943.

29. Timoshenko, S. and Goodier, J., *Theory of Elasticity*, 2nd Ed., McGraw-Hill Book Co., New York, N. Y., 1951.

VITA

Billy Bruce Mazanti was born November 26, 1925, in Pine Bluff, Arkansas. He graduated from Pine Bluff High School in 1942. After a short period of work, he entered the U. S. Marine Corps and served with it until 1946. He studied pre-engineering at Conway State Teachers College, Conway, Arkansas, and entered Georgia Institute of Technology in 1947. He received both a Bachelor of Civil Engineering degree and a Master of Science in Civil Engineering degree from Georgia Institute of Technology in 1951 and 1955, respectively. Mr. Mazanti has worked in industry approximately six years in a variety of positions concerned with soil mechanics and foundation engineering. He has practiced as an independent, registered civil engineer, and acts as consultant to several companies. He has held a position as Assistant Professor of Civil Engineering at Georgia Institute of Technology since 1960.